

https://dspace.org/

Analysis of pillar/rockmass failure and propagation dynamics due to mining in hard rock Platinum Mines

Mushangwe, Patrick Chenjerai

2018

https://hdl.handle.net/10539/28910

Mushangwe, Patrick Chenjerai (2018) Analysis of pillar/rockmass failure and propagation dynamics due to mining in hard rock Platinum Mines, University of the Witwatersrand, Johannesburg, <http://hdl.handle.net/10539/28910>

Downloaded from a DSpace repository. https://dspace.org/

ANALYSIS OF PILLAR / ROCKMASS FAILURE AND PROPAGATION DYNAMICS DUE TO MINING IN HARD ROCK PLATINUM MINES

Patrick Chenjerai Mushangwe

A research report submitted to the Faculty of Engineering and the Built Environment, University of the Witwatersrand, Johannesburg, in fulfillment of the requirements for the degree of Master of Science in Engineering

Johannesburg 2018

DECLARATION

I declare that this research report is my own, unaided work. It is being submitted for the Degree of Master of Science in the University of the Witwatersrand, Johannesburg. It has not been submitted before for any degree or examination in any other University.

…….

(Signature of candidate)

…….. day of …….. (year)……..

at……..

ABSTRACT

The propagation of failure of a pillar system has often resulted in catastrophic consequences, this research establishes key variables that govern failure propagation in hard rock platinum mines. In order to critically analyse failure propagation, the available literature was reviewed to guide the research on key focus areas that may govern propagation. A review of the global and local geotechnical environment was done leading into detailed analysis of the data and rock mass behaviour from a case study mine to establish key variables and behaviour correlations. Available literature point towards failure largely due to mining practice issues and to some extent ground conditions. Joint orientation has been proven, in literature, to have an influence on the strength of pillar systems in particular when the joints dip adversely at 45° to the pillar / loading axis. This research also establishes that ground conditions, as described by rock mass quality and the effect of major sub-horizontal shear structures on pillar systems, have significant influence on the direction of failure propagation. This research further establishes that the failure prefers a direction 45° to the major vertical to subvertical joint set. The angle between the direction of migration and major subvertical joint is a phenomenon that had not been largely explored in terms of influence on failure propagation. The influence of mining practice issues, like pillar position and factor of safety, on failure direction is comparatively lower. This research also shows that barrier pillars should be designed taking into account the strike of major subvertical joint sets/structures in order to improve the ability to stop the propagation of failure. The analysis of the ground monitoring parameters, closure rates in particular, can be used to inform evacuation plans and reduce the impact of failure propagation on safety and production.

To my wife, Sharon and kids, Tadiwanashe and Makanaka, for affording me their precious time off family to work on this research. Above all thanks and praise be to God.

ACKNOWLEDGEMENTS

I acknowledge the effort and guidance provided by my supervisors, Prof Halil Yilmaz and Prof Francois Malan in ensuring this work comes out right.

Finally I thank Zimplats for allowing me to do this research and use data from its operations and reports which was very vital in this research.

CONTENTS

DECLARATION ii
ABSTRACT i
ACKNOWLEDGEMENTS iii
CONTENTS iv
LIST OF FIGURES vii
LIST OF TABLES ix
LIST OF ABBREVIATIONS x
LIST OF SYMBOLS xi
1. INTRODUCTION 1
1.1. Introduction 1
1.2. Project Background 3
1.3. Problem Statement 3
1.4. Research Objectives 5
1.5. Research Methodology 5
1.6. Areas Covered in this Research Report 6
2. LITERATURE REVIEW 7
2.1. Introduction 7
2.2. Rock Mass failure and Propagation / Migration of Failure. 7
2.2.1. Ground related conditions 7
2.2.2. Design considerations 11
2.2.3. Mining practice 17
2.2.4. Time related rock failure – creep 20
2.3. Conclusion 29
3. GEOTECHNICAL SETTING AND CASE STUDY MONITORING 30
3.1. Introduction 30
3.2. Geology of the Great Dyke 30

3.3. Structural Geology of the Great Dyke. 33
3.3.1 Regional structural geology history 33
3.3.2 Local geology of the case study area 36
3.3.3 Mutambara shear 38
3.4. Rock Properties 41
3.5. Mine History 41
3.6. Rockmass Response to Mining and the Shear 44
3.6.1 Monitoring results 44
3.6.2 Design of the monitoring system 44
3.6.3 Stress zone monitoring 46
3.6.4 Closure monitoring 47
3.6.5 Seismic Monitoring 48
3.6.6 Surface Monitoring 48
3.7. Conclusion 49
4. RESULTS ANALYSIS 50
4.1. Introduction 50
4.2. Macro-Scale Analysis 50
4.2.1 Tectonic activity 50
4.2.2 Rock mass Quality / Ground Conditions 54
4.2.3 Mutambara Shear 56
4.3. Micro-scale analysis 58
4.3.1 Pillar sizes 58
4.3.2 Pillar position 61
4.3.3 Joint properties 61
4.4. Ground Monitoring Results Analysis 66
4.4.1 Stress migration 66
4.4.2 Closure 67

4.4.3 Seismic events 69
4.4.4 Rainfall 71
4.5. Detailed Results Analysis 72
4.6. Formulation of the migration model. 75
4.6.1 Formulation of a probability function 78
4.7. Conclusion 82
5. CONCLUSION AND RECOMMENDATIONS 83
5.1. Conclusions 83
5.2. Recommendations 84
5.3. Recommendations for further study 84
REFERENCES 86
APPENDICES 89

LIST OF FIGURES

Figure 2.1 Variation of effect of jointing with pillar width to height ratio 9
Figure 2.2 Effect of joint dip on pillar strength. 10
Figure 2.3 Impact of shear on strength and pillar width 12
Figure 2.4 Plan of the Coalbrook mine at the time of collapse 18
Figure 2.5 Idealised creep curve. 23
Figure 2.6 Commonly used viscoelastic models 26
Figure 2.7 Pillar failure modes 27
Figure 2.8 Partially failed surface spalling with isolated internal fractures 28
Figure 2.9 Partially failed contacts with extensive internal fractures 28
Figure 2.10 Failed pillar with internal shear fractures 28
Figure 2.11 Effects of scaling, buckling and spalling on pillars 28
Figure 3.1 Location of the Great Dyke on the Zimbabwean craton 30
Figure 3.2 Generalised geological succession 31
Figure 3.3 Detailed geological succession of the Great Dyke 32
Figure 3.4 Post Great Dyke tectonic history in Ngezi area 34
Figure 3.5 Typical orthogonal network of granite dykes 35
Figure 3.6 General stratigraphy of Southern Africa 35
Figure 3.7 Ngezi structural model 36
Figure 3.8 Position of the Mutambara shear 39
Figure 3.9 Thickness of the Mutambara shear 40
Figure 3.10 Bimha Mine plan showing failure and progression 43
Figure 3.11 Stages of rock mass failure 45
Figure 3.12 Stress meter and read out unit 46
Figure 3.13 Installed closure measuring devices 47
Figure 3.14 Bimha monitoring stations 49
Figure 4.1 Direction of migration in relation to tectonic events 51
Figure 4.2 Direction of migration in relation to structures 51
Figure 4.3 Direction of migration in relation to Aplitic dyke structures 53
Figure 4.4 Correlation of stress migration and very poor ground conditions 55

Figure 4.5 Failure migration in relation to Mutambara Shear thickness 56
Figure 4.6 Failure migration in relation to the position of the shear 57
Figure 4.7 Distribution of the pillar height 58
Figure 4.8 Distribution of the w/h ratio 59
Figure 4.9 Distribution of the Factor of safety 60
Figure 4.10 Pillar position with respect to design. 61
Figure 4.11 Failure migration with respect to joint roughness 64
Figure 4.12 Failure migration in relation to joint alteration. 65
Figure 4.13 Bimha monthly stress migration 66
Figure 4.14 Cumulative stress migration curve 67
Figure 4.15 Closure trend. 68
Figure 4.16 Typical inverse closure rates 69
Figure 4.17 Seismic events trend 70
Figure 4.18 Rainfall trend 71
Figure 4.19 Comparison of the Monitoring trends 73
Figure 4.20 Stress meter readings 74
Figure 4.21 Failure areas by period 76
Figure 4.22 Plot of the key variables 78
Figure 4.23 Sine – Cosine curves 80
Figure 4.24 Angle difference $(sin\theta cos\theta)^2$ curve 80
Figure 4.25 Failure factor 81

LIST OF TABLES

Table 2.1 Pillar design formulae. 16
Table 2.2 Coalbrook failure - key parameter changes 17
Table 2.3 Comparison of key stability variables 20
Table 3.1 Distribution of the joints based on the joint analysis 37
Table 3.2 Rock mass quality parameters 38
Table 3.3 Key intact rock parameters 41
Table 3.4 In-stope pillar design parameters 44
Table 4.1 Dyke frequency for the mine 53
Table 4.2 Rock mass classes 54
Table 4.3 Rock mass ratings comparison 56
Table 4.4 Joint roughness and alteration numbers 63
Table 4.5 Seasonal rainfall comparison 71
Table 4.6a Correlation coefficients for first year 72
Table 4.6b Correlation coefficients for second year 72
Table 4.7 Key variables in the different areas 77
Table 4.8 Failure factor for the different areas 81

LIST OF ABBREVIATIONS

BMSZ	Base of the main sulphide zone
CPF	Cascading pillar failure
CSIR	Centre for Scientific and Industrial Research – (South Africa)
DIPS	Joint analysis software code
E	East
ESE	East-southeast
FoS	Factor of safety
LB	Limpopo mobile belt
m	Metres
Ma	Million Annuals (years)
MSZ	Main Sulphide zone
N	North
NE	North-east
NNE	North-northeast
NW	North-west
Pa	Pascals
Q	Rock mass quality
S	South
SE	South-east
SW	South-west
SGMI	Small ground movement instrument
UCS	Uniaxial compressive strength
UDEC	Universal Distinct Element Code (Numerical modelling software)
W	West
WNW	west-northwest
WSW	west -southwest

LIST OF SYMBOLS

Degrees	°
Total strain	ε
Instantaneous elastic strain	ε_e
Function expressing the decelerating creep of the primary phase	$\varepsilon(t)$
Steady state creep component	$\mathrm{C}t$
Function expressing the accelerating creep	$\varepsilon_{\mathrm{T}}(t)$
Failure function	F
Angle between failure direction and major subvertical joint set	θ
Rate of steady state creep	$\dot{\varepsilon}_{\mathrm{SS}}$
Pearson's correlation coefficient	R

1 INTRODUCTION

1.1. Introduction

The failure of a pillar system in mines is an unwanted event which normally starts with a few pillars, propagating with a domino effect to cover large areas, in some catastrophic cases, propagating to the whole mine. Some of the major mine/pillar failures in hard rock metal mines have been associated with the existence of extensive geological structures and weak rock layers. Historical examples of such failures in metal mines include pillar failure due to the hangingwall contact shear such as the cases at Everest Mine, Wonderkop Chrome Mine in South Africa in 1998 where a 0.17m thick clay layer was 0.5-1.0m above the footwall and at Bimha Mine (Zimbabwe 2014) where an undulating (Mutambara) shear zone with thicknesses up to 1.0m was found within, above and below the mining horizon. Of interest is the fact that the failure at Bimha Mine initiated in an area where the clay filled shear plane was 0.5-1.2m in the footwall (Zimplats, 2014). Other major pillar failures that have been reported in metal mines have been associated with high extraction, secondary mining and pillar splitting (Zipf, 2000).

Rock mass by its nature is neither homogeneous, continuous nor isotropic (showing same properties in all directions). The existence of geological structures, competent and weak zones within the same rock mass has been observed in rock masses resulting in unexpected behaviour and failure mechanisms. The variability in rock mass properties make the projection and prediction of failure and propagation mechanics very complex to formulate. The layered rock masses such as the Bushveld Complex of South Africa, the Stillwater Complex in America and the Great Dyke of Zimbabwe are no exception to extensive weak layers within the rock mass. The weak layers tend to follow a similar layering to that of the host rock mass or weaknesses within. On the Great Dyke of Zimbabwe, Unki Mine is reported to have a weak layer within the footwall while Zimplats is also reported to have a weak layer which largely contributed to the collapse of the bottom half of Bimha Mine in 2014.

The onset of failure has been observed to be triggered by zones of poor designs/mining and those with weak rock layers. Typically, areas where pillars have been formed below the design sizes e.g. Coalbrook disaster in South Africa in 1960 (Malan, 2012) are prone to failure. The propagation/migration of failure once triggered has also been observed to follow zones of weak layer/parting, low pillar strength or very high extraction which form the lines of weaknesses. This kind of behaviour has been observed at a number of case study failures and in particular at the epicentre of failure. Propagation of failure has other variables controlling the behaviour as they appear to be dissimilar on different cases. The later stages of the failure migration at Bimha Mine seemed not to follow the initial trends as well as observations from other metal mines. At Bimha Mine, the failure continued to areas where a weak layered rock did not exist and where it has less influence on the pillar system hence the need to study and understand the other variables defining the migration direction. From the available literature, less attention has been given to establishing the key variables that influence the direction of propagation once the failure has initiated.

Studies of pillar failure in the room and pillar metal mines in the United States of America (USA) also indicated the influence of pillar height, panel span, percentage extraction, width to height ratio and panel length on pillar failure propagation (Zipf, 2000). It is also important to note that the propagation of failure in the USA analysis shows a higher positive correlation to pillar and excavation parameters. Similarities are drawn from these observations to the case study analysis in terms of the absence of barrier pillars, low width to height ratios, high extraction and presence of a weak layer. However, the properties, nature and occurrence of the weak layer was unique and dissimilar to those of known pillar failures at metal mines.

From analysis of the literature on different pillar failure cases, weak zones and mining height are the key variables for onset of pillar failure while other variables such as span and depth come into play for the migration of the failure. These

variables influencing the onset and propagation of failure will be enumerated and analysed to come up with a probability of failure function that can be used for prediction of failure migration.

1.2. Project Background

Room and pillar mining is the most common mining layout for hard rock shallow platinum mines and is applied to all the existing operations on the great dyke of Zimbabwe. Experience at Zimplats Bimha mine and other mines has proven that it is difficult to stop cascading pillar failure once it starts to propagate. Cascading pillar failure is a collapse/failure of pillars covering a large area in a room and pillar mine, starting from a particular point and spreading with a domino-effect (Zipf, 1996). One difficult question that is always asked is 'which pillar/ block is going to fail next?' The variability in rockmass properties make the projection and prediction of failure very difficult and complex to formulate. This project seeks to address the question of failure probability and prediction by establishment/formulation of a probability of failure function that can be used to locate the areas prone to the onset of failure as well as the migration. The function was tested against the observed behaviour. The establishment of a way of predicting failure propagation behaviour can be used to inform evacuation plans and can be incorporated in pillar designs as well.

1.3. Problem Statement

Mining is a capital intensive business and capital efficiency should be maintained at highest possible levels. In order to achieve maximum capital efficiency, a mine must be able to live its planned life. Any pillar system or rockmass failure which results in any loss is an unwanted event as it lowers the capital efficiency of a mine. In case of a pillar failure, thought the first price is to prevent pillar failure, it is important to know and understand the root cause of the failure so as to predict

how and where the failure will propagate to. It is also important to understand what failure system or mode of failure and under which conditions will the mine operator be able to halt any propagation of failure in a room and pillar mine set up. It is critical that a good understanding of the expected behaviour of the failure process be sought. The following critical questions were addressed;

- What is the direction of propagation of a failure?
- What will delay and/or stop propagation of the failure?
- At what point does evacuation become necessary?

Understanding the onset and propagation of failure within a pillar system as well as the rockmass brings valuable information on the critical variables that need to be analysed and considered in coming up with evacuation plans as well as future designs and mitigation measures. The pillar failure at Bimha mine which is largely attributed to the existence of a shear structure was of interest to this research (Zimplats, 2014). The shear structure was described as a low angle undulating open shear system with infill comprising brecciated altered clayey / mylonite gouge of varying thickness up to 1.0m (Zimplats, 2014). The shear structure is pervasive at Bimha mine and has a variable position with respect to the mining horizon, varying thicknesses as well as infill material properties. Analysis of the fill material characteristics and detailed structural evaluation of the shear structure was carried out at various times during the investigation of the Bimha mine collapse case. Understanding and modelling of such variability will make prediction of behaviour as well as incorporation into designs valuable.

1.4. Research Objectives

The objectives of the research are;

- To establish why rock mass failures propagate in a particular direction and use the results to recommend input into mine evacuation plans, pillar layout and design that will delay or even stop failure propagation
- To establish a formulation that can be used to identify zones prone to high probability of failure propagation within a pillar system
- To analyse the trends from ground monitoring results to guide decision making on evacuation should the need arise in case of a future collapse thus reducing exposure to risky conditions and minimizing loss (production or any other).

1.5. Research Methodology

The methodology used was to analyse a major pillar failure from Zimplats Bimha mine as well as other mines with similar mining methods in both hard and soft rock mining or geotechnical setting using the following techniques;

- Back analysis
- Geological interpretation
- Geotechnical and rock property tests
- Identification of key parameters that govern the behaviour of the rockmass in failure.

Once the key parameters were identified, an analysis that takes into account the variability in rock parameters was done in an attempt to yield results close to real life behaviour. This then lead into a formulation that can be used to predict probable behaviour.

Analysis and correlations was done covering the following;

1. Pillar failure propagation
2. Stress propagation
3. Geotechnical and ground conditions

4. Effect of pillar geometries
5. Effect of jointing (Location, fill, dip and dip direction)
6. Pillar sizes and positions
7. Mining heights
8. Mining depth below surface
9. Shear plane position and thickness

This research investigated the onset and propagation of failure in relation to the interplay of the above variables. These were then used to formulate a function to predict failure direction which can be used to inform evacuation plans and pillar designs.

1.6. Areas Covered in this Research Report

A thorough review of available literature and case histories is covered in Chapter 2 detailing similarities and differences with the case study. Some of the variables to be included in the case study were established from a study of cases in history. Chapter 3 follows with detail on the geological setting and geotechnical conditions of the case study as established from the research as well as some literature. Regional geotechnical conditions and settings are also covered in this chapter. Chapter 4 focusses on analysis and correlations of the failure propagation trends and ground monitoring results as established. The analysis was used to come up with a formulation that can be used to guide and establish potential direction of migration / propagation of the failure. The establishment of direction of migration together with results of monitoring can be used to inform evacuation plans for the mine. The results of the analysis can further be incorporated as input into pillar design. Chapter 5 covers the conclusions from the research work in understanding the direction of migration of failure to inform evacuation plans, loss minimisation as well as recommendations for further study and implementation.

2 LITERATURE REVIEW

2.1 Introduction

This chapter examines the literature that is available in relation to pillar failure and the propagation of the failure. The literature analysed cover the causes of pillar failure spanning from in situ ground conditions, design of pillars, excavations, mine design and the implementation of the design i.e. mining practice to time related deterioration of ground conditions. This is carefully examined to guide the focus areas in terms of analyzing the variables that govern mechanics of failure propagation.

2.2 Rock Mass failure and Propagation / Migration of Failure.

Analysis has been done on the available literature with focus on rock mass and pillar system failure and propagation due to mining. The causes of such failure and propagation can be grouped into four major domains. These domains which are analysed in this research cover the following key areas;

1. Regional geology, in situ rock mass and ground related conditions
2. Design issues related to the design of excavations, pillars and mining sequence
3. Operational issues around the correct implementation of the design during the process of mining
4. Creep – time dependent failure / rheological propagation of failure.

2.2.1 Geology and ground related conditions

According to More O'Ferrall & du Plessis (2017), the impact of geological structure is often overlooked in design and in most cases leads to massive instability. They noted that failure and propagation of the failure often depends on the tectonic events that resulted in the formation of such structures, the orientation, width, infill, ability to dissipate energy and mining induced stress

either enhance or reduce instability. The geotechnical behaviour of the parameters mentioned above is in most cases non-linear and very difficult to model and predict due to their variability (More O'Ferrall & du Plessis, 2017).

The difficulty in predicting failure and its propagation in rock is a great concern and difficult to formulate owing to the variation in rock properties and geological structures which govern behaviour and deformation. Such complexities can only be understood by increased research into establishing the underlying causes and drivers of failure and its propagation in a particular direction which is one of the key objectives of this research.

The difficulty in coming up with a formulation for failure propagation in conditions with variable properties is best explained by the study done by Carla et al (2017) even though it was on open pit slopes. Carla et al (2017) (1, page 76) indicated that the laws used to describe displacements of failing slopes do not take into account the mechanical properties of the material and their influence on failure. The analysis of 78 case histories of mine slope failures, showed that "*reliable mathematical expressions with ability to comprehensively characterize the observed events could not be found*" (1, page 77). Carla et al (2017) (4, page 79) concluded that "*there is a striking linear correlation between the average acceleration in the final 3 hours before failure and the average acceleration in the final 24hrs before failure with a positive correlation of 0.99*". It has been observed in this and other analysis related to rock mass failure with time that the failure rate cannot be directly related to just one variable like velocity or displacement rate as other variables (e.g. geo-mechanical and geological properties of the rockmass) play a significant role in governing rockmass failure and propagation. It therefore becomes important to analyse and correlate the failure trends observed, to as many variables in order to use, in the formulation of a relationship. The difficulty in obtaining mathematical expressions that can accurately characterize rock failure raises interest in this research to work towards a formulation that can express the behaviour of rock and pillars in failure propagation.

The key geo-mechanical properties of the rock mass that determine the strength of pillars are geological structures such as joints and faults. Studies done by Esterhuizen (2000) on coal and metal mines to understand the effect of jointing on pillar strength gave relationships between the pillar strength and the variables. The numerical modelling done in UDEC to understand the effect of jointing showed that "*the effect of jointing on pillar strength diminishes as the width to height ratio of a pillar increases*" (Esterhuizen, 2000) (page 287) as shown in Figure 2.1.

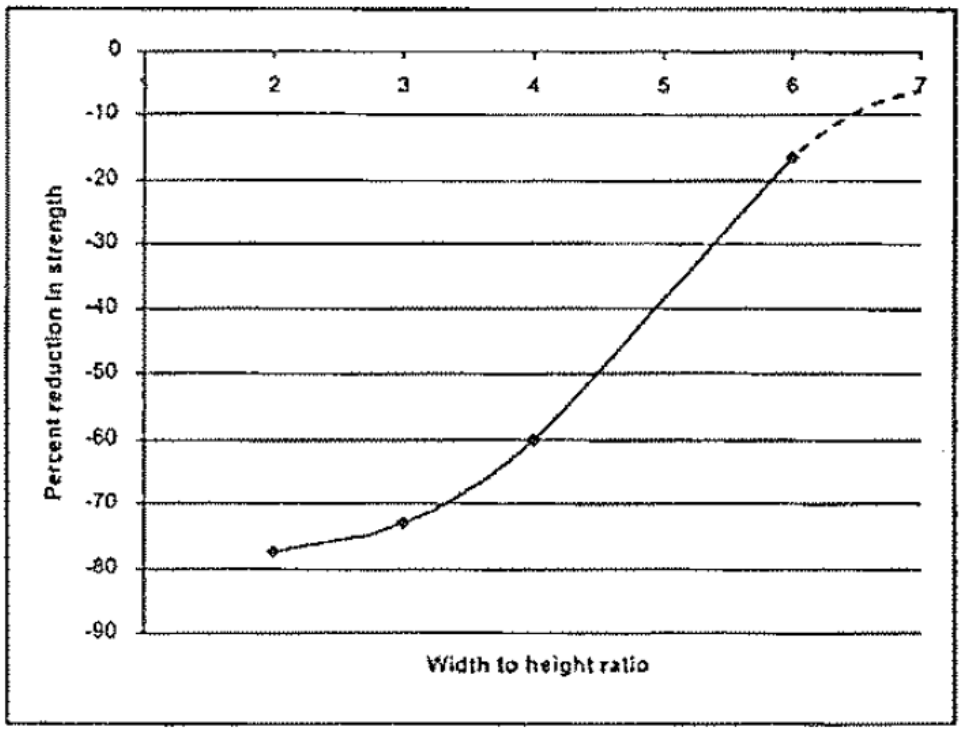

Figure 2.1 Variation of effect of jointing with pillar width to height ratio (Esterhuizen, 2000)

From the above trend, the expectation is that pillars with a higher width to height ratio are less prone to failure when compared to pillars with a low width to height ratio.

Further analysis was done on the effect of joint dip to the strength of the pillar. "*It was seen that the pillar strength reaches a minimum when the joints dip at 45°*" (Esterhuizen, 2000) (page 287). The reduction in pillar strength particularly for width to height ratios less than five can be attributed to the fact that a 45° joint

set is highly likely to daylight on opposite sides of the pillar forming a potential surfaces for deformation and eventual failure. The same analysis also showed that "*pillars with a large width to height ratio are less affected by the presence of joints than narrow pillars*" as shown in Figure 2.2 (Esterhuizen, 2000) (page 287).

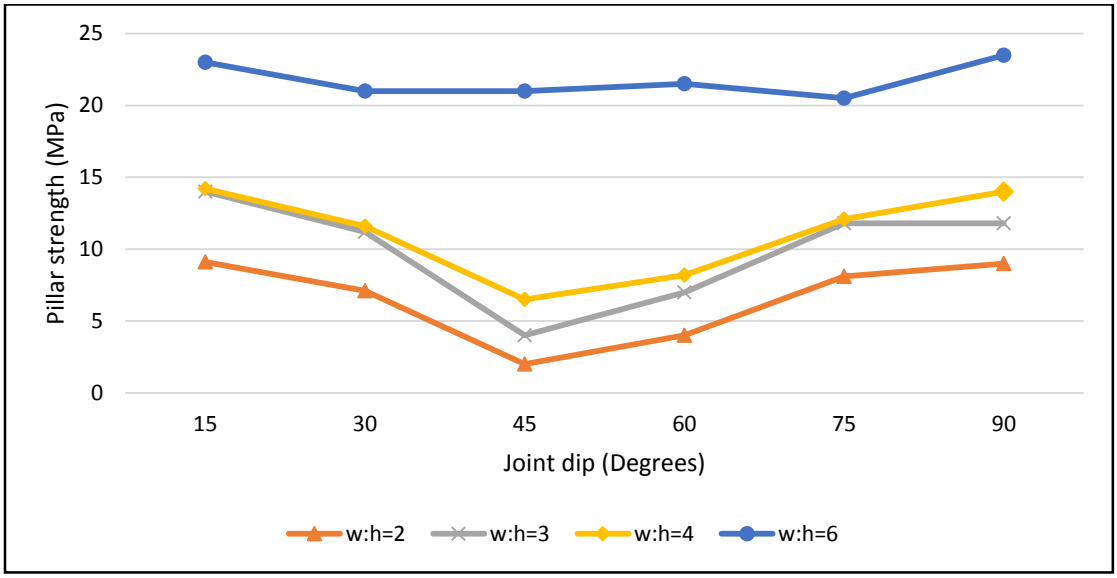

Figure 2.2 Effect of joint dip on pillar strength. (Esterhuizen, 2000)

The trend in Figure 2.2 clearly shows that the adversely dipping joints (45 degrees) reduce the strength by as much as 50% for width to height ratio less than 5, hence the importance of considering the joint set dips and orientations.

Esterhuizen (2000)'s analysis has proven the impact of joint dip on pillar strength and this research on failure propagation dynamics will further test the impact of jointing and pillar strength on failure propagation.

Most of the research work that has been reviewed focused on the impact of ground conditions and geological structures to the strength of pillars and or failure of excavation with less focus on the propagation of failure. The focus of this research goes further into understanding the behaviour beyond the failure point. While one of the important controls in mine stability will be to prevent failure, the analysis of failure propagation will open up information guiding the response to be taken in the event of failure and hence heighten emergency preparedness.

2.2.2 Design considerations

More O'Ferral and Malan (2012) (page 8) analysed different pillar design methods in South African mines, and indicated that there are two main approaches which follow either empirical methods or numerical modelling. Their conclusion was that "*none of the pillar design methodologies employed take into congnisance the existence of weak layers within the pillar material or in the immediate foundation*". The assertions by More O'Ferrall and Malan (2012) point to the infancy of the understanding of the behaviour of pillars under the influence of geological structures and in particular weak layers. One weakness with most methodologies for pillar design is that assumptions which do not take into account the variability of the different geological structures are made in determining pillar strength. Most of the methods assume homogeneous rock masses. Furthermore, most of the empirical methods of pillar design would normally work accurately in environments similar to where they were formulated to an extent that disclaimers are put for use of some of the methods to extrapolated environments. In a chrome mine case study, More O'Ferral and Malan, (2012) (3, page 3) indicated that "*a change in the direction of loading orientation on the pillar resulted in a large-scale pillar failure associated with a weak layer*". The understanding of the impact of the direction of loading, reef dip and orientation of major geological structures becomes a key point, in this study, that attempts to establish the propagation of failure in pillars. Analysis on a platinum mine failure indicated that, where the weak parting was 1m into the footwall, there was a marked weakening effect on the pillar strength (More O'Ferral and Malan, 2012). The case study in this research also indicated a similar weakening effect when the weak layer is in the footwall, however, the effect tends to diminish as the position gets deeper into the footwall. From the research, it can be reasoned that a pillar system may have a unique position of the weak layer where the impact on pillar strength is significant.

The Southern African Platinum mining industry has largely used the Hedley and Grant power formulae which was formulated based on case histories from Uranium mines in Canada. This is a different geotechnical environment and might

have limited applicability. However it has been used and has registered lots of success which could be an indication of conservativeness of the method in the Platinum industry. The few failures that have been noted in platinum mines are an indication of inadequacies in the methods or omissions in the inputs to the design. Such inadequacies and omissions result in pillar failures which then need to be managed once initiated. The management of which can be done if there is a well laid approach with prediction of likely behaviour.

UDEC analysis done by Muaka, et al. (2017) proved that the impact of shear structures within the footwall or hangingwall on pillar strength is more severe. Figure 2.3 shows the impact of the shear at different pillar sizes as established by Muaka et al. (2017)

The propagation of failure within a pillar system is ultimately expected to trace the line of weakest strength pillars. The trends in Figure 2.3 show that the greatest impact on pillar strength is when the shear is in the footwall and hangingwall and least when it is on the reef horizon. This research examines and tests the correlation of these findings to the case study.

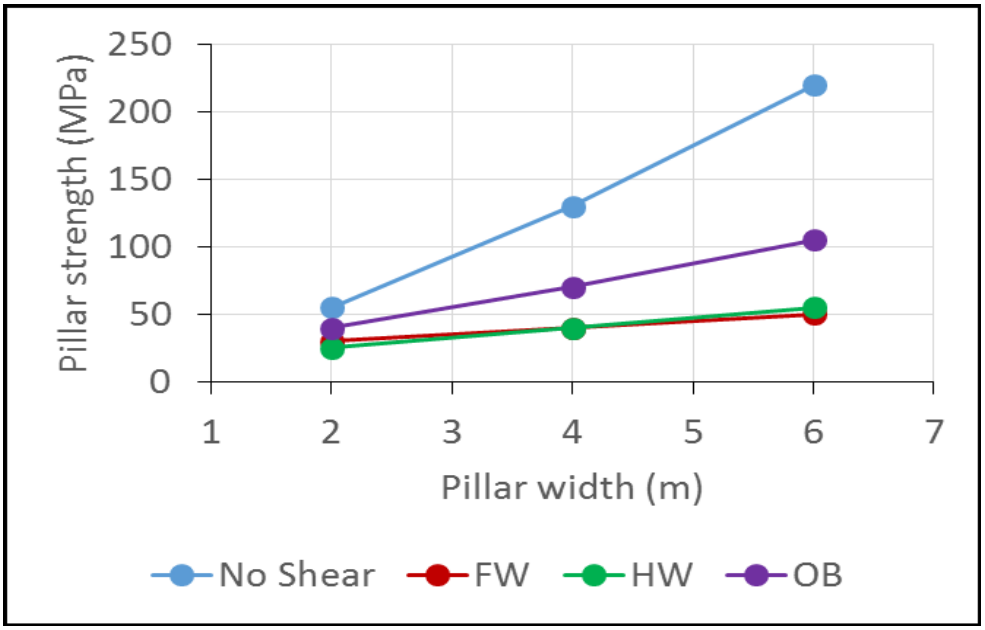

Figure 2.3 Impact of shear on strength and pillar width (Muaka, et al., 2017)

The design of a mine cannot be done competently without taking into account the quality of the inputs into the design as it determines the stability of the mine. Since a number of variables and assumptions are taken into design, if any of such variables is not accurately represented in the design, it results in a flawed design which can lead to eventual failure. One such variable that feeds into design is the rockmass conditions as well as existence of major geological structures. If such variables are not properly enumerated right from exploration and accurately incorporated into design, the resultant design is often inadequate for the conditions.

Pillar design

A number of pillar formulae used in the design of room and pillar layouts have been analysed. Table 2.1 shows some of the common formulae in use showing the key variables that are input into the design formula. The base of most pillar designs is pillar strength to pillar stress ratio which provides a certain factor of safety. The input into the determination of the two independent variables of pillar strength and stress is so complex that some assumptions are taken into consideration. The estimation of these two variables therefore becomes key for a design to be adequate. Some of the key variables that can affect pillar strength include;

- Intact rock strength parameter as determined from laboratory test programs e.g. uniaxial, shear and triaxial tests
- The geometry of the pillar as determined by its dimensions in all the three dimensions of length width and height
- The rockmass properties of the pillar forming material and how it responds to excavations made in rock.

While the intact rock properties are determined based on strict guidelines, the conversion / extrapolation of these parameters into the rock mass parameters

can be very difficult leading to errors in design with the end result of failure of the design to perform to the expected standard. The geometry of pillars and excavation are a physical shape measurable parameter hence of limited variability as compared to rock parameters. If the design does not cater for the unexpected event of design failure, major losses and even fatalities can result. The impact of unexpected failure can be mitigated if there is a good understanding of the behaviour, post failure initiation.

Mining practice issues also contribute to pillar strength, and includes issues to do with pillar mining quality, adherence to design in terms of shape, size, and position including the impact of blasting and process water management. If process water is not correctly managed, it can easily percolate, lubricate structures and increase the risk of deformation.

Some major geological structures like faults and shears have the effect of reducing the strength of the pillar (Esterhuizen, 2000) and they become the points of weakness which can form the epicenter of failure. This also includes the size, shape, orientation, and position of such structures which have been shown to have an impact on the strength of the pillars.

The stress within a pillar is also complex to estimate as it is determined not only by the weight of the overburden (virgin stress) but also the effect of mining induced stress.

Geological structures like faults and shears have also been known to have an influence on stress as most are associated with tectonic stress. These stresses largely emanate from the phenomenon that resulted in their formation and certain residual stresses may become active as a result of mining close or in such structures. (More O'Ferral and Malan, 2012).

Ground water is a key parameter in determining pillar strength as it affects pore water pressure as well as provide lubrication on major geological structures.

Broadly speaking the pillar design methodologies can be classified into four groups (Potvin, 1985), (Hanekom, 2017);

- Heuristic – based on experience of what has worked and should continue to work (rule of thumb)
- Empirical – based on case studies and experience
- Theoretical – based on exact properties which are very variable in rock masses
- Numerical – based on very accurate pillar stress levels

The different methods have been applied in different case histories with varying degrees of success/failure. One major shortcoming of the Heuristic methods is that they are based on the performance and modification of an initial solution where results can be worse if the initial one fails. It must be noted that there is a lot of literature where one method has performed in one situation and failed in another. This brings out the important fact of the variability in the ground conditions where the different methods are applied. If any of the methods are applied in the right environment, the results will be positive and it therefore becomes important to understand the environment of application of a particular method. Some of the methods are based on limited case histories and data which at times is specific to a mining method or geotechnical environment and therefore applicability in all environments will be met with varying degrees of success. The varying degrees of success can be attributed to the differences in the intact rock properties, rock mass properties, structural geology, tectonic history, stress and other key factors that influence rock mass behaviour and pillar integrity. Numerical methods have gained a lot of application in design with one major disadvantage being that complex assumptions are used to build the models which can often lead to incorrect results particularly cases where there is limited experience. On the other hand the major advantage is the ability of models to handle and analyse large volumes of input data.

Pillar design methods

From the above groups, Table 2.1 shows some of the widely used formulae for pillar strength.

Table 2.1 Pillar design formulae (Martin & Maybee, 2000), (Potvin, 1985), (More O'Ferral and Malan, 2012).

Name	Formula	Pillar application
Size effect	A+B*(w/h)	Stub and inclined
Shape effect	Kw^a/h^b	Stub and inclined
Salamon	Kw_e^a/h^b	Stub and inclined
Shorey and Singh	K1/2(w_1+w_2)^a/h^b	Stub and inclined
Hoek and Brown curves	$\sigma_1 = \sigma_3 + \sqrt{m\sigma_c\sigma_3 + s\sigma_c^2}$	Separation stub and inclined
Salamon and Munro	$\sigma_s = K\, w^{\alpha}/h^{\beta}$	Regular square pillars
Hedley and Grant	$\sigma_s = k\frac{w^{0.5}}{h^{0.75}}$	Regular pillars

From the different approaches to design, it is clear that there are quite a number of assumptions on the ground conditions as depicted by the use of constants such as K whose determination is quite varied.

In the analysis of the strength of hard rock pillars, Martin & Maybee (2000) (6-page 1246) observed the predominant mode of failure as "*progressive slabbing and spalling*". They also suggested that "*the conventional Hoek-Brown failure envelops over predict the strength as the failure process is largely governed by cohesion loss where frictional strength components are not mobilized*". In the application of empirical formulae, it is important to note that the application environment is similar to the environment from which the formula was derived. Hence empirical methods are specific. Where they are applied to a different environment, certain parameters will have to be adjusted to suit application in the new environment. In the analysis of pillar failure in hard rock mines in Elliot Lake, it was noted that the stress induced spalling dominated in the early stages while the latter stages were dominated by typical hour glass shape failure, slip along planes and joints played

a significant role in the failure process (Martin & Maybee, 2000). Effectively this means that stress plays an important role in the initiation of failure while the impact of joints becomes significant in the propagation / migration of failure.

Most of the literature on pillars design focus on obtaining a formulation that will ensure excavation stability and no inadvertent failure of pillars. However a number of assumptions are built into the formulae and hence into the design of the mine. In the event that there are inadequacies in the inputs or assumptions, the design might fail and once failure has initiated, the options become very limited to trying to stop the failure and safe evacuation. The understanding and prediction of direction of propagation therefore becomes important in such situations as well as the timing of the evacuation process become critical to the safety of man.

2.2.3 Mining practice

Review of the reported cases of pillar failures was done in different commodities and geotechnical settings in order to guide this research as well as establish key variables that govern the stability and failure of pillars.

One of the major pillar failure disasters in the history of South African coal mining is the Coalbrook disaster (Van Der Merwe, 2006) where a pillar system failed leading to 437 fatalities. Investigations and analysis concluded that the failure was primarily driven by reduced barrier pillar size from initial 24.4m (1905-1932) to 18.3m (1932-1950) then 13.1m (1950-1959) at the time of collapse on 21 January 1960 as shown in Table 2.2 with other parameters included.

Table 2.2 Coalbrook failure - key parameter changes (Van Der Merwe, 2006)

Parameter	**1905-1932**	**1932-1950**	**1950-1960**	**Comment**
Barrier pillar width (m)	24.4	18.3	13.1	Decreased
Pillar centres (m)	24.4	19.8	19.8	Decreased
Bord size (m)	6.7	6.7	6.7	Maintained
Mining height (m)	2.4	2.4	4.3-5.5	Increased

A total mining area of 324 hectares collapsed in this disaster as shown in Figure 2.4 and it is important to note that the failure could not migrate into areas mined prior to 1950 where the barrier pillars were bigger and mining height was still at 2.4m (Van Der Merwe, 2006).

The Wonderkop chrome mine pillar failure (Spencer, 1999) is a typical example of failure in hard rock mines where a weak layer within the mining horizon caused the failure.

Everest mine pillar failure in South Africa - Bushveld exemplifies the influence that shear structures have on pillar stability and rock mass failure. Jointing can also have serious negative influence on pillar stability (Esterhuizen, 2000). In this example a slippage along the pillar contacts with the hangingwall occurred. The Everest mine slippage shares similarities to what could have happened at Bimha Mine due to the following common findings; clay filled shear structure, presence of water, high extraction ratio (above 75%) and pillar width to height ratio of less than 2 as shown in Figure 2.4.

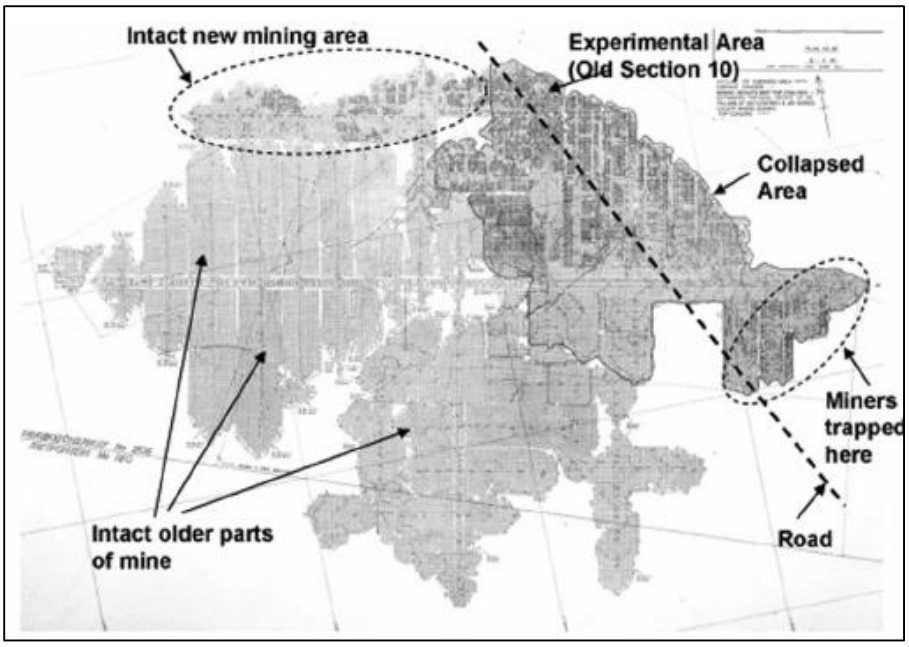

Figure 2.4 Plan of the Coalbrook mine at the time of collapse (Van Der Merwe, 2006)

The variables that govern the onset of failure have proven to be different from what determines the direction and rate of failure migration. Zipf (2000) (page 5) established from a study of several US metal mines, that, where pillar failure occurs and migration of the failure follows;

"*(1) High extraction above 60%*
(2) Width-height ratios less than 3, 2 and 1 for coal, metal and other mines respectively
(3) Reached maximum tributary area load and minimum panel width of 80m
(4) Substantial barrier pillars with width-height ratios more than 10 are absent from the mine layout
(5) Although CPF seems more prevalent in shallow mines less than 100 m deep, this may be only a reflection of the prevalence of shallow room-and-pillar mines"

Table 2.3 shows the key variables that govern stability as well as propagation of failure at different case studies analysed.

While there are some similarities, the data in the table clearly indicates that there are certain unique variables that trigger instability as well as propagation of the instability.

Analysis of the failure of a rock mass was extensively analysed by Milne (1997) where he made use of a hydraulic factor which takes into account the complex shapes involved in mining. The application of such factors in analysis of this research is expected to yield correlations that are important in formulating a prediction of failure propagation.

No large scale pillar and rock mass failure in shallow depth hard rock platinum mining environment in Zimbabwe has been recorded prior to Bimha mine failure in 2014. However numerous failures of large magnitude involving underground operations in room and pillar mines have been extensively analysed for soft rock mines e.g. the coal brook disaster, Van Der Merwe (2006) such as in coal, limestone and some metal mines such as chrome and platinum mines. This study focused on failure propagation behaviour based on experience on a platinum mine. In most cases where failure of large spans has occurred, access is often

restricted for safety reasons and hence analysis of failure propagation is often limited. However, understanding the behaviour as well as the ability to predict behaviour is important for every mine operator. It gives the mine operator the flexibility to continue working until the right time to evacuate is reached and reduce the impact on production as well as man exposure to potential risk.

Table 2.3 Comparison of key stability variables (Van Der Merwe, 2006), (Spencer, 1999) , (More O'Ferral and Malan, 2012), (Zimplats Internal report, 2014) .

	Coalbrook	**Wonderkop**	**Everest**	**Bimha**
Bord size	6.7	5	10	7
Pillar width (m)	13.1	8	5	4-5
Mining height (m)	4.3-5.5	2	2	2.5
Pillar width to height ratio	2.4-3	4	2.5	1.6-2
Barrier pillar width (m)	13.1	Nil	Nil	Nil
Extraction (%)	+44	40	83	82
Rock type	Coal	Chromitite	Pyroxenite	Bronzitite
Weak layer position / horizon	Nil	Ore	H/wall contact and ore	H/wall, ore and F/wall
Weak layer thickness	N/A	0.2	0.3-0.5	Up to 1.0m
Depth (m)	140	100	80-180	150-260
Water ingress into shear	Nil	Some	Yes	Yes

2.2.4 Time related rock failure – creep

Creep behaviour on jointed rock masses is largely driven by the time dependent response of the intact rock as well as the joints (Khoshboresh, 2013). In his analysis of creep behaviour, Khoshboresh (2013) noted that creep deformations in fractures overshadows intact rock creep in intact rock masses. This is the case because generally the shear strength of a joint is less than that of intact rock particularly where the joints have infilling. This points out to the importance of understanding the jointing and fractures contribution to this research.

It also becomes important to understand the fundamental mechanism underlying creep. Ryder & Jager (2002) noted that the fundamental mechanism is "*chemical weakening of bond strengths of multitudes of overstressed crack tips in an already damaged rock mass, and consequent stress re-distribution due to growth of these cracks*" (Page 54, Chapter 2.7.2). The analysis agrees very well with the understanding that creep is more pronounced in fractured rock when compared to intact rock. Moreover joints and fractures play a significant role in creep behaviour as compared to intact rock creep. It is also important to note that "*time-dependent stress re-distribution can lead to overloading of unstable structures remote from mining faces leading to seismic events at random times well apart from the blasts*" (Ryder & Jager, 2002) (Page 33, Chapter 4.4). This concept of stress redistribution and random seismic events becomes important to the case study as there was record of random seismic events at Bimha Mine in 2014.

According to Drescher and Handley (2003) there are at least four mechanisms responsible for time-dependent hard rock deformation, namely:

- compression creep of the intact rock material
- material dilation as a result of stress damage
- shear creep on pre-existing discontinuities and stress induced discontinuities in the rock
- dilation of discontinuities as shear displacements grow with time

Rock has rheological behaviour and studies by Drescher and Handley (2003) (Page 329) from laboratory shear creep tests of hard rock, quartzite and lava concluded that creep rate depends on the following variables;

1. "*Shear stress to shear strength ratio*
2. *Moisture content*
3. *Ratio of grain size to infilling thickness as well as the grain size distribution*
4. *Infill particle comminution due to discontinuity* "

According to Drescher and Handley (2003), creep itself is not a driving mechanism of failure, it is merely an outwardly measurable manifestation of

failure processes taking place in a stressed material. Thus, creep is a measure of the complex interaction between loading of a material, the material damage developing within by whatever mechanism, and the slow resulting reduction of the stress: strength ratio towards unit, where creep rates increase dramatically and failure occurs. Mechanistically, creep is a physical measure of a material's ability to:

- dissipate strain energy in material damage, and therefore is a rough measure of the potential violence of material failure
- withstand the current loading for a given amount of time

In analyzing different models to simulate rheological rockmass behaviour, (Malan, 1999) (page 140) concluded that "*hard rock time dependency is a direct consequence of the failure process and the solid rock behaves essentially elastically*" and is difficult to simulate. From his earlier experiments, Malan also concluded that "*if a rock specimen is loaded close to the uniaxial strength, creep rate and eventual creep failure occur faster than for a low stress. For a particular volume of rock under high stress, creep fracture will therefore form more rapidly, resulting in a faster loss of cohesion in the rock than for low stress*" This brings into perspective that under high stress and highly fractured rock, cohesion loss is faster and therefore rock failure risk is higher. From the analysis by Malan (1999) it can also be concluded that time-dependent closure data can be used to deduce important information on rock mass behaviour hence the importance of analyzing closure data to guide decision making on failure propagation.

2.2.4.1 Creep Stages

Creep has generally been divided into three major stages, primary, secondary and tertiary as shown in Figure 2.5.

Primary creep is characterized by rapid increase in strain in the early stages and eventually slows down leading to the onset of secondary creep stage. The secondary creep stage is characterized by a constant strain rate and with time

the strain rate will accelerate (tertiary creep) and eventual failure at the end of the tertiary creep stage. The tertiary stage is characterized by hyperbolic acceleration of the strain leading to failure.

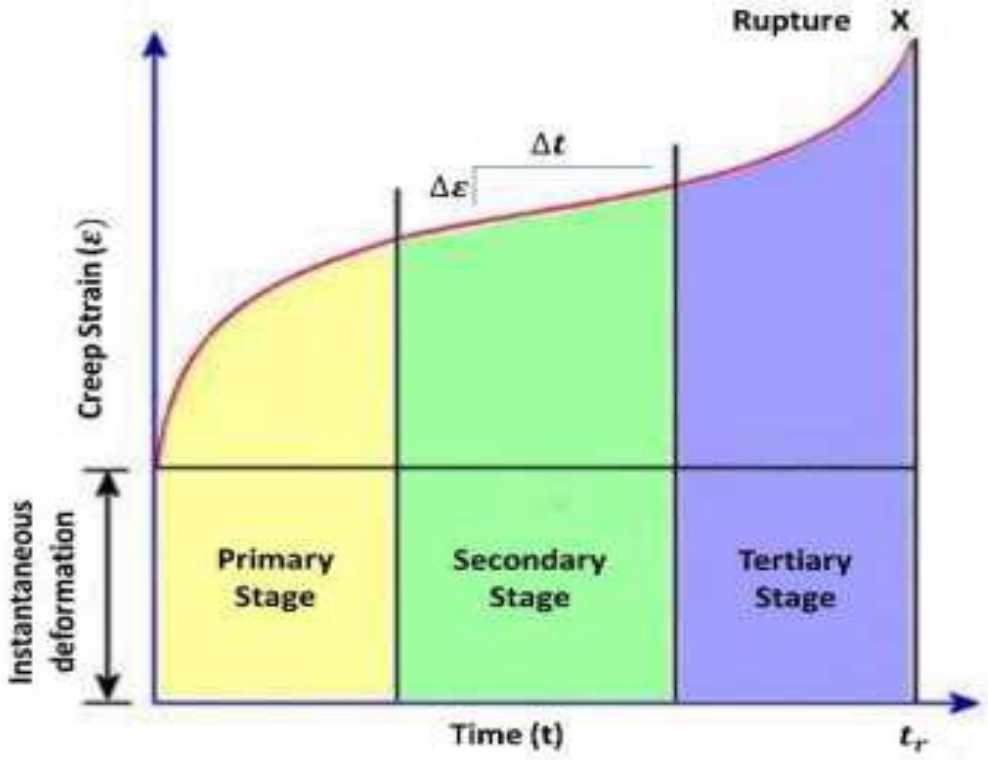

Figure 2.5 Idealised creep curve (Khoshboresh, 2013).

Ryder & Jager (2002) described 3 major theories governing time dependent behaviour of hard rock brittle rock masses namely

1. Empirical laws
2. Viscoelastic theory and
3. Elasto-viscoplastic theory

Empirical laws

The generalized empirical equation for creep is shown in equation 1.

$\varepsilon = \varepsilon_e + \varepsilon(t) + \mathrm{C}t + \varepsilon_{\mathrm{T}}(t)$ - 1

Where;

ε is total strain

ε_e is instantaneous elastic strain

$\varepsilon(t)$ is a function expressing the decelerating creep of the primary phase

Ct is the steady state creep component

$\varepsilon_T(t)$ is a function expressing the accelerating creep of the tertiary phase

The primary creep behaviour has been represented by various empirical laws which (Ryder & Jager, 2002) have expressed in a differential form as shown in equation 2.

$\dot{\varepsilon}(t) = Bt^{-m}$ (0<m<1) - 2

Where

B is a constant.

With different values of the constants and variables, equation 2 takes the form of the different laws that have already been established for example when m=1 it forms the creep law and when m=1/3 it takes the form of the power law of Andrade. However no correlation or link has previously been established linking the formulae to field and laboratory primary creep responses (Ryder & Jager, 2002).

The secondary stage of creep is represented by the widely used equation 3

$\dot{\varepsilon}_{ss} = A(\sigma_1-\sigma_3)^n e^{-Q/RT}$ - 3

Where;

A is a constant

$\dot{\varepsilon}_{ss}$ is the rate of steady state creep

σ_1 and σ_3 are the major and minor principal stresses respectively

R is the universal gas constant

T is the temperature in Kelvin

Q is the creep activation energy

The tertiary creep stage is attributed to increased micro-fracture and coalescence leading to macroscopic failure. However, more studies need to be directed

towards this stage as there is no equation that relates very well to observed behaviour has been established.

Visco-elastic theory

The theory largely hinges on two key modes of deformation which are elastic as exhibited in most failures as well as viscous behaviour. Studies have shown that this model largely depends on viscosity values of stress, temperature and chemical environment. Figure 2.6 shows some of the models that are used in laboratory and experimental analysis of creep (Ryder & Jager, 2002).

Elasto-Visco-plastic Theory

This is a plastic model where time rate rule is incorporated in the model. An Elasto- visco-plastic shows viscous behaviour only in the plastic region.

One major shortcoming of this type of model is that the model cannot simulate creep behaviour of discontinuities (Ryder & Jager, 2002).

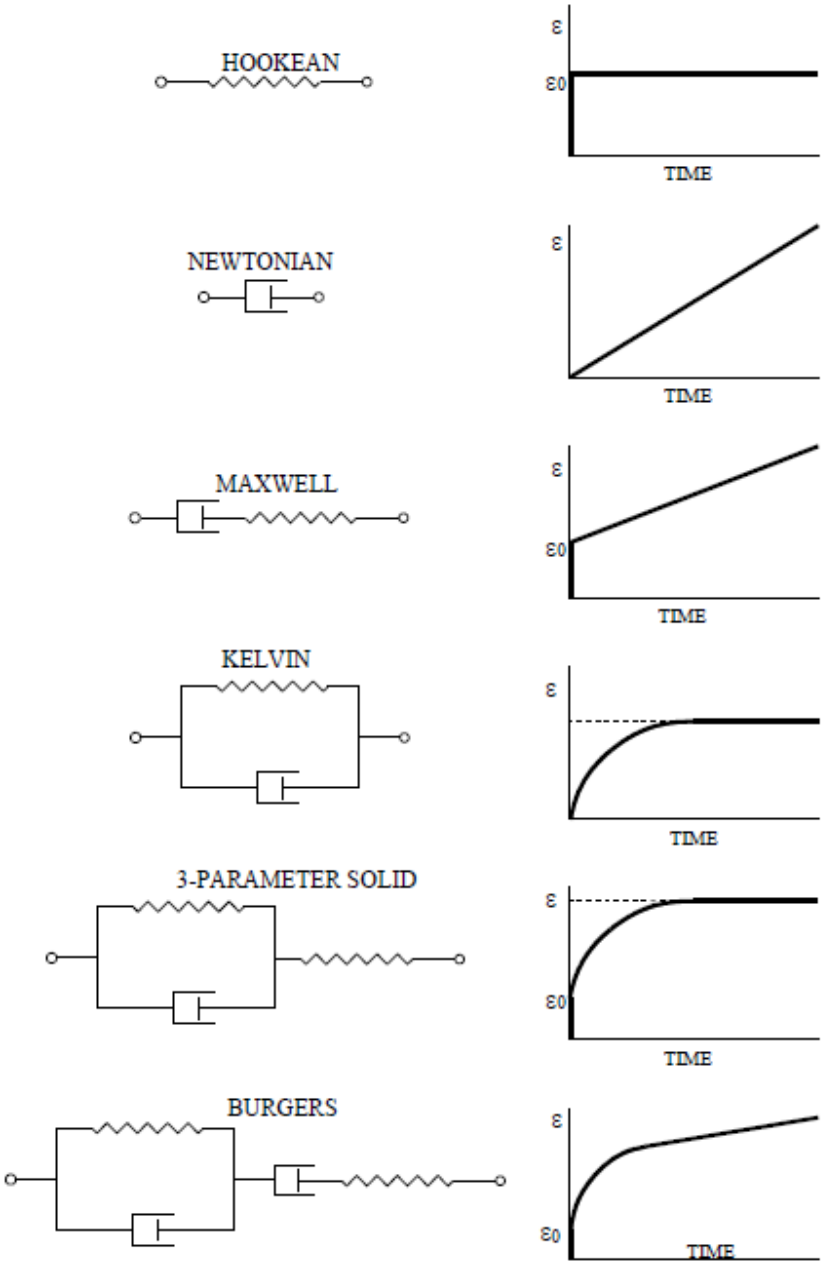

Figure 2.6 Commonly used viscoelastic models and their respective strain-time behaviour for a stepwise application of constant stress adapted from (Ryder & Jager, 2002)

Creep has been studied in detail and different mechanisms detailed as related to rockmass failure. In any system where there is rock mass failure, the contribution of creep cannot be overlooked particularly in underground excavations where

there is always an overburden load acting on the rockmass. In this research of a pillar system failure, understanding and investigating the effect of creep on failure can provide answers to the observed behaviour during rock mass/ pillar system failure in particular, the “stick slip” behaviour observed from closure monitoring results.

2.2.4.2 Pillar failure models and mechanisms

Brady & Brown (2005) (13.2 page 372) noted that “*for states of stress in a pillar less than the in situ rock mass strength, the pillar remains intact and responds elastically to the increased state of stress”.* Pillar response to mining induced stress is largely determined by four key variables

1. Rock material properties
2. Geological structures
3. Absolute and relative dimensions (geometry) of the pillar and
4. Nature of surface constraints applied on the pillar by the host rock, Brady & Brown (2005)

These key parameters therefore become important in understanding the behaviour of the pillar as well as propagation of failure once the pillars start to fail.

A number of studies have been carried out to analyse the different modes of pillar failure. Figures 2.7 to 2.11 show some of the common modes of pillar failure together with the description.

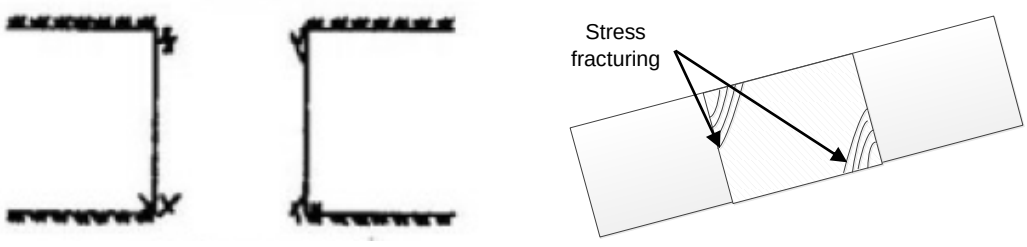

Figure 2.7 Pillar failure modes (Brady & Brown, 2005)

Localized shear failure; cracking at excavation abutments and starting with the 2 diagonally opposite sides if the pillar is inclined.

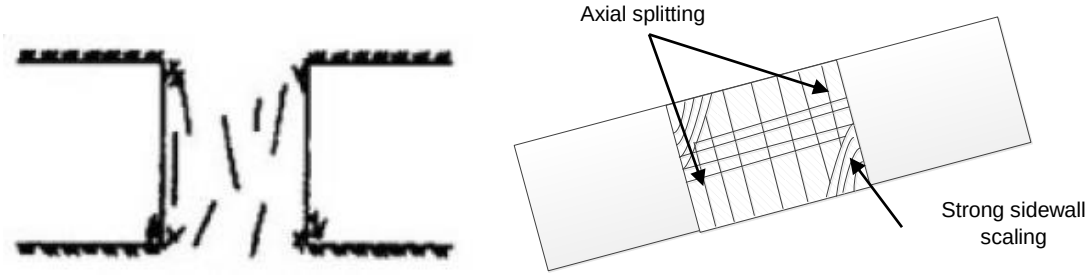

Figure 2.8 Partially failed surface spalling with isolated internal fractures (Brady & Brown, 2005)

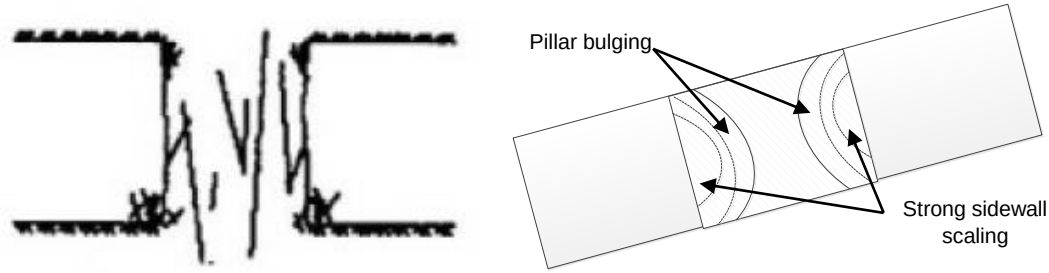

Figure 2.9 Partially failed contacts with extensive internal fractures (Brady & Brown, 2005)

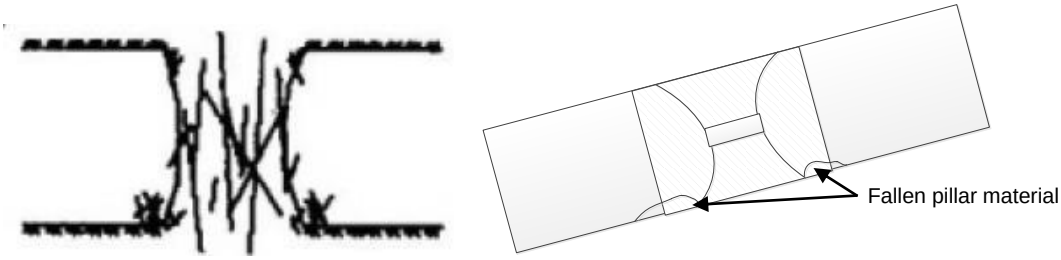

Figure 2.10 Failed pillar with internal shear fractures (Brady & Brown, 2005)

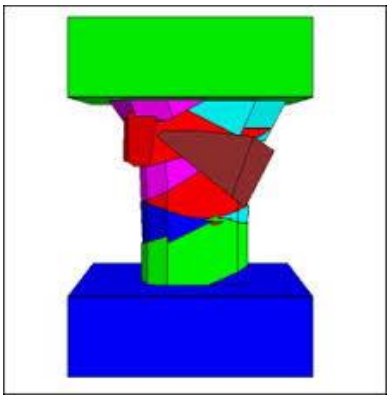

Figure 2.11 Effects of scaling, buckling and spalling on pillars (Pritchard and Hedley, 1993)

2.3 Conclusion

From the available literature studied, the key geotechnical parameters that can potentially influence the migration of failure are; geotechnical setting of the mine and its interaction within mining, design and implementation of the design and time dependent failure (creep). These variables have been studied in detail for a number of case studies as recorded and present technical differences which need to be explored further, in particular the behaviour and process after failure has initiated. The rockmass conditions are always found in situ but the design is made and therefore can be adjusted to suit the conditions. However, due to limited information at design stage, assumptions are made and built into the designs. The competence of the design depends on the accuracy of the input parameters. In case of omissions the design may result in the failure of a pillar system. Natural processes and events like creep eventually contribute to pillar system failure. The case studies presented have also shown that once initiated, it is difficult to halt failure of a pillar system as the loads continue to be transferred to the remaining stable pillars (cascading pillar failure). The halting of a failure, impact minimisation or successful evacuation can only be implemented if the behaviour of failure propagation is well studied, understood and can be predicted. Researching on these key variables is therefore important in order to understand the failure propagation. The upside potential of the ability to predict behaviour of a failing system is, reduced man exposure to risk and the increase of the available production time to a point where it really becomes necessary to evacuate, (not too early or too late). Research into failure propagation and behaviour could therefore unlock such potential.

3 GEOTECHNICAL SETTING AND CASE STUDY MONITORING

3.1 Introduction

This chapter presents the case study geotechnical conditions and setting in relation to the key parameters analysed in chapter 2. The key parameters are further split into geological setting, major geological structures and how they relate to the propagation of failure in the case study of Bimha Mine. This chapter further looks at the geotechnical design considerations of the case study, brief history of the actual mining and finally introduces the monitoring system implemented to assess time related failure trends and failure propagation.

3.2 Geology of the Great Dyke

The Great Dyke is a layered mafic-ultramafic complex that transects the Zimbabwean Achaean Craton in a NNE-trending direction as shown in Figure 3.1. The Dyke is highly elongate, slightly sinuous, 550km long, with a maximum width of 12 km. It developed as a series of initially discrete magma chamber compartments, which joined up as the chambers filled (Wilson & Prendergast, 2001). The emplacement of the dyke is estimated at 2575 ± 0.7 Ma (Wilson & Prendergast, 2001).

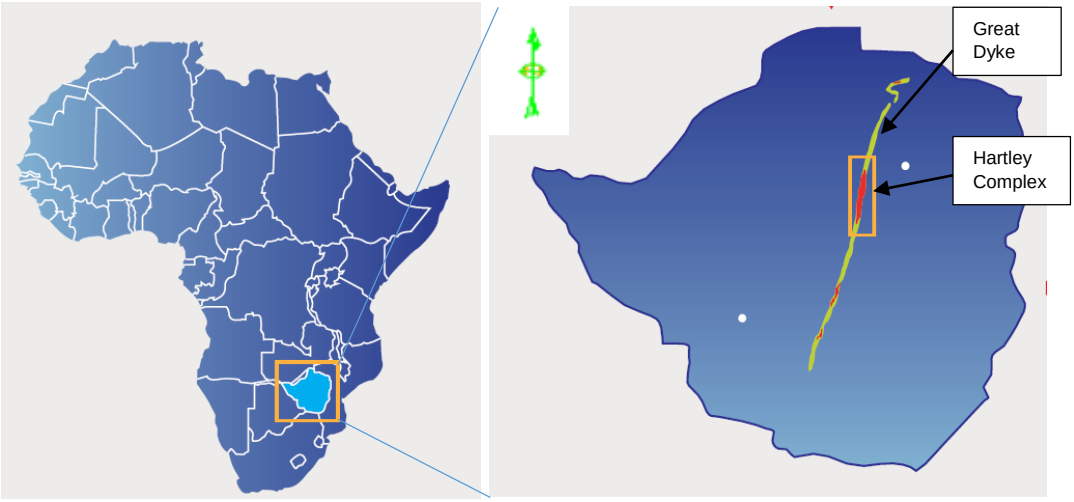

Figure 3.1 Location of the Great Dyke on the Zimbabwean craton (Zimplats, 2017).

Stratigraphically, the Dyke is divided into two major successions, a lower ultramafic sequence dominated from the base upwards by cyclic repetitions of dunite, harzburgite and bronzitite (pyroxenite), and an upper mafic sequence consisting mainly of gabbro and gabbronorite as shown in Figures 3.2 and 3.3. Much of the mafic sequence has been removed by erosion over the time from emplacement about 2575 ± 0.7 Ma (Wilson & Prendergast, 2001).

The Main Sulphide Zone (MSZ) covered in this case study is preserved in a continuous zone stretching 90km from Lake Manyame to Ngezi Dam, known as the Hartley Complex. Typically, the MSZ consists of 4-8m wide zone below the websterite and bronzitite contact with enrichment in base metal suphides and platinum group metals. The plane immediately below the Peak platinum position is used as a reference plane, the Base of Main Sulphide Zone (BMSZ). The Hartley Complex straddles two sub-chambers, namely Darwendale and Sebakwe. Ngezi Mines lie towards the southern tip of the Sebakwe Sub-chamber (Zimplats, 2017). Figure 3.2 shows the generalized geological succession with the layering that forms the Great Dyke.

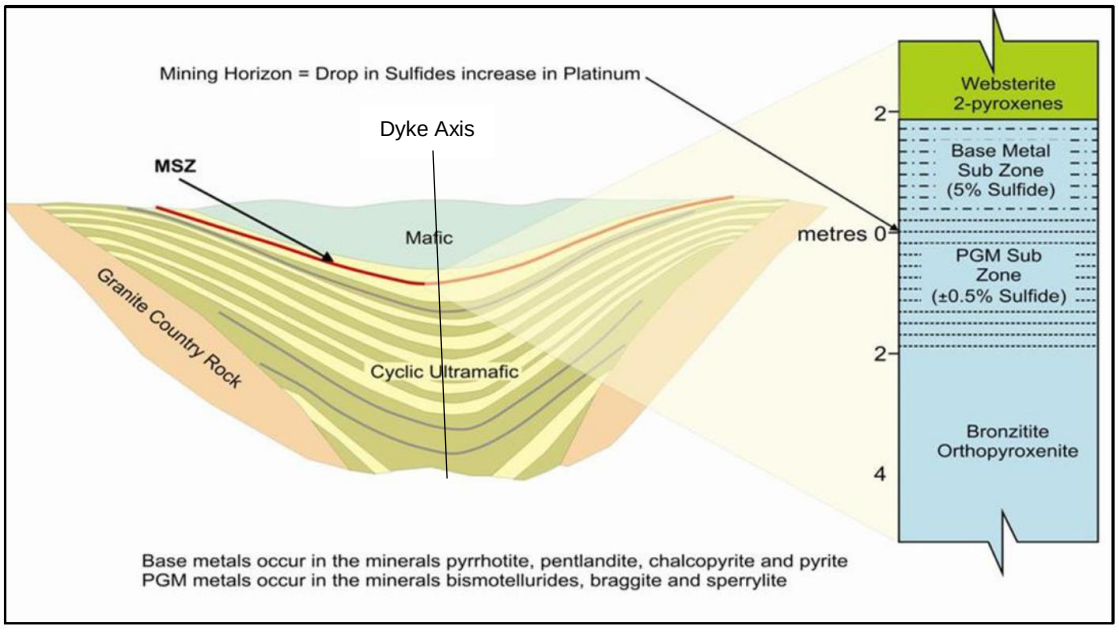

Figure 3.2 Generalised geological succession (Walls & Mpunzi, 2017)

The MSZ which is the mineralised platinum rich horizon is hosted by the bronzitite. The reef dip is generally steep in the flanks flattening towards the dyke axis where it is flat as shown in Figure 3.2. The detailed geological succession showing the different rock types forming the Great Dyke are shown in Figure 3.3.

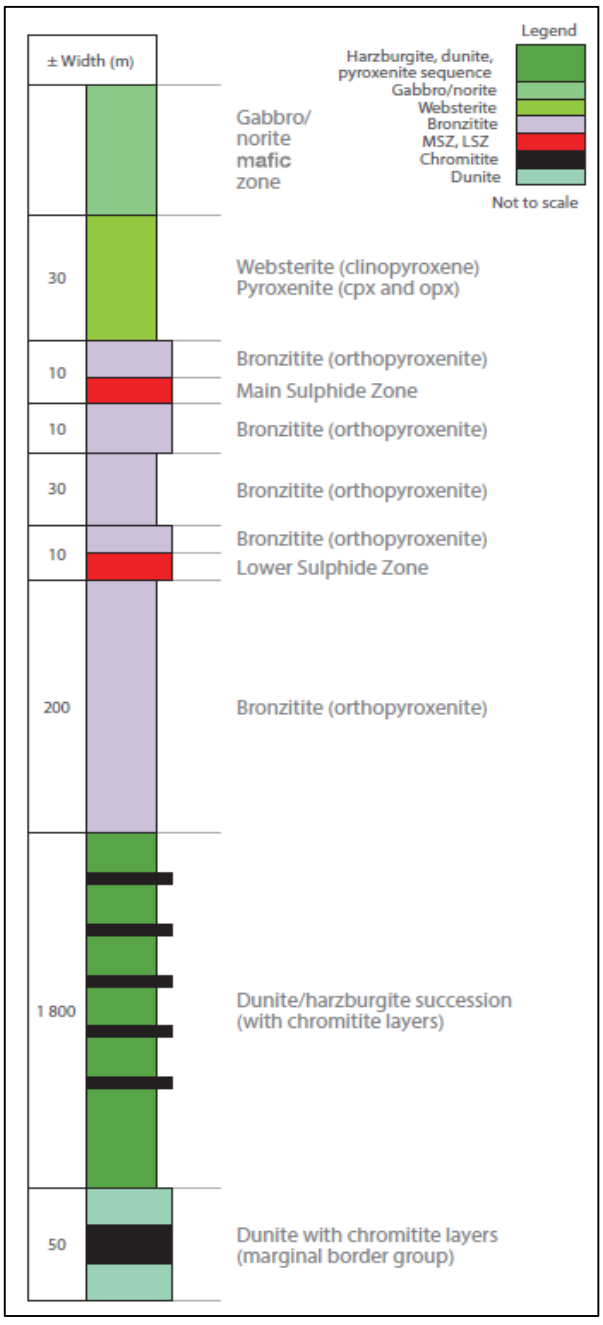

Figure 3.3 Detailed geological succession of the Great Dyke (Zimplats, 2017)

3.3 Structural Geology of the Great Dyke.

3.3.1 Regional structural geology history

The post intrusion structural footprint of the Great dyke was analysed in relation to the overall history of the Zimbabwean craton as well as local structures. From analysis done by Blenkinsop (2014) six phases could be observed and interpreted from the structures present in the Ngezi area. These phases are shown in Figure 3.4. The first conjugate set is perpendicular and parallel to the Great Dyke margins and formed as cooling joints and dyke sagging during the placement of the dyke. These were then intruded by granitic magmas (stage 2) and has been confirmed by the orthogonal granitic dykes observed underground typically shown in Figure 3.5. Stage 3 was the formation of the NW and NE strike slip faults with dextral sinistral movement respectively. Most of the major fault systems in Ngezi area are NW trending though less frequent. The next phase was driven by the NS thrust with shortening of NW and NE faults in response to the Limpopo orogenic events. The EW shortening is associated with the Magondi orogeny and further reactivation in the opposite sense is associated with the Zambezi orogeny (Blenkinsop, 2014).

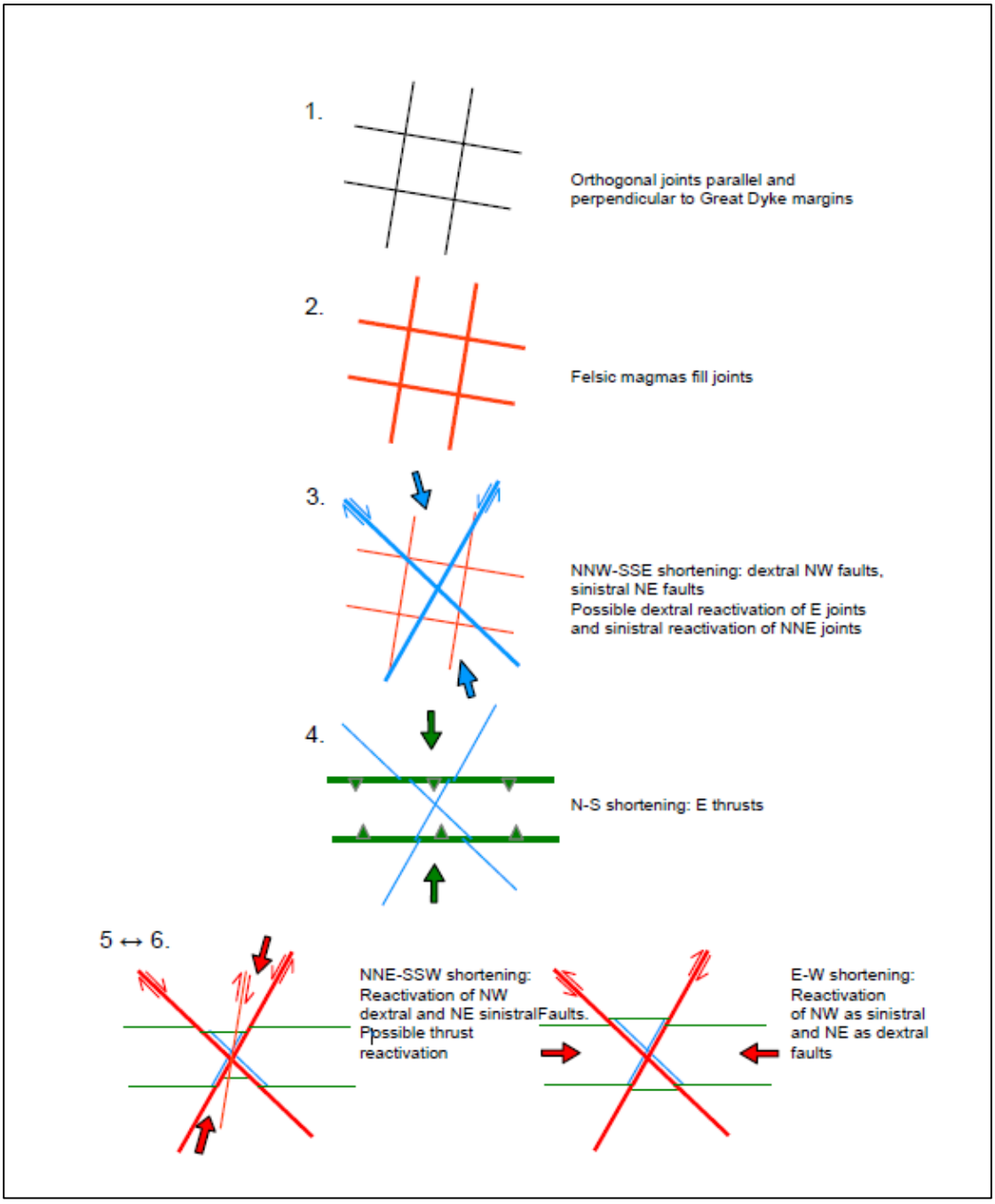

Figure 3.4 Post Great Dyke tectonic history in Ngezi area. (Blenkinsop, 2014)

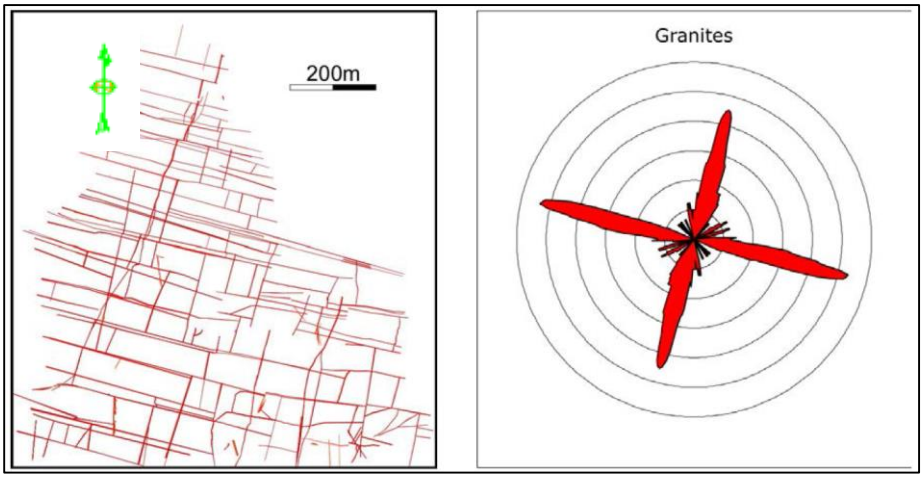

Figure 3.5 Typical orthogonal network of granite dykes as mapped in Bimha north. With the equal area rose diagram of the strikes. (Blenkinsop, 2014)

Figure 3.6 shows the different mobile belts on the generalised stratigraphy of Southern Africa as this is important in understanding the regional scale tectonic history and how it relates to the geological structure of the Great Dyke and in particular the case study area.

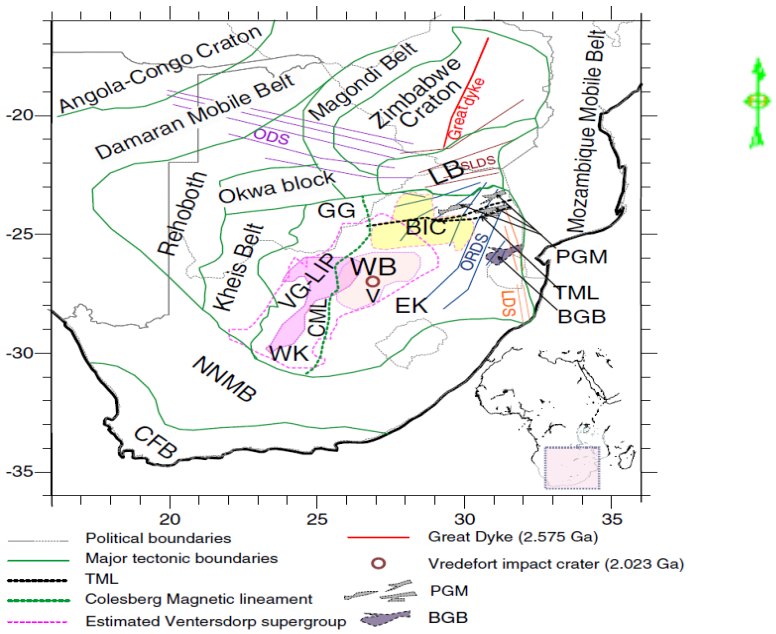

Figure 3.6 General stratigraphy of Southern Africa (Youssof et al, 2013)

3.3.2 Local geology of the case study area

Figure 3.7 shows the structural model of the Ngezi area. The NE-SW and NW-SE conjugate set is the most common of the major fault systems in Ngezi (Zimplats Internal Report, (Kock S.), 2015). The orientation of these faults corroborate well with formation shown in the stage 3 explained by Blenkinsop (2015) in Figure 3.4.

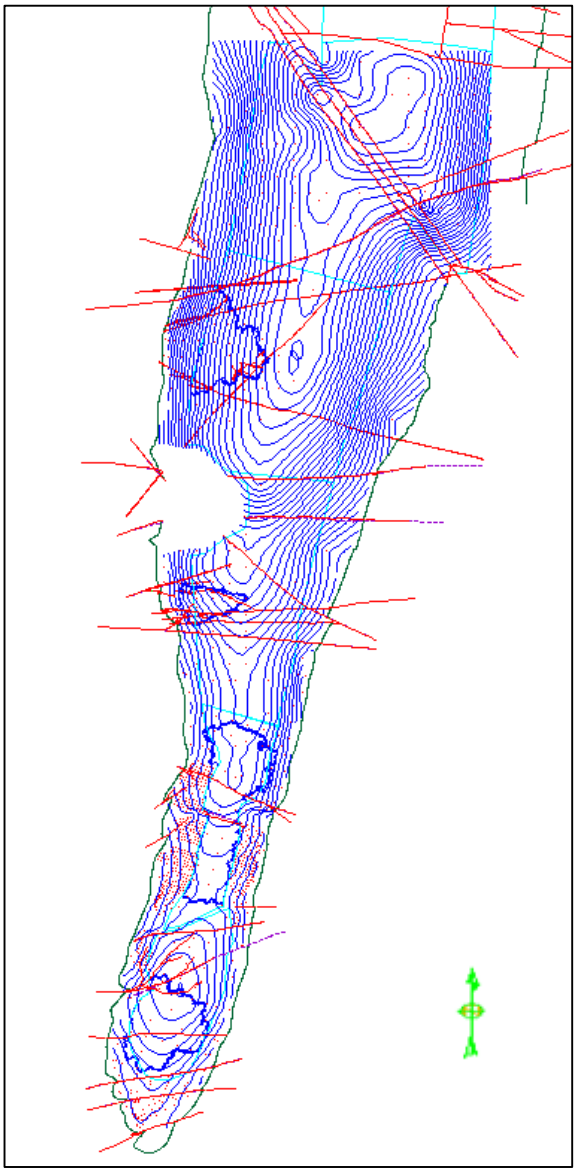

Figure 3.7 Ngezi structural model (Zimplats Internal Report (Kock S.), 2015)

3.3.1.1 Joint analysis

Joint analysis was done in order to establish if there are any preferential trends. The analysis done using DIPS showed that generally the most common conjugate set is the NE-SW and NW-SE and in particular the subvertical joints. This is also consistent with the analysis done by Blenkinsop in 2014, (see appendix 1). Table 3.1 summarises the analysis of the jointing as established using DIPS. These joints were taken from Bimha Mine before the collapse.

Table 3.1 Distribution of the joints based on the joint analysis

			JOINT DIP			Strike direction of High (60°-90°)	Collapse direction	Diff.
Area of the mine	**Site**	**Gen Direction**	**Low (0°-30°) %**	**Medium (30°-60°) %**	**High (60°-90°) %**			
Upper north	5N	NW-SE	12	12	76	120	40	80
Mid north	26N	NW-SE & NE-SW	16	16	68	100	40	60
Centre North	30N	NE-SW	3	38	59	45	40	5
Centre south	31S	NNE-WSW	10	40	50	100	40	60
Mid-south	20-30S	NE-SW	20	23	57	10	40	-30
South of centre south	44S	WNW-ESE & NE-SW	7	14	79	100	40	60
Bottom	70	NW-SE	20	65	15	165	40	125

From Table 3.1, the collapse direction is generally within 30-60 degrees of the jointing direction.

Further analysis was done to establish if there were any variations between north and south based on the geotechnical logging done during the time of mining the excavations. Table 3.2 summarises the findings and it is evident that the southern section, in comparison to the north, generally has worse ground conditions largely driven by higher SRF and joint alteration.

The south side's weaker ground conditions show a positive correlation to joint alteration and joint water. This results from the negative impact of moisture ingress and oxidation on jointing strength. In comparison to the north, the south

section is generally shallower as the great dyke plunges to the north. The existence of more seasonal surface streams on the south in comparison to the north further exacerbate the oxidation situation in the south. The preferred collapse migration direction is further corroborated by the DIPS analysis where the propagation tends to correlate positively to the direction at 45° to the 60-90 degree joints. The 60-90 degree joints are near vertical which bring moisture from surface thus further weakening the rockmass through weathering and oxidation.

Table 3.2 Rock mass quality parameters (Averages)

	Rock Quality Designation RQD	Joint Set number Jn	Joint Roughness Jr	Joint Alteration Ja	Joint water Jw	Stress reduction factor SRF	Rock Quality rating Q
North	100	11.8	2.19	2.75	1.00	2.48	2.72
South	100	11.9	2.16	2.80	0.97	2.80	2.25

3.3.3 Mutambara shear

The Mutambara Shear occurs in Bimha Mine as a sub horizontal mylonitic shear structure dipping to the east and undulating in nature both on strike and on dip and very friable in some areas. The thickness varies from less than a millimetre in areas where it appears as tight joint to 1.0m. The fill has picrolite, chlorite and serpentine in some areas all of which are closely associated with mylonite. Geotechnical logging of cores done concluded that the sub-horizontal thrust shear was very difficult to delineate as a continuous structure as it varies substantially over short distances. Cases where the sheared material varied from thick to thin, granular to smooth mylonite to slicken sided serpentine pinched joint like feature repeated once or multiple location in one hole further proved the complexity in variability of the structure (Zimplats Internal Report (SRK Cosulting), 2016b).

Figures 3.8 and 3.9 shows the nature, position and thickness (respectively) of the shear with respect to mining horizon. The variability as well as the randomness both in terms of position and thickness as shown in the Figures 3.8 and 3.9 make the projection of its behaviour very difficult and complex. In adjacent blocks, the shear can be mapped in the hangingwall in one block and in the footwall in the next block with no visible transition from hangingwall to the footwall making the interpretation complex.

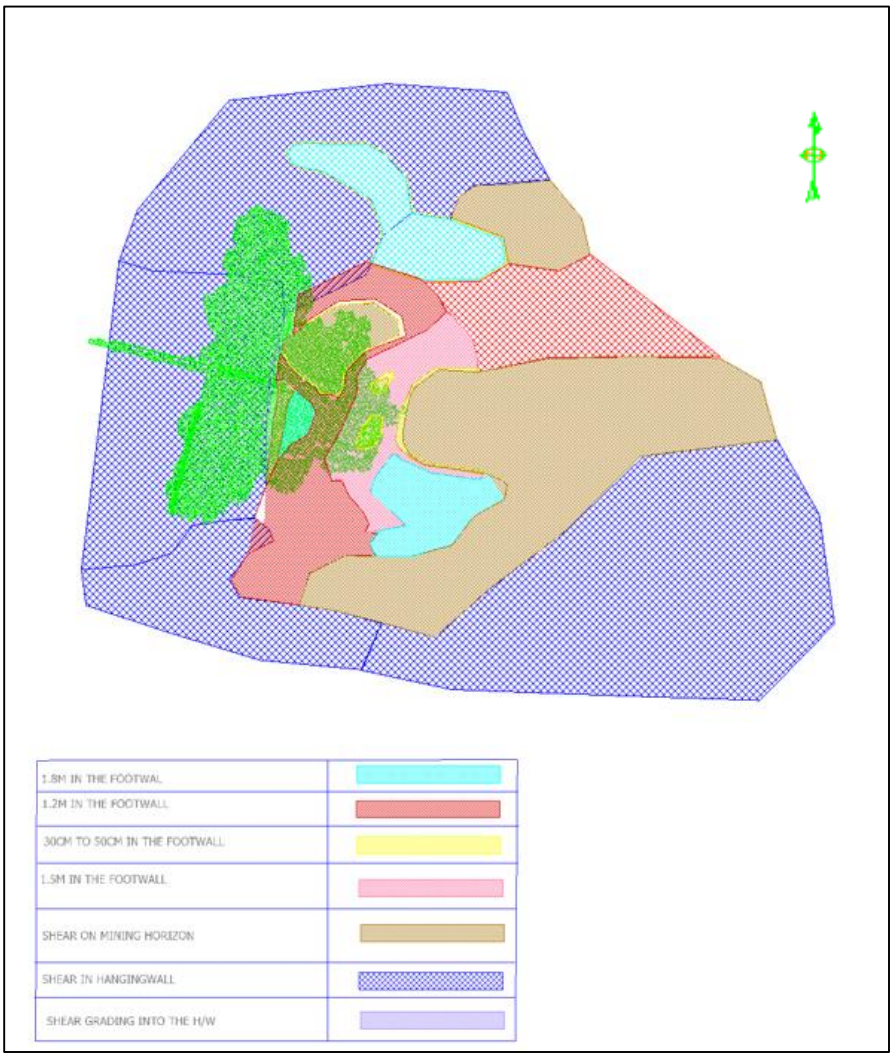

Figure 3.8 Position of the Mutambara shear with respect to the mining horizon (Zimplats Internal report, 2014)

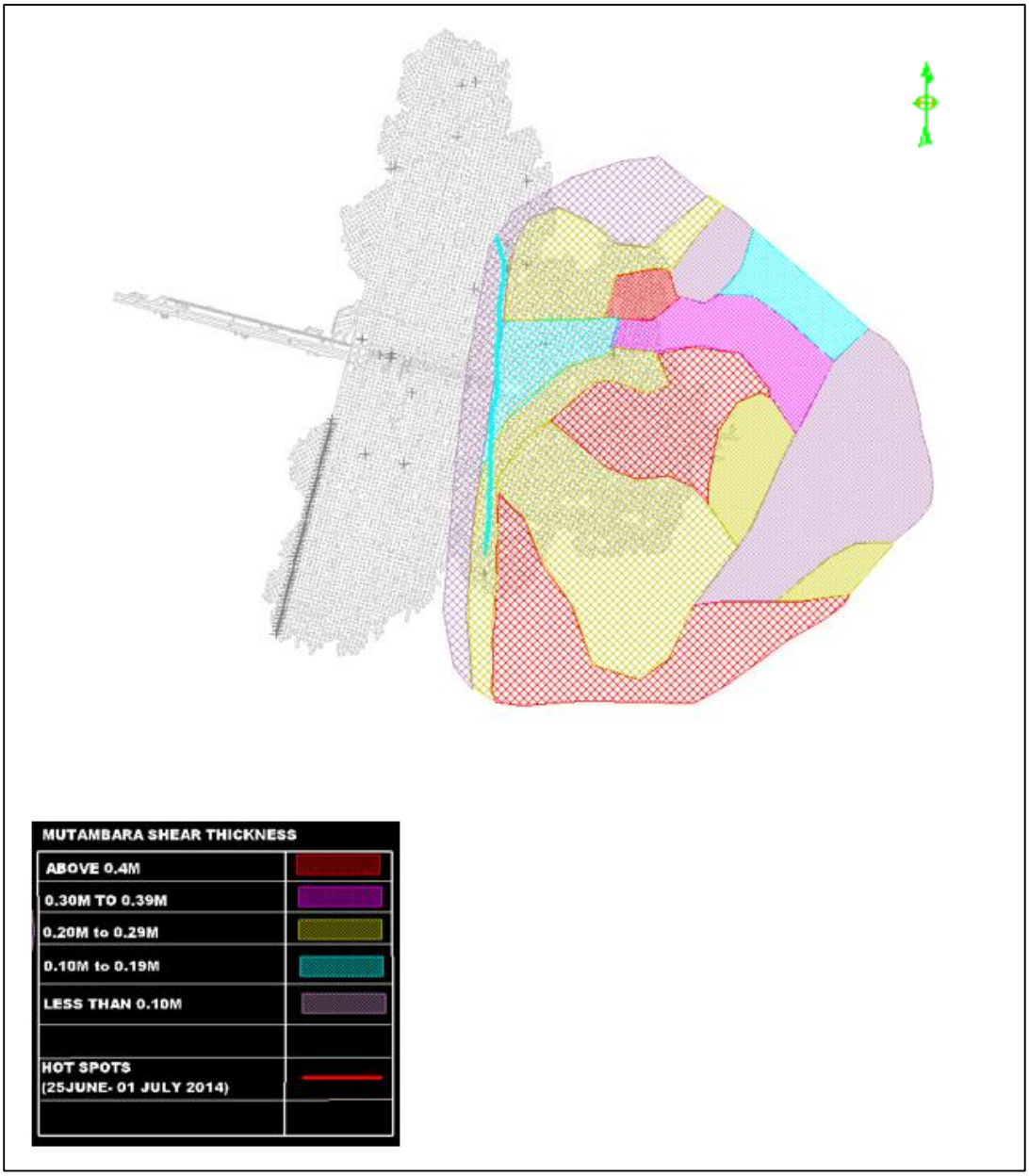

Figure 3.9 Thickness of the Mutambara shear (Zimplats Internal report, 2014)

3.3.1.2 Geotechnical properties of the shear

The geotechnical behaviour of the rock mass to the Mutambara Shear is generally in response to the presence and nature of its occurrence. Where the structure is thicker, the risk of movement along the structure is higher due to the reduction of the friction angle. The presence of mylonite, picrolite, chlorite and serpentine with well-known response to presence of moisture or water (making

them slippery and hence prone to movement) increase the risk of slippage along any plane where they are found. Any structures (e.g. joints) that interact with such structures, depending on their nature of occurrence, will increase the chances of blocks falling off. Areas with a weak layer in the footwall are susceptible to footwall heaving as the material is squeezed out in between pillars “toothpaste effect”. This results in footwall heaving as witnessed in the bottom section of the mine where the shear was in the footwall and thicker.

3.4 Rock Properties

Platinum mining on the Great Dyke is from the MSZ which is hosted by the Bronzitite, (Orthopyroxenite). Bronzitite is considered a fairly competent hard rock with an average UCS above 200MPa. Intact rock testing programs conducted for rock properties are summarized in Table 3.3 with the full results in appendix 2. Please note that failures along planes/joints were excluded from mean and standard deviation calculations.

Table 3.3 Key intact rock parameters (Bronzitite)

Parameter	**Mean**	**Standard deviation**
Intact Rock		
UCS (MPa)	220	22
Poisson’s ratio	0.27	0.05
Modulus of elasticity (GPa)	147	10
Base friction angle (°)	37	3
Joints		
Friction angle (°)	26	5

In order to understand the Mutambara Shear itself, tests were done to establish the shear strength and is was found to be very weak with an average shear strength of 18kPa (Zimplats internal report, (Jacobsz), 2015). With such low shear strengths, the potential of movement along the shear will be very high.

3.5 Mine History

The mine design was done by consultants as a typical room and pillar mine with the Hedley and Grant (1972) power formula used to determine the pillar strength. The bulk strength of the pillars was obtained by down-rating the intact rock strength by 75% (Zimplats Internal Report (SRK Consulting), 2006). The design calculations gave a minimum pillar size of 4x4m at 150m depth below surface up to 7x5m at 300m depth below surface (increasing with depth).Table 3.4 shows the typical values of the pillar sizes with depth based on the Hedley and Grant power formula. It is important to note that the pillar design assumptions did not take into account the existence of the Mutambara shear as it had not been picked as a continuous geological structure from the exploration mapping and geotechnical logging. The development of the mine started first with the box cut, in January 2007, reaching ore contact in May 2008 and attaining design production of two million tonnes per annum in May 2011. In the same year (2011) a shear, which was initially identified as very poor ground conditions in the north section of the mine was, first intersected. The different patches of very poor ground conditions were later joined together, forming what is now known as the Mutambara Shear. The very poor ground conditions were managed according to the existing procedures, blocking out larger pillars and applying shotcrete where necessary.

Mining progressed and in 2013 in the lower southern section of the mine, footwall heaving was observed. Investigations of the footwall heaving revealed the existence of the shear in the footwall with varying thickness and position. The condition of pillars continued to deteriorate with footwall heaving spreading to the north, movement was observed along joints in jointed pillars and blocks started falling off pillars. The lower section of the mine starting on the southern side eventually collapsed in July 2014, which covered an area of approximately 38 hectares. Figure 3.10 shows the layout of the mine, the epicenter of the failure and the propagation of the failure front. Monitoring of the old footprint continued in the upper, safe and stable sections of the mine. A new mine design was put

in place to redevelop the mine leaving a boundary pillar between the old and new mines.

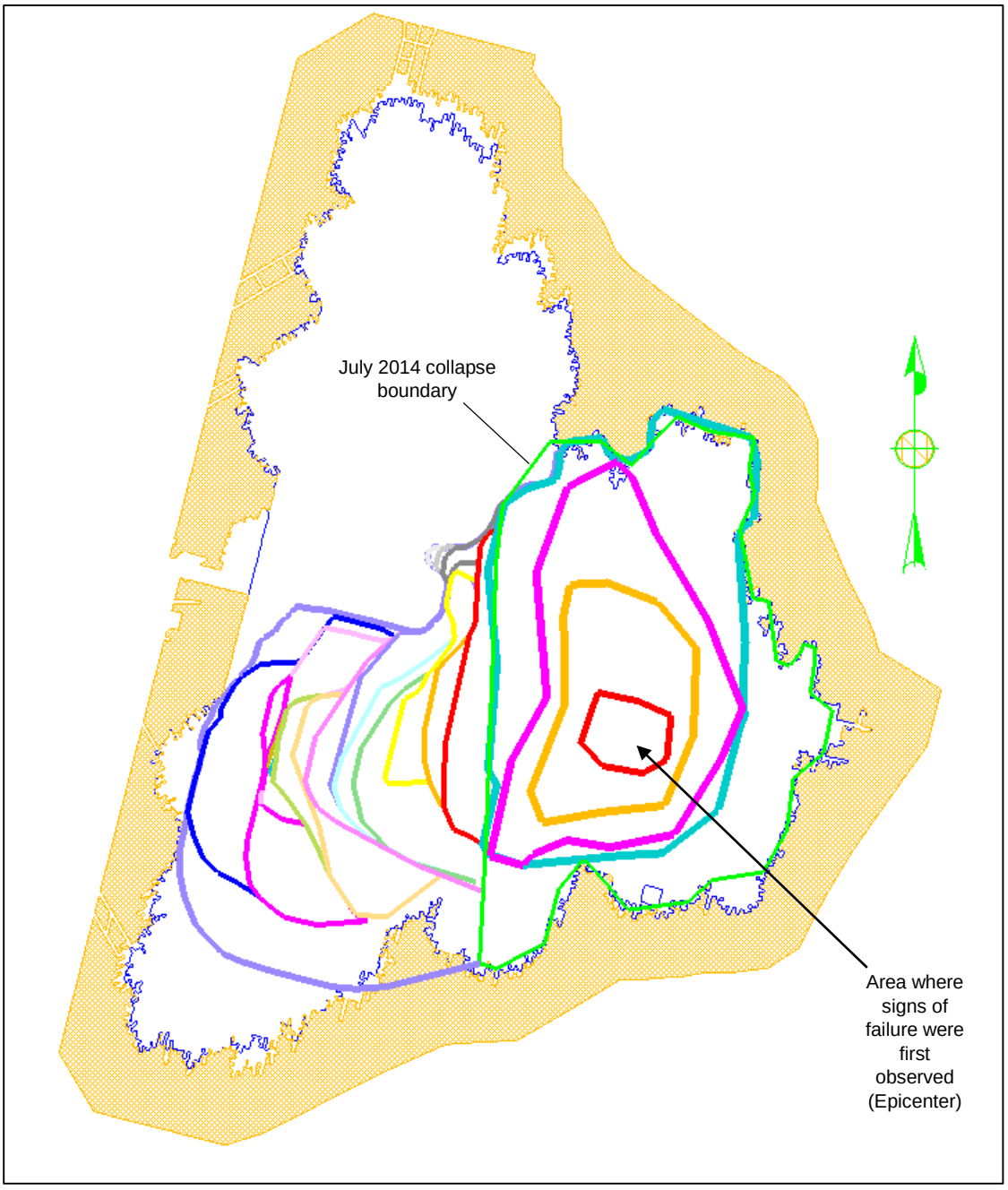

Figure 3.10 Bimha Mine plan showing failure and progression

Table 3.4 In-stope pillar design parameters (Zimplats Internal Report, (2006)

Average depth (m)	Average virgin stress (MPa)	Pillar dimensions			Effective pillar width (m)	Areal extraction (in panel) (%)	Pillar strength (MPa)	Pillar Stress (MPa)	Safety factor
		Pillar length (m)	Pillar width (m)	Height (m)					
150	4.8	4	4	2.5	4	86.8	60.3	36.1	1.67
160	5.1	4	4	2.5	4	86.8	60.3	33.6	1.57
170	5.4	5	4	2.5	4.44	84.8	63.6	35.7	1.78
180	5.7	5	4	2.5	4.44	84.8	63.6	37.8	1.68
190	6	5	4	2.5	4.44	84.8	63.6	39.9	1.6
200	6.4	5	5	2.5	5	82.6	67.4	36.6	1.84
210	6.7	5	5	2.5	5	82.6	67.4	38.5	1.76
220	7	5	5	2.5	5	82.6	67.4	40.3	1.68
230	7.3	5	5	2.5	5	82.6	67.4	42.1	1.6
240	7.6	6	5	2.5	5.45	80.8	70.4	39.7	1.78
250	7.9	6	5	2.5	5.45	80.8	70.4	41.3	1.71
260	8.3	6	5	2.5	5.45	80.8	70.4	43	1.64
270	8.6	7	5	2.5	5.83	79.2	72.8	41.2	1.77
280	8.9	7	5	2.5	5.83	79.2	72.8	42.7	1.71
290	9.2	7	5	2.5	5.83	79.2	72.8	44.2	1.65
300	9.5	7	5	2.5	5.83	79.2	72.8	45.8	1.59

3.6 Rockmass Response to Mining and the Shear

3.6.1 Monitoring results

When the lower section of Bimha mine collapsed, a team was assigned to monitor the ground conditions in the old footprint. This was done to ensure that any migration of the pillar failure was detected early, long before it could affect the new mine development. The monitoring crew was scheduled to enter the old workings daily and provide reports on the conditions. The key parameters that were (and are still) monitored include progression of the collapse zone/front, progression of the stress zone/front, stope closure levels, seismic activity (in whatever form). Surface monitoring included surface subsidence and rainfall.

3.6.2 Design of the monitoring system

The key parameters for monitoring were driven by the need to establish the stress zone and the failure zone. Understanding the migration of these key parameters was important in order to inform the decision for evacuation if need arose. In this analysis, the following key stages are defined in order to guide the analysis in terms of consistency.

Stage 1 – Stress zone – This is the area where signs of stress start to show on the mining horizon e.g. stress fracturing on the pillars, cracking on the pillars,

signs of movement along existing joints, footwall heaving and closure. Typical examples are shown in Figure 3.11a and b.

Stage 2 – Intermediate – These are areas where blocks start to fall off the sidewalls / pillars with the hangingwall remaining intact Figure 3.11c.

Stage 3 – Collapse – This is defined in areas where blocks have fallen from the hangingwall and pillars Figure 3.11d.



(a) (b)

(c) (d)

Figure 3.11 Stages of rock mass failure (a) Stress fracturing, (b) Footwall heaving, (c) Intermediate stage, (d) Hangingwall collapse stage

In order to clearly define and pick the above stages, monitoring systems were put in place starting with visual identification of the cracks in the sidewalls to an online closure monitoring system. The online monitoring system was installed in 2016 to reduce men exposure to high risk / collapsing environment.

3.6.3 Stress zone monitoring

Monitoring was done on two key variables which are stress fracturing (visual) and stress monitoring (using stress meters). Initial monitoring from 2014 was done with people going towards the stress front on a daily basis and defining the front based on the visual inspection and status of the pillars ahead of the stress front. The data from visual observations was plotted on a plan, showing the boundary of each variable (stress or collapse). The individual boundaries (stress or collapse) were then monitored to track the rate of migration in the different directions. Once new pillars showing signs of fracturing or failure were identified, the boundary was then moved to the new position.

Stress meters were installed in August 2016 to monitor the stress change in the boundary pillar separating the old and the new footprint. A program has been put in place to install more stress meters in the boundary pillar in order to record the stress change around the old footprint as well as the stress gradient within the pillar. Figure 3.12 shows a picture of the typical stress meter and the readout device. While the measurements were not intended for quantifying the virgin in-situ stress levels, the stress meters provide a measure of the change in stress levels in the rockmass as the time progresses.

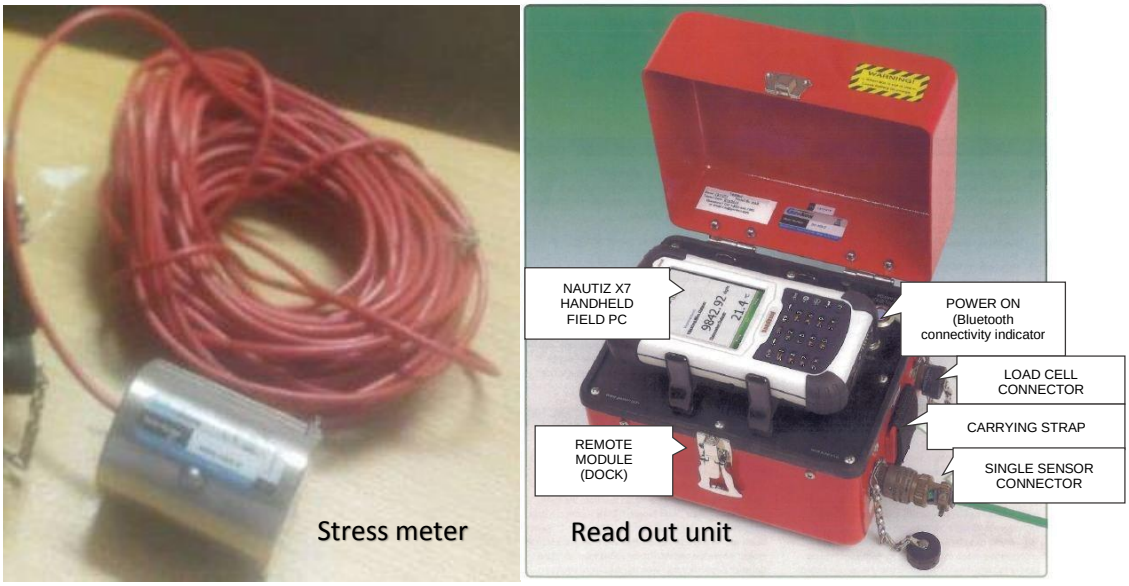

Figure 3.12 Stress meter and read out unit

3.6.4 Closure monitoring

Closure can be defined as the amount by which the cross-sectional dimension of an excavation is reduced by the combined effect of convergence and additional in-elastic movements, such as bed separation (Implats Rock Engineering, 2003). The closure levels in Bimha Mine were initially measured by the use of standalone closure loggers, supplemented by the recent commissioning of a system of ultra-sensitive closure sensors with online reporting. Figure 3.13 shows the position of an installed closure logger and closure sensor. The positioning of the meters was based on a regular grid with increased density around the active stress boundary. The technicians were trained by the equipment manufacturer on installation, reading, maintenance and calibration of the closure meters in order to achieve accurate and consistent readings.



(a) (b)

Figure 3.13 Installed closure measuring devices (a) Closure logger, (b) Online closure sensor

3.6.5 Seismic monitoring

The level and rate of seismic activity (both pillar bursts and overburden tensile failure) was initially monitored by a set of four strategically-located Small Ground Movement Instruments (SGMI) manufactured by CSIR. The data recorded by these single-seismometer instruments was downloaded weekly, for analysis of recorded events within each unit's sensitive radius of 500m. A new network of tri-axial seismometers was commissioned at Ngezi in March 2017 and is now fully operational. While seismic activity is not normally associated with shallow mining operations, it is important to monitor particularly in a case like this where some events have been recorded. This will ensure conclusive location of the source and implementation of strategies to manage such.

3.6.6 Surface monitoring

A number of variables were monitored on surface for correlation with underground rock mass behaviour. These included rainfall levels, development and extension of surface cracks and measurement of subsidence using survey beacons. The plan in Figure 3.14 shows the location of the different monitoring stations currently being used in this program.

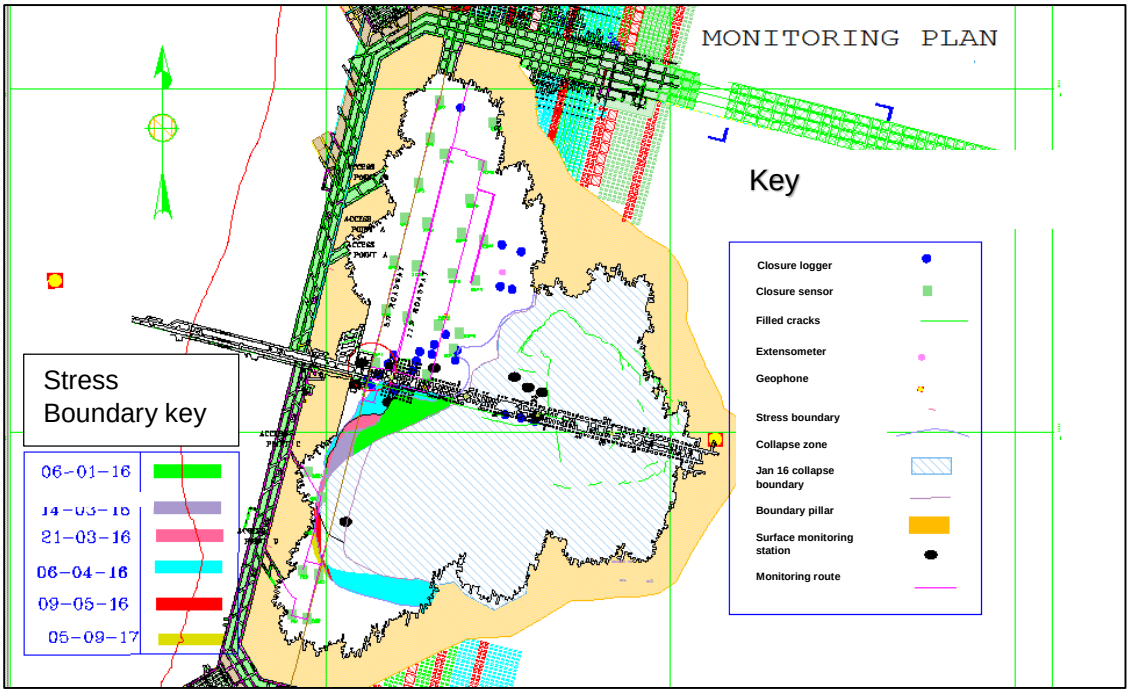

Figure 3.14 Bimha monitoring stations

3.7 Conclusions

The analysis of the geotechnical setting in relation to the failure indicate to a relation to failure propagation which relation need to be thoroughly scrutinised to provide solutions to why the failure propagated in a particular direction. Design considerations, in particular key parameters like shears that had not been taken into account at design stage, have a high potential to influence the propagation of failure. These relations are therefore further analysed in relation to the results of the monitoring sytem and failure propagation. Earlier presentations of case histories in literature review pointed to an influence of most of the parameters and variables presented in this chapter. An in depth analysis of the correlation of the different variables to the failure migration is therefore necessary to provide clarity on the noted behaviour and trends under the conditions and environment discussed in this chapter.

4 Results analysis

4.1 Introduction

This chapter looks at the data collected and its analysis in relation to the migration of the failure front. Data was collected to establish the geological and geotechnical conditions and behaviour of the rockmass. The data collected included a total of 6 400 pillars covering 100 Hectares with focus on different variables including pillar shape, position, and ground conditions. The ground conditions cover regional geology and local structures as well as major geological structures – in particular the Mutambara shear. Recordings of the ground monitoring system implemented are also analysed in detail and correlated with failure front migration.

4.2 Macro-Scale Analysis

4.2.1 Tectonic activity

This section analyses the stress and collapse fronts (failure front) in relation to the tectonic history of the great dyke and the Zimbabwean craton. The analysis is meant to establish any correlations that can explain the preferred direction of migration as observed underground. The general trend of the migration after the July 2014 collapse was from northeast to southwest. The initial direction of migration in July 2014 from the epicenter of collapse was towards the northwest. Reading this in the context of the geotechnical conditions explained in chapter 3, in particular the formation of the major faults on the great dyke, is important. Blenkinsop (2014), explained the formation of NE and NW strike slip fault systems with the NW faults being more prevalent. Shortening of these faults was due to the orogenic activity in the Limpopo mobile belt. The formation of the NE and NW faults points to a creation of a lines of weakness in the NE and NW directions. Figure 4.1 shows the correlation of the dyke with respect to the orogenic events. The same direction is observed in the direction of migration of the stress front and could potentially be correlated.

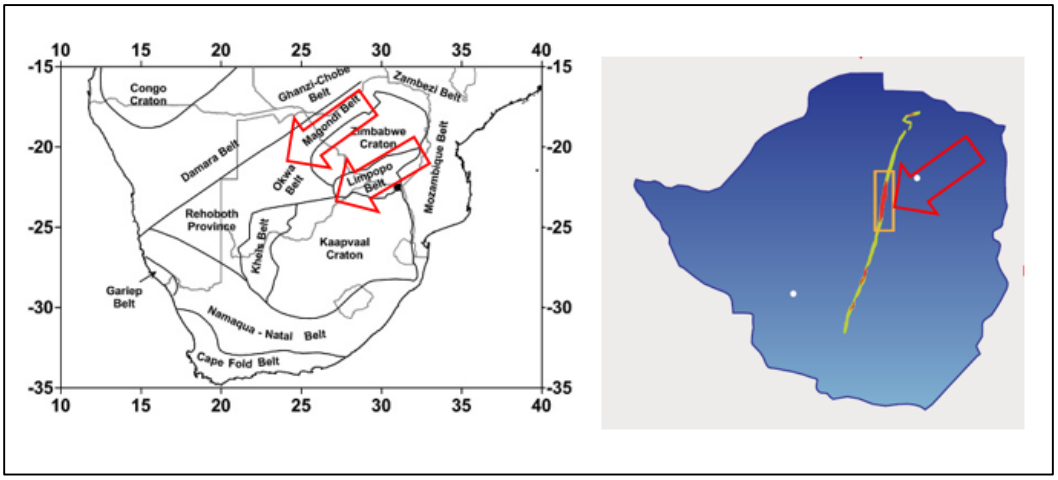

Figure 4.1 Direction of failure migration in relation to the regional tectonic events

Blenkinsop (2014) also explained the formation of the conjugate set of joints that formed at the placement of the Great Dyke with the set being perpendicular and parallel to the Great Dyke strike as shown in Figure 4.2. This set was intruded by granitic material which exhibit underground as conjugate aplite dykes.

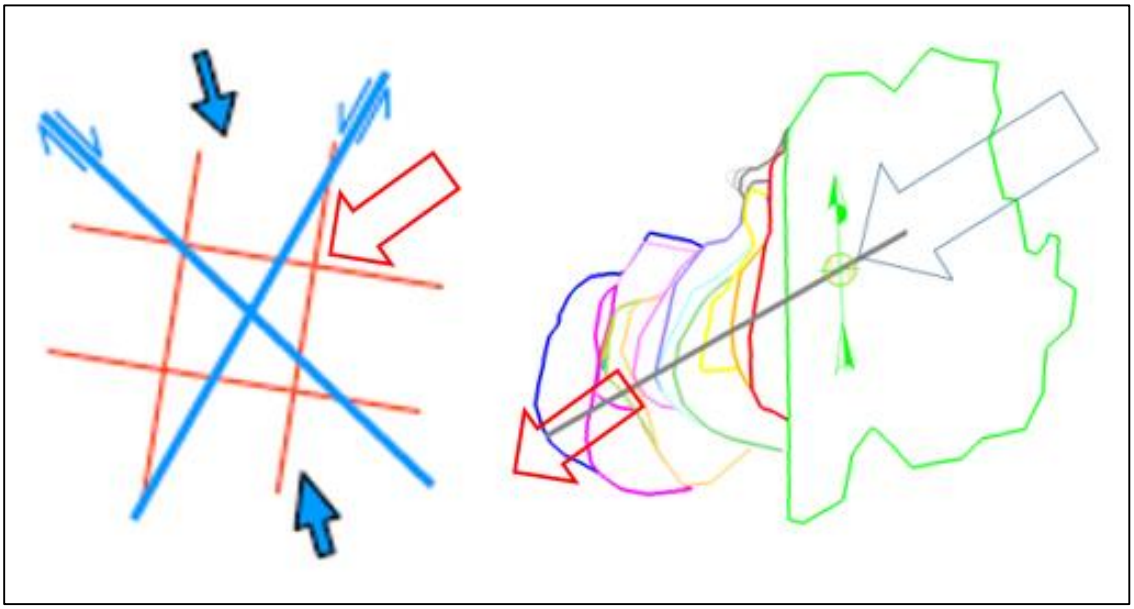

Figure 4.2 Direction of failure migration in relation to the Great Dyke structures at Bimha Mine

Similarities can be drawn from the work done by Esterhuizen (2000) in Figure 2.2 showing that the impact of jointing on pillar strength is worst when the joints are at an angle of 45° to the direction of loading and the current study. These similarities are limited to the angles and not necessarily the direction of loading. The direction of migration is at an angle of 45° ± 10° to the conjugate set of dyke intrusions (Aplitic Dykes) that forms parallel and perpendicular to Great Dyke axis as shown in Figure 4.3 and Table 3.1. It can be drawn that the impact of joints oriented at 45° to axis under consideration is not only on pillar strength but also on defining direction of failure migration. The direction of migration is the bearing of the line joining the centroid of initial area of failure to the centroid including the extended area of failure (including area of new migration), figure 4.3 insert.

The direction of migration is closely related to the structures that formed at the time of placement of the dyke i.e. 45° to the structures. In comparison to the south, the north part of the mine has a lower density of the N-S aplitic dykes to form complete conjugates as shown in the dyke frequency Table 4.1. The frequency was calculated by taking a scan-line in the particular direction and counting the number of dykes that cross the scan-line. Frequency is the calculated by dividing total scan-line length by the number of dykes intersected.

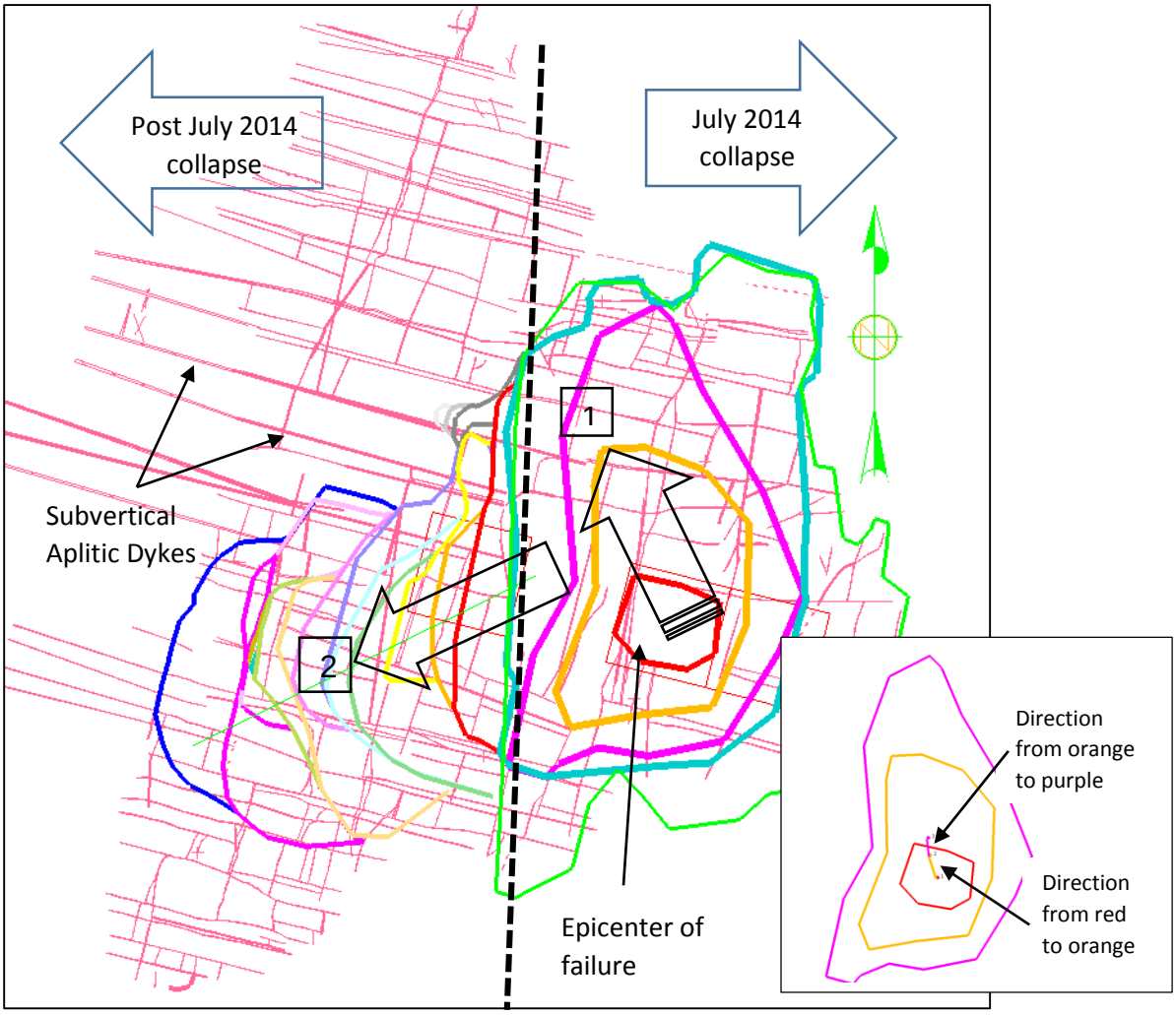

Figure 4.3 Direction of migration in relation to aplitic dyke structures showing pre and post July 2014 propagation and (insert) determination of direction of migration.

Table 4.1 Dyke frequency for the mine

	Strike* frequency (m per dyke)	**Dip** frequency (m per dyke)**
North	34	89
South	35	60

* Based on strike direction being along the Great dyke strike
** Based on strike direction being along the Great dyke dip

4.2.2 Rock mass quality / ground conditions

The rock mass quality was measured from the results of mapping, geotechnical logging and rock mass quality ratings of the excavated bords of the mine based on Barton's rock mass classification system (Barton N, 1988). The classification system used was adapted in order to better manage the very poor ground conditions. The adapted system basically classifies the rock into four distinct classes as shown in Table 4.2.

Table 4.2 Rock mass classes (Source – Zimplats ground classification tables)

Ground class	Description of conditions	Q-Value	Colour
A	Good	10+	Blue
B	Fair	4-10	Green
C	Poor	2-4 (1-4)*	Yellow
D	Very poor	0-2 (0-1)*	Red

* - Original Barton classification system ranges. (Full spectrum range is 0.001-1000)

The trend or direction of migration of the failure shows similar trend to that of the very poor ground conditions. From the epicenter of the collapse, the failure front migrated to the northwest (Direction 1 in Figure 4.4) until it stopped near the boundary of the very poor ground conditions. The failure front then started migrating to the southwest (Direction 2 in Figure 4.4) again in a direction where there was a higher prevalence of very poor ground conditions.

The influence of very poor ground conditions is therefore significant in the determination of the direction of migration of the failure front.

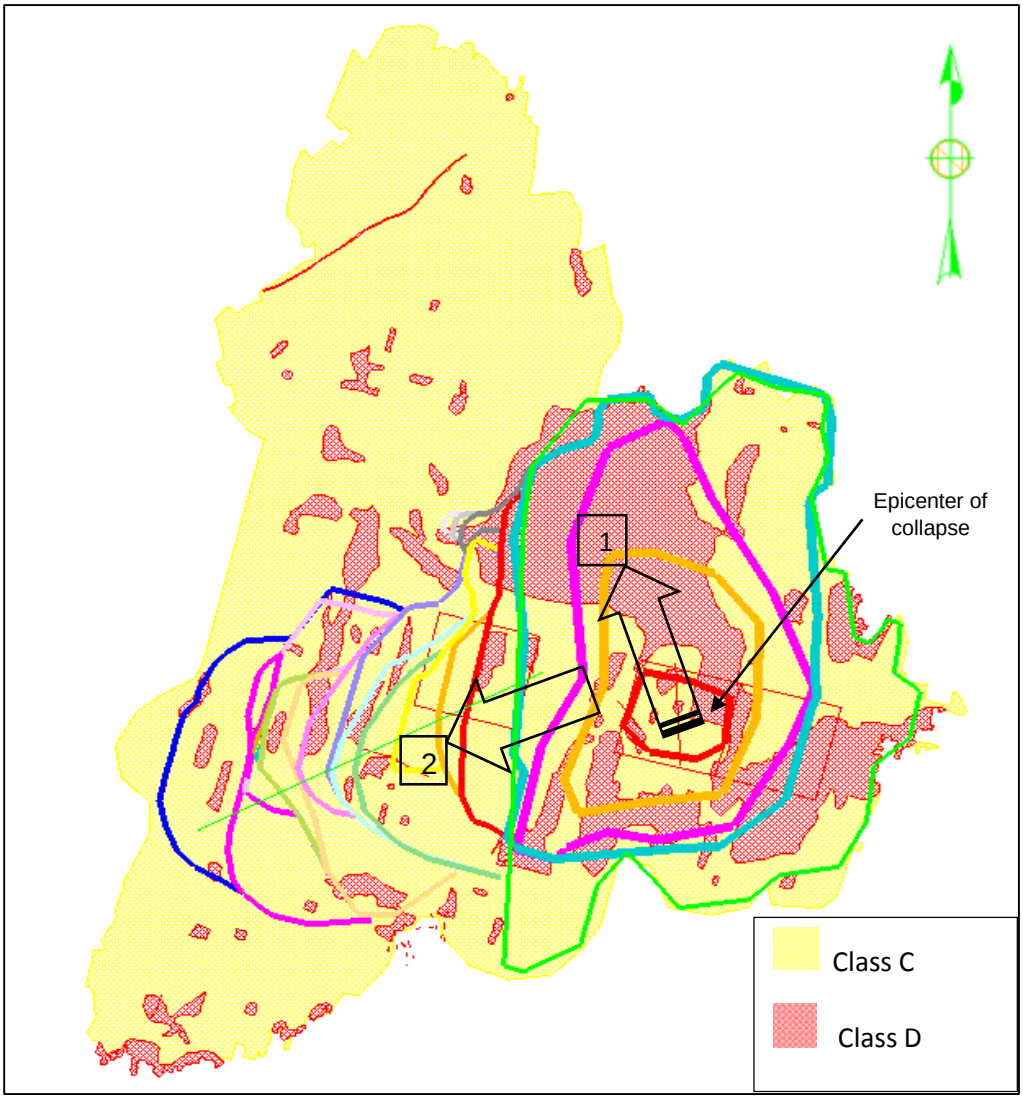

Figure 4.4 Failure migration in relation to very poor ground conditions

In order to validate the ground class ratings that were done, an exercise was done to calculate the ratings based on two different methods i.e. the Q system and the Rock Mass Rating RMR89 system (Bieniawski, 1989). This was further verified independently by a third person. Eight different areas in the current workings that had been logged and classified were used for verification. Table 4.3 summarises and compares the results. The data shows that the variances in the results is small and insignificant which is a reflection of the appropriateness of the classification that was done and used in this research.

Table 4.3 Rock mass ratings comparison

Area	Based on actual logging				Calculated RMR		
	PM	Initial	Independent	RMR89	PM*	Initial*	Independent*
88S	2.2	1.4	1.8	53.0	51.2	46.9	49.0
29S	2.8	2.8	2.1	54.0	53.2	53.3	50.6
30S	3.0	2.5	3.3	54.0	53.8	52.2	54.8

* calculated based on the relationship RMR=9lnQ+44

4.2.3 Mutambara Shear

The relationship between the existence of the shear and the epicenter of failure as well as the propagation of the failure is shown in Figure 4.5. Figure 4.5 and 4.6 show the relation between the migration of failure to the thickness and position of the shear with respect to the mining horizon.

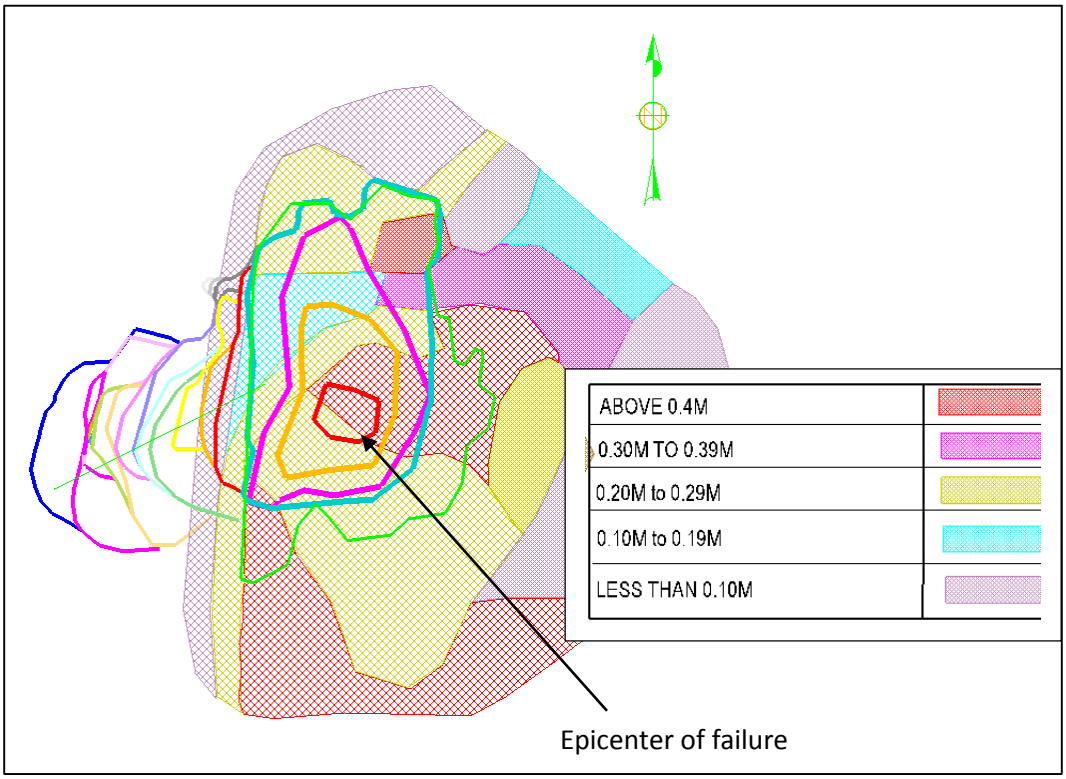

Figure 4.5 Failure migration in relation to Mutambara Shear thickness

The failure front started off from an area where the shear was more than 0.4m thick moving out to areas with reduced thickness. Of note is the brief stoppage of the migration front after the July 2014 collapse. The plane of stoppage also

coincides with the plane where the shear is less than 0.10m thick as shown in Figure 4.5. The brief halt in propagation with the thin shear can be inferred to signify the influence that the thickness of the shear has on failure propagation.

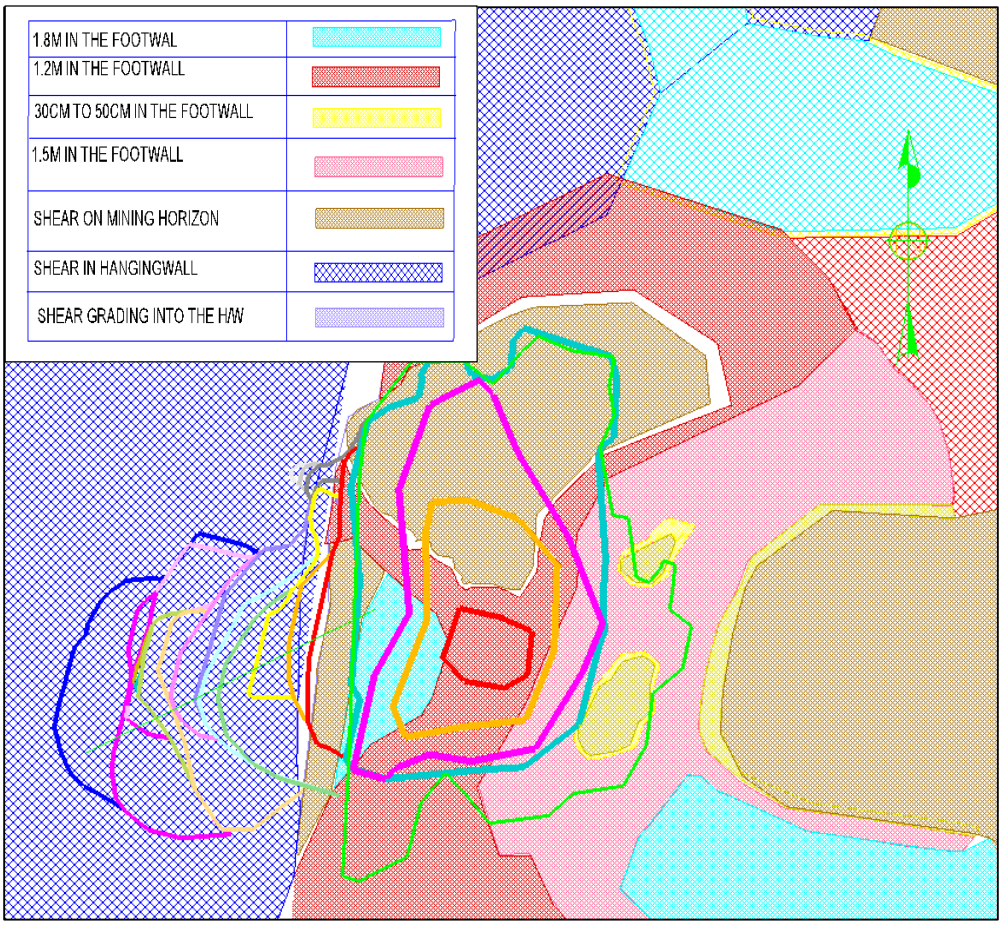

Figure 4.6 Failure migration in relation to the position of the shear

From the evidence shown in Figure 4.6, the collapse started in an area where the shear is 0.5m-1.2m in the footwall and more than 0.4m thick. The failure front migrated towards the area where the shear is on the mining horizon rather than towards the area where the shear lies deeper in the footwall. A brief halt in rapid migration is noted where the shear thins out, also coincide with the shear going into the hangingwall. Analysis by (Muaka, et al., 2017), as discussed in chapter 2, corroborates with the observed behaviour of reduced negative influence on pillar strength when the shear is in the hangingwall when compared to when the shear is on the reef horizon and very close to the footwall. Post-July 2014, the

failure propagated towards areas where the shear is in the hangingwall as a tight joint, proving that there are other variables that continue to influence the failure direction besides the shear position.

4.3 Micro-Scale Analysis

4.3.1 Pillar sizes

Design pillar size is governed by ground conditions, pillar height and pillar width. Figures 4.7 and 4.8 show the plot of the pillar height and width to height ratio together with the relative frequency distribution.

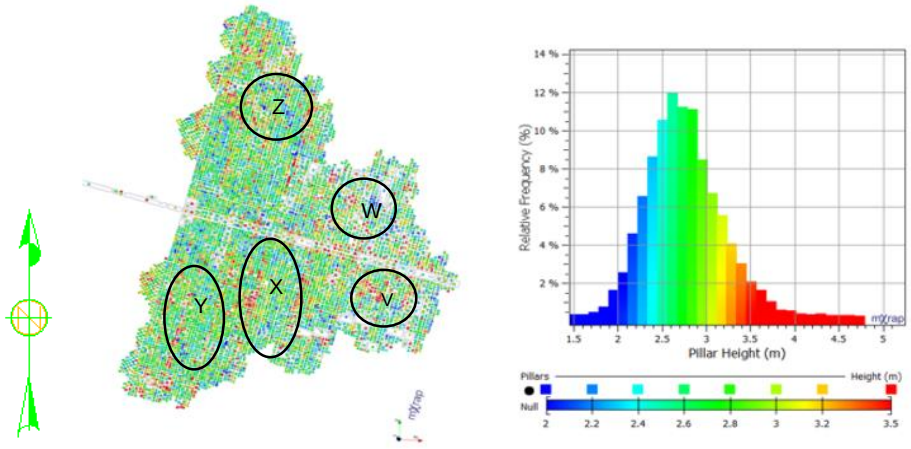

(a)

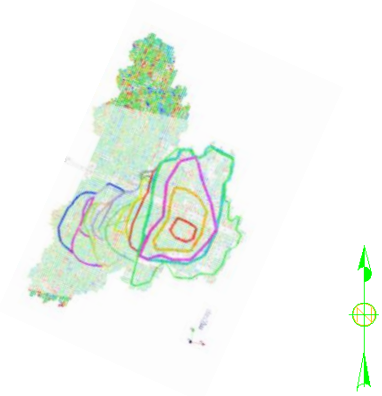

(b)

Figure 4.7 Distribution of the pillar sizes a) Distribution of pillar height, b) Pillar height compared to failure direction (Zimplats Internal report (SRK), 2016a), (Walls & Mpunzi, 2017)

The pictures in Figure 4.7 show a generally even distribution of all the pillar heights. Of note are some of the clusters with above normal heights circled out with “V” representing the epicenter of the collapse and the general trend of the failure migration towards areas “W” and “Y”.

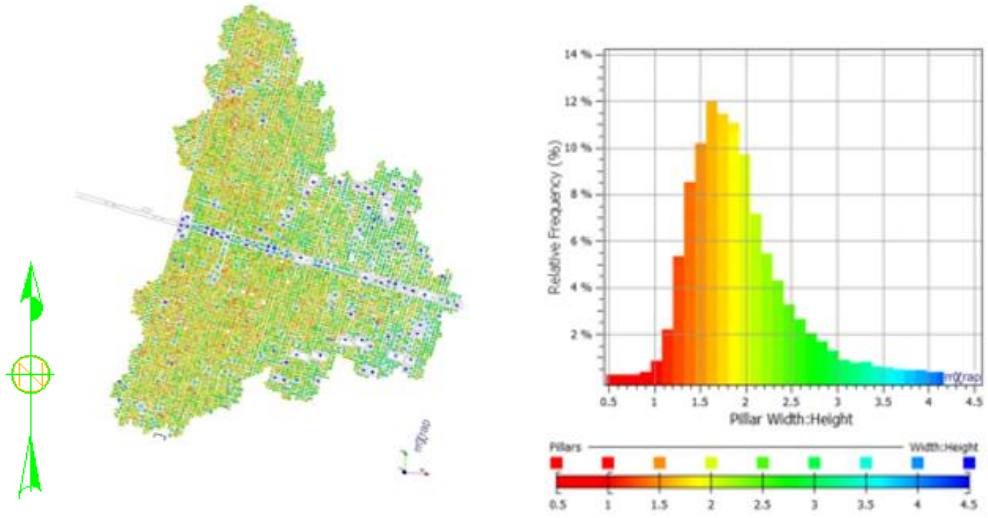

Figure 4.8 Distribution of the w/h ratio (Zimplats Internal report (SRK), 2016a), (Walls & Mpunzi, 2017)

From Figure 4.8, no significant clusters with low w/h ratios can be singled out as potentially problematic, hence a seemingly low correlation to failure front migration. While there are areas/ clusters with poor pillar heights, the same is not observed on the w/h plots. This is attributable to the controls in the mining of splits to ensure mine stability.

Figure 4.9 shows the distribution of the factor of safety and comparison with the failure migration. The distribution in Figure 4.9 shows higher concentration of the lower factor of safety on the southern side in comparison to the north. From this model used, it can be concluded that the estimation of the K-value in the bottom areas of the mine is more accurate to these conditions in comparison to the upper areas (Walls & Mpunzi, 2017). Therefore, the contribution of lower factor of safety to the failure migration trend is critical and cannot be overlooked as it should be taken into consideration in the determination of pillar strength and stress.

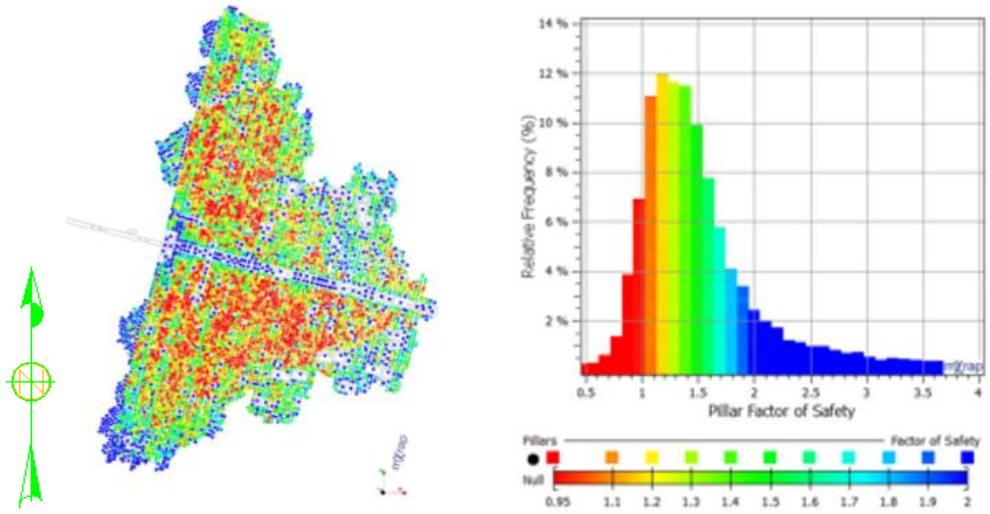

(a)

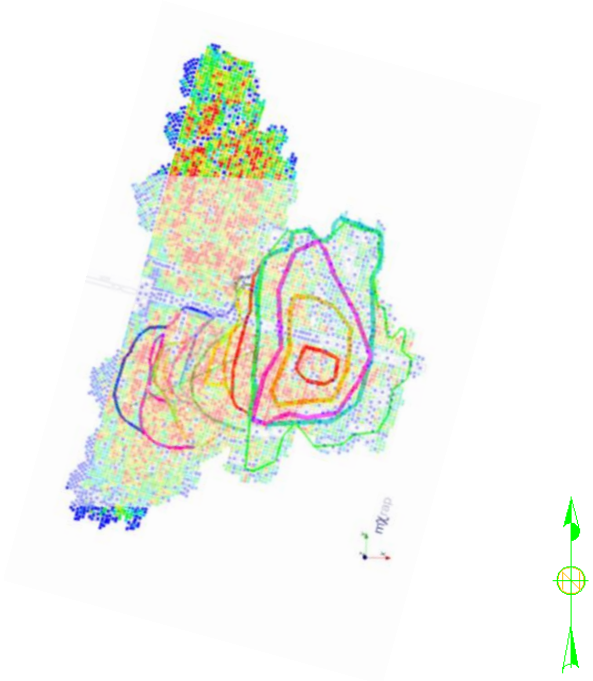

(b)

Figure 4.9 Distribution of the Factor of safety (a)Distribution of factor of safety, (b)Comparison of factor of safety to failure migration (Zimplats Internal report (SRK), 2016a), (Walls & Mpunzi, 2017)

4.3.2 Pillar position

Figure 4.10 shows the distribution of the distance between the planned pillar centroid and the actual pillar centroid position. The analysis was done using Vulcan software from Maptek. The plot shows an even distribution of the distance between design and actual pillar centroid position with no clear and direct correlation to the failure migration front. To this end, it can be seen that the pillar position has low influence on the direction of failure migration.

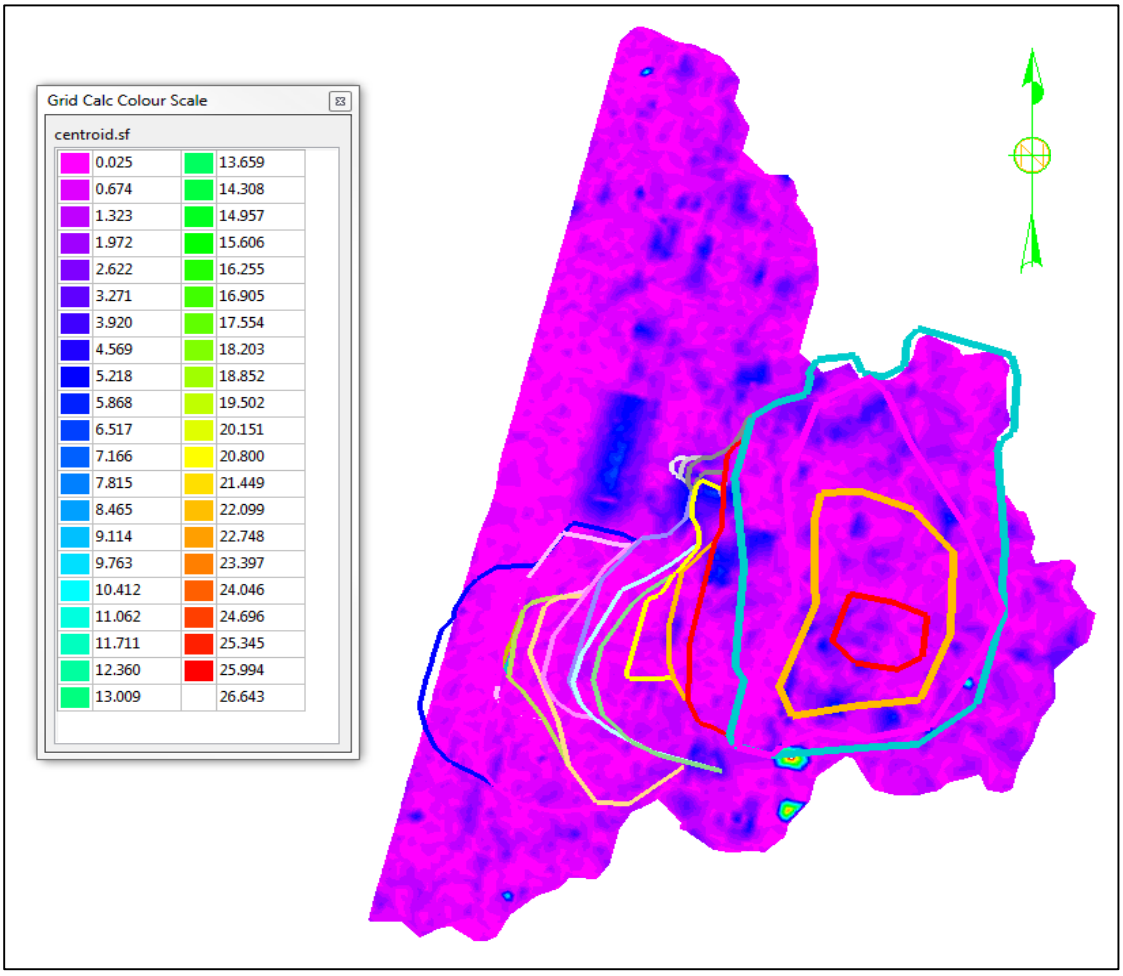

Figure 4.10 Pillar position with respect to design.

4.3.3 Joint properties

Analysis of joint properties was done on limited data that could be obtained post collapse (i.e. data mapped during the mining phase). The available data on joint

properties largely cover the areas mined up to 2012. Figures 4.11 and 4.12 show the relationship between joint roughness and alteration to the failure propagation, where the roughness and alteration are based on the Barton classification system as shown in Table 4.4 (Barton, 1988). The joints analysed in this section exclude the aplite filled joints that have been analysed separately in an earlier section.

Table 4.4 Joint roughness and alteration numbers (Barton, 1988)

	Joint Roughness Number	J_r
a) Rock-wall contact, and b) rock-wall contact before 10 cm shear		
A	Discontinuous joints	4
B	Rough or irregular, undulating	3
C	Smooth, undulating	2
D	Slickensided, undulating	1.5
E	Rough or irregular, planar	1.5
F	Smooth, planar	1.0
G	Slickensided, planar	0.5
Note: i) Descriptions refer to small scale features and intermediate scale features, in that order.		
c) No rock-wall contact when sheared		
H	Zone containing clay minerals thick enough to prevent rock-wall contact	1.0
J	Sandy, gravelly or crushed zone thick enough to prevent rock-wall contact	1.0
Note: i) Add 1.0 if the mean spacing of the relevant joint set is greater than 3m. ii) J_r = 0.5 can be used for planar slickensided joints having lineations, provided the lineations are oriented for minimum strength.		

	Joint alteration number	ϕ_r approx.	J_a
a) Rock-wall contact (no mineral fillings, only coatings)			
A	Tightly healed, hard, non-softening, impermeable filling, i.e., quartz or epidote.	--	0.75
B	Unaltered joint walls, surface staining only.	25-35°	1.0
C	Slightly altered joint walls. Non-softening mineral coatings, sandy particles, clay-free disintegrated rock, etc.	25-30°	2.0
D	Silty- or sandy-clay coatings, small clay fraction (non-softening).	20-25°	3.0
E	Softening or low friction clay mineral coatings, i.e., kaolinite or mica. Also chlorite, talc, gypsum, graphite, etc., and small quantities of swelling clays.	8-16°	4.0
b) Rock-wall contact before 10 cm shear (thin mineral fillings).			
F	Sandy particles, clay-free disintegrated rock, etc.	25-30°	4.0
G	Strongly over-consolidated non-softening clay mineral fillings (continuous, but < 5 mm thickness).	16-24°	6.0
H	Medium or low over-consolidation, softening, clay mineral fillings (continuous, but < 5 mm thickness).	12-16°	8.0
J	Swelling-clay fillings, i.e., montmorillonite (continuous, but < 5 mm thickness). Value of J_a depends on per cent of swelling clay-size particles, and access to water, etc.	6-12°	8-12
c) No rock-wall contact when sheared (thick mineral fillings)			
KLM	Zones or bands of disintegrated or crushed rock and clay (see G, H, J for description of clay condition).	6-24°	6, 8, or 8-12
N	Zones or bands of silty- or sandy-clay, small clay fraction (non-softening).	--	5.0
OPR	Thick, continuous zones or bands of clay (see G, H, J for description of clay condition).	6-24°	10, 13, or 13-20

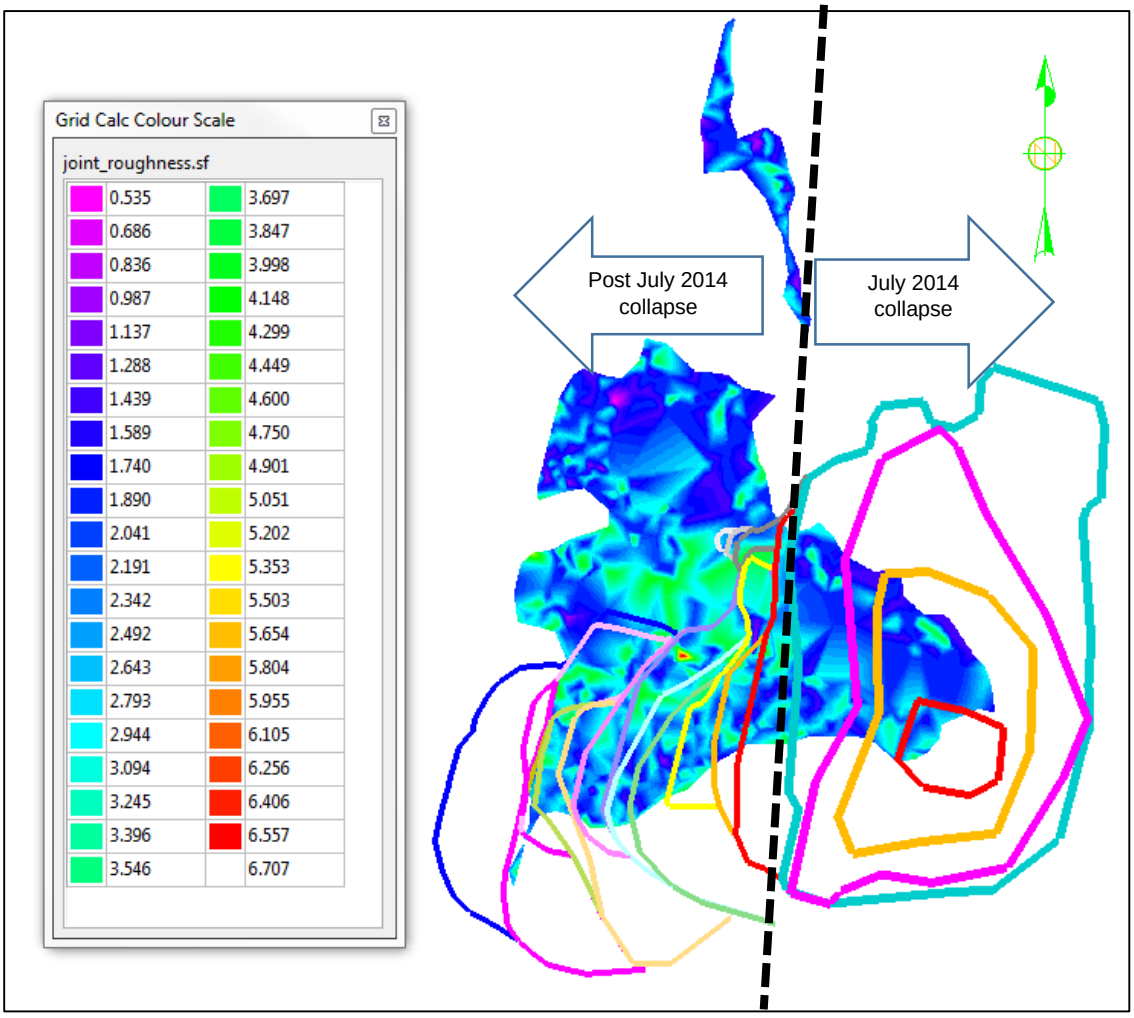

Figure 4.11 Failure migration with respect to joint roughness

Joint roughness correlates well on the 2014 migration but has a low correlation post July 2014 collapse. In the 2014 migration area, the Mutambara shear is mostly more than 0.4m thick and close to the mining horizon and hence the influence of the shear to the joint properties could be significant. In subsequent migration events, the influence of the shear is reduced. Joint roughness therefore has limited independent influence on direction of failure front migration.

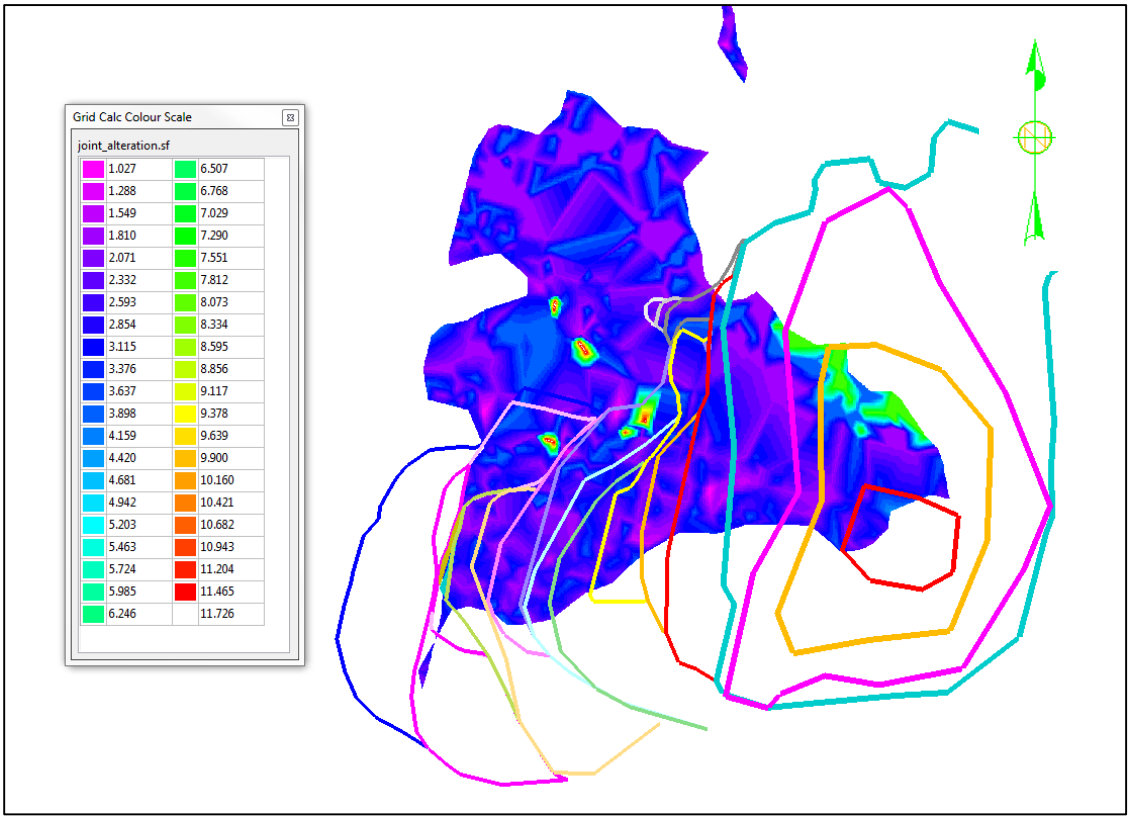

Figure 4.12 Failure migration in relation to joint alteration.

No correlation can clearly be established between direction of migration and joint alteration. Similar to joint roughness, the lack of correlation between joint alteration and failure migration direction point to the limited influence the joint alteration has on the failure front migration.

4.4 Ground Monitoring Results Analysis

4.4.1 Stress migration

Figure 4.13 shows the historical monthly stress migration rates, and is used to trend the failure front migration rates since 2014. In the graph, North (W) means westward migration on the northern section of the mine, likewise South (N) means northward migration of the stress front in the south section of the mine. The last stress front migration event was recorded in August 2017. It is however important to note that some of the pillars within the stress zone have shown signs of increasing stress. The migration from the south towards the north appears to have been slowed down by the larger decline pillar separating the north and the south in the upper portion of the mine.

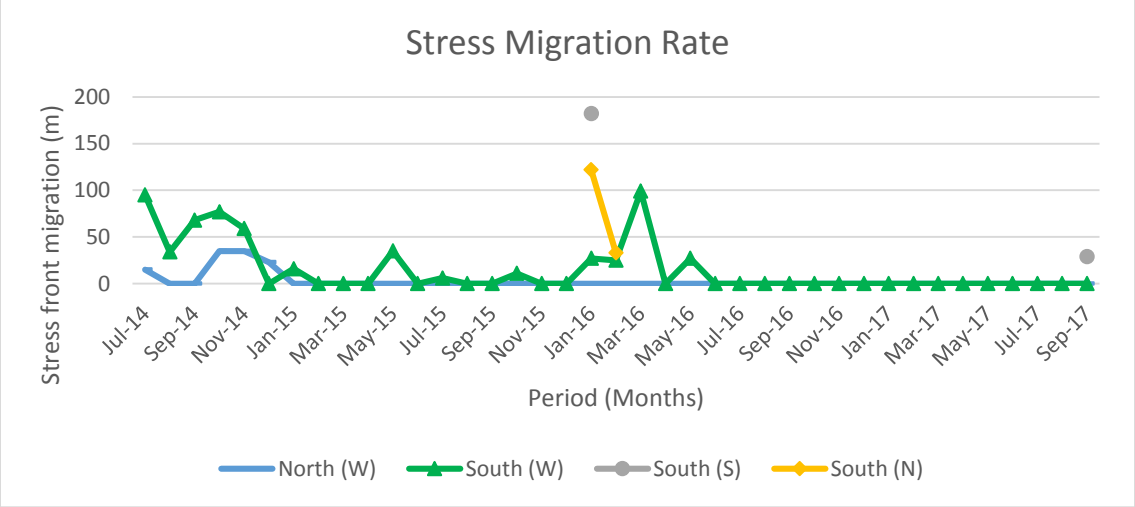

Figure 4.13 Bimha monthly stress migration

The cumulative stress migration curve shown in Figure 4.14 shows the influence of creep on failure propagation. The steps in the cumulative curves can be related to the major collapse events in October 2014, January 2016 and August 2017 (Failure front with dates is shown in Figure 4.21). The 'slip-stick' movement can be seen and also related to rainfall shown in Figure 4.18 and moisture increase as explained in chapter 2 under factors influencing creep rates. Creep therefore is an important factor influencing failure and its propagation.

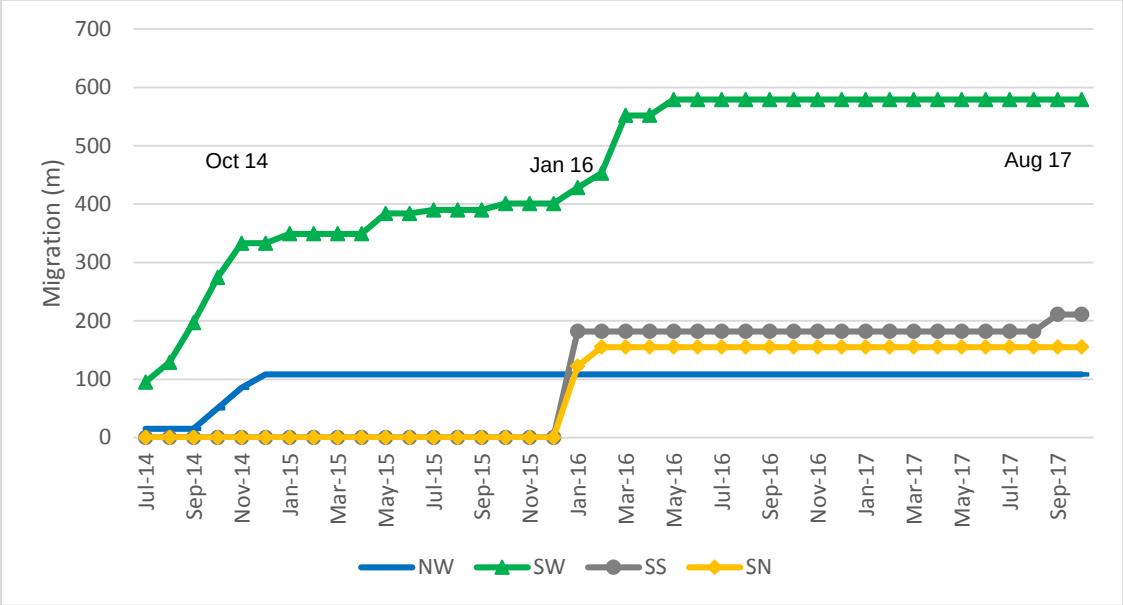

Figure 4.14 Cumulative stress migration curve

4.4.2 Closure

In this analysis, the total closure of the closure monitoring stations is used for trending the rockmass behavior in both the north and south sections. The total closure is the sum of the closure recorded on closure stations in the section. For the purpose of this analysis, closure from stations ahead of the failure front was summed up. The recording stations were kept within 70m of the failure front on dip and spaced within 150m on strike. Figure 4.15 shows the trend obtained from closure monitoring. The graph shows a higher rate of closure for the south when compared to the north. Weaker rockmass is prone to higher closure as it fails easier than good ground conditions. This also followed the trend recorded on the stress migration front. Close analysis of the daily closure rates have shown that when rates of more than 1.5mm per day are sustained for more than three days at a station, a major collapse event follows within a week. Both the total closure

and individual station closure are important to track as the total closure provides information on regional events while individual station closure informs evacuation plans.

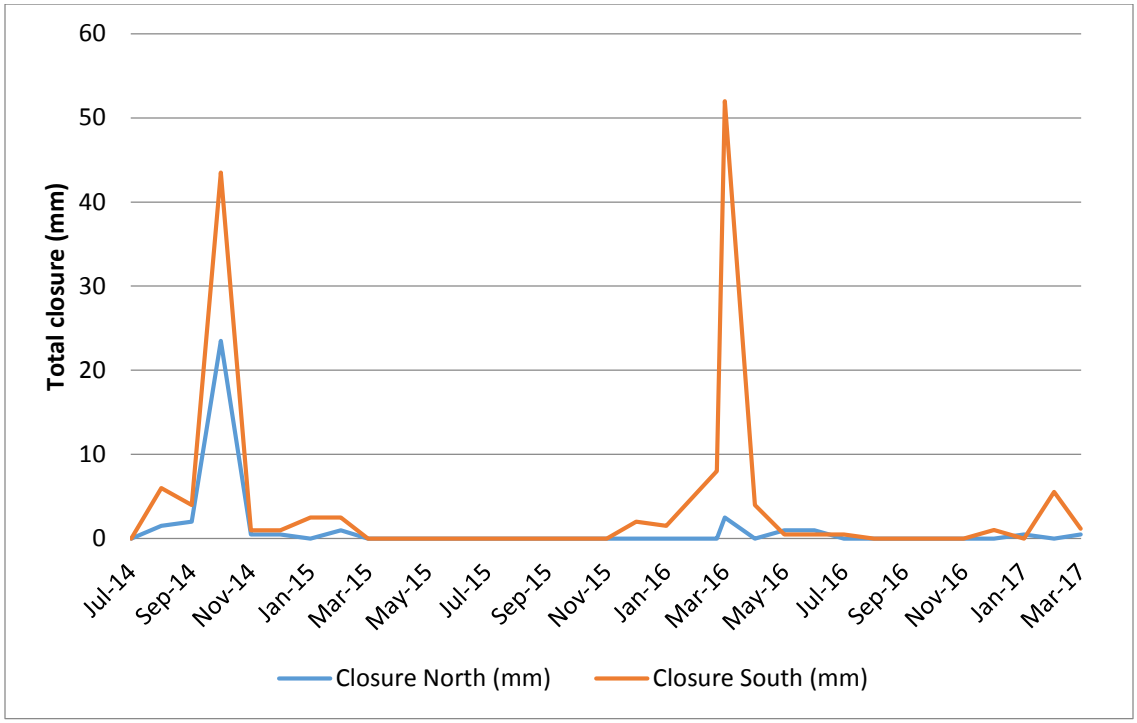

Figure 4.15 Total closure trend.

Typical individual station closure trends for two selected stations are shown in Figure 4.16. These have been reduced to an inverse closure rate calculated from the inverse of closure. The trend is projected to reduce to zero when closure is maximum which corresponds to total closure. The trend can therefore be used to establish a trigger point to evacuate. In this case the trigger point would be to evacuate when the inverse closure rate is still above 1 in order to give a buffer of at least one week before the major collapse event.

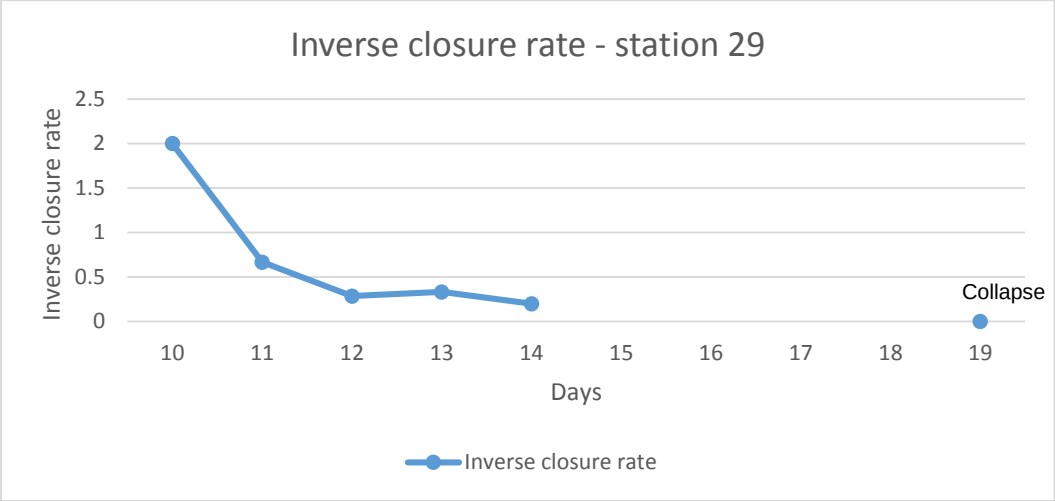

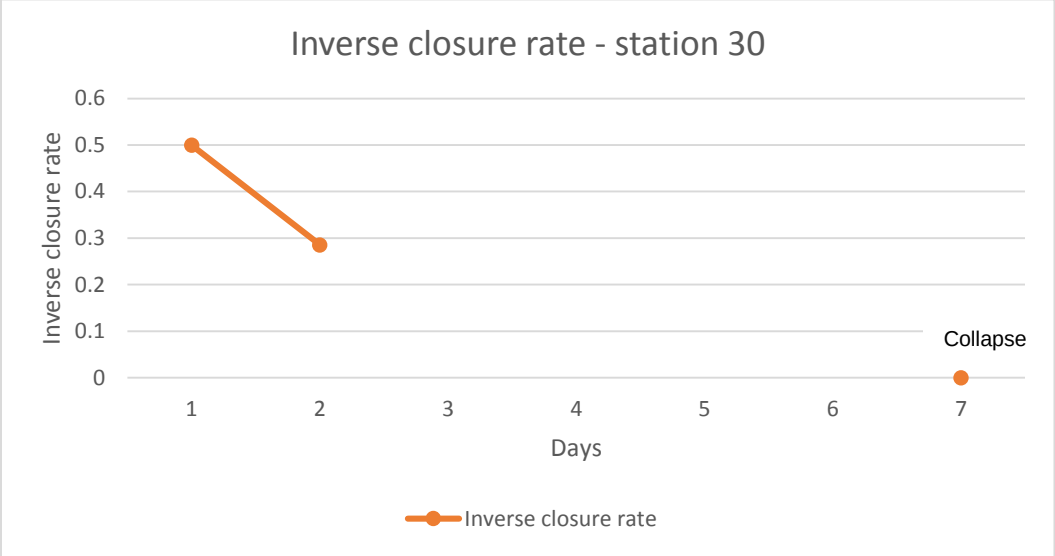

Figure 4.16 Typical inverse closure rates for stations 29 and 30

From the analysis of the trends in Figure 4.16, if an inverse closure rate of less than 1 is sustained for more than three days, a major collapse event is witnessed within seven days.

4.4.3 Seismic events

The trend in Figure 4.17 shows the recorded seismic events. Small ground movement indicators (SGMIs) from CSIR South Africa were used to monitor seismic events. These were located as shown in the insert in figure 4.17 with a

sensitivity of -1 and a location radius of 500m. The graph shows that the event rate increases around major stress migration and collapse events.

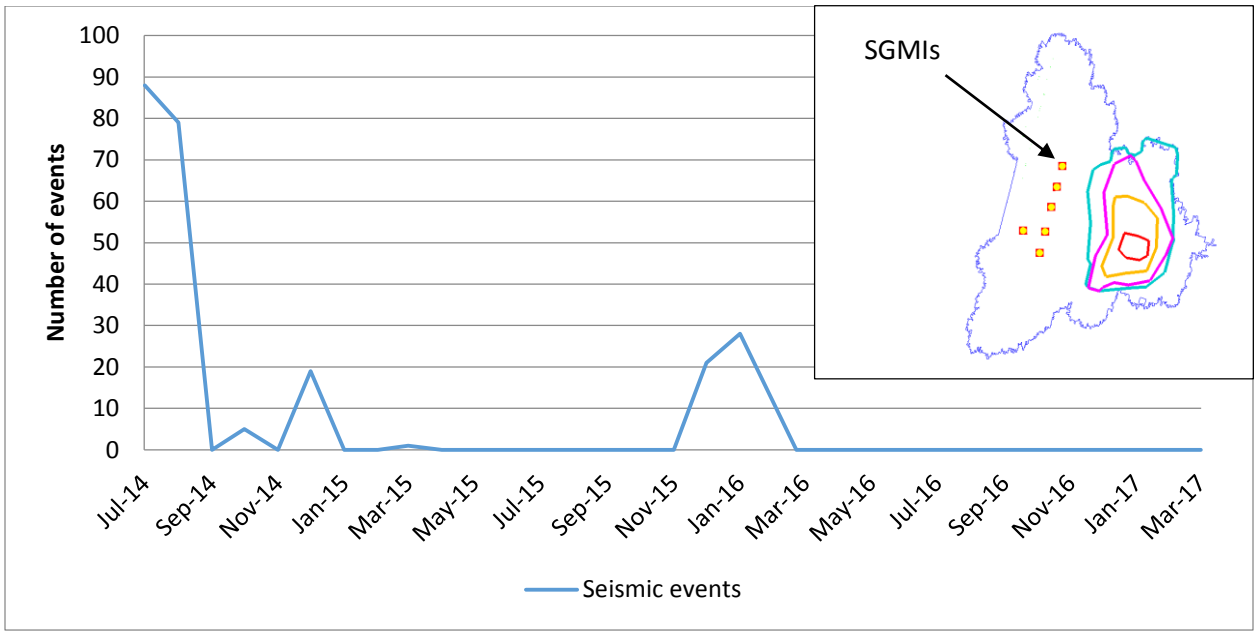

Figure 4.17 Seismic events trend and location of the SGMIs (insert)

The events increase around major events as intact rock fracture during failure and collapse. Two major sources of mining induced seismic events are intact rock rapturing and the geology related events which are associated with faults and dykes (Ryder & Jaeger, 2002). Mining induced seismic events are normally associated with deep mines and least expected in shallow mines like in this case study. The occurrence of the recorded events coincide with the major collapse events hence the seismic events are due to the collapse itself not necessarily stress related. It however becomes important to monitor the seismic activity in the shallow mine in order to confidently establish the source of the events. This will enable setting up of necessary systems to prevent accidents related to seismic events.

4.4.4 Rainfall

The rainfall trend in Figure 4.18 shows that the 2016-2017 rain season had higher rainfall when compared with the first two seasons after Bimha collapse (Table 4.4). Of note in the 2017 season is the fact that the effects of the increased rainfall have however not directly translated into additional progress of the failure front as witnessed in the 2015-2016 season (figure 4.19). This is attributable to the failure front abutting with the boundary / protection pillar left in place to stop any migration of the failure into the new workings.

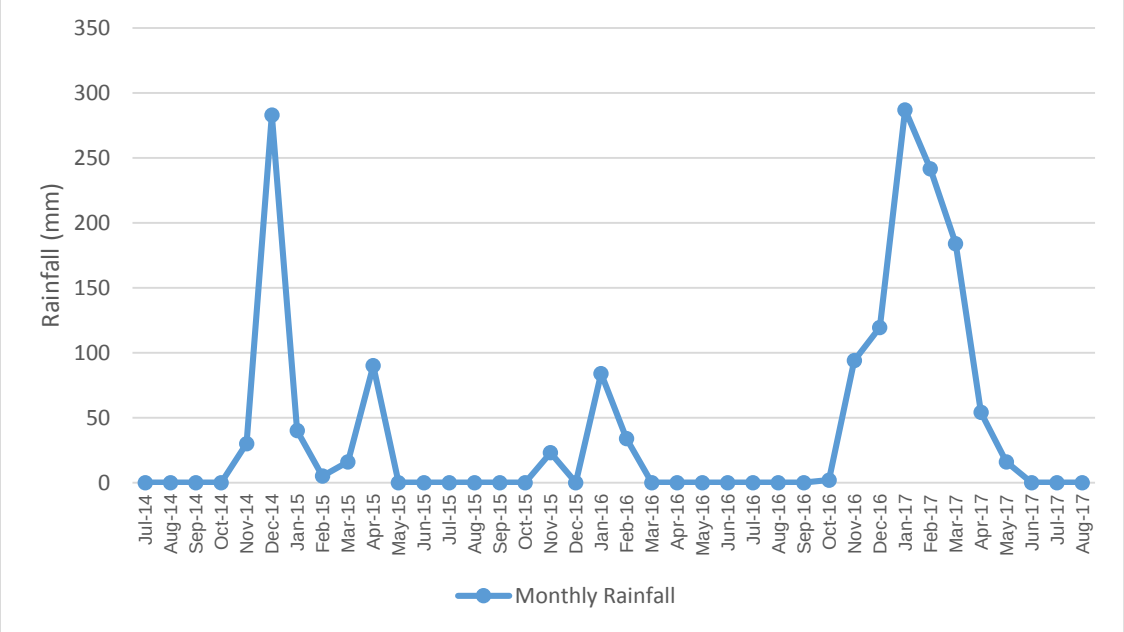

Figure 4.18 Rainfall trend

Table 4.5 compares the total annual rainfall for the three consecutive seasons up to 2017.

Table 4.5 Seasonal rainfall comparison

Year / Season (October – September)	Annual rainfall (mm)	Comment
2014-2015	464	Average rainfall
2015-2016	141	Very low rainfall
2016-2017	998	Very high rainfall

4.5 Detailed Results Analysis

Tables 4.6a and b shows the calculated correlation coefficients (R) for the different variables for the first and second year after the July 2014 collapse. The detailed calculation of correlation coefficient is shown in appendix 3. The third year was not included in the correlation analysis as the failure front abutted the boundary pillar in the west as well as being slowed down by decline pillars on the South (N) migration. The abutment of the failure front on the boundary pillar and slowing down on decline pillars introduces new constraints and changes which distort the comparisons as the front is no longer freely moving. Figure 4.19 shows all the different trends superimposed to gain further information on correlations of the different variables that were being monitored.

Table 4.6a Correlation coefficients for first year

Year 1			
	Seismic events	*Total closure*	*Monthly Rainfall*
total closure	-0.1		
Monthly Rainfall	-0.1	-0.2	
Total migration	0.4	0.5	-0.2

Table 4.6b Correlation coefficients for the second year

Year 2			
	Seismic events	*Total closure*	*Monthly Rainfall*
total closure	-0.1		
Monthly Rainfall	0.7	-0.1	
Total migration	0.7	0.2	0.9

Key
Green – Strong correlation
Yellow – Fair correlation
Orange – Low correlation

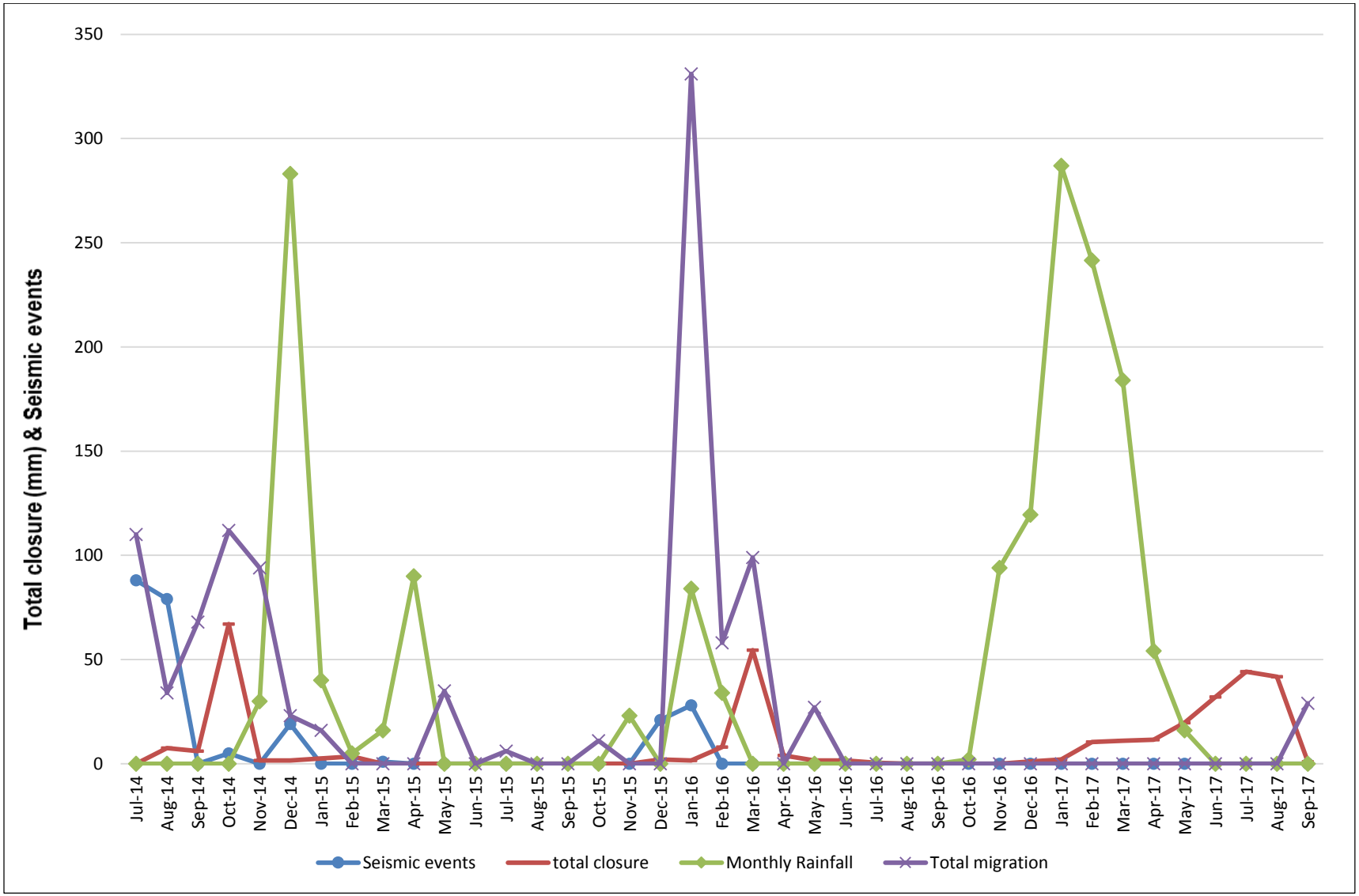

Figure 4.19 Comparison of the Monitoring trends

The trends in Figure 4.19 shows the behaviour of the four key variables being monitored. The correlations were analysed for the first two years after the July 2014 collapse as there are no new constraints to the migration in both years. The January 2016 major collapse event happened within the failing zone and thus explains why not as much closure was recorded. However, there was an increase in the closure and stress migration in March 2016 though there was no major collapse event. Fair to strong correlations are seen amongst most of the different variables as shown in Tables 4.6a and b. Although the 2017 rainfall has been much higher (table 4.5), the other variables have not responded as in the previous seasons. This is due to the fact that the stress boundary had reached the boundary pillar on the south and no further westward migration is possible. Stress meters installed in the boundary pillar on the west have not shown any significant increase in the stress levels as shown in Figure 4.20. The marginal increase noted in July and August 2017 is consistent with the collapse event noted at the end of August 2017 at 1S60 in the old footprint.

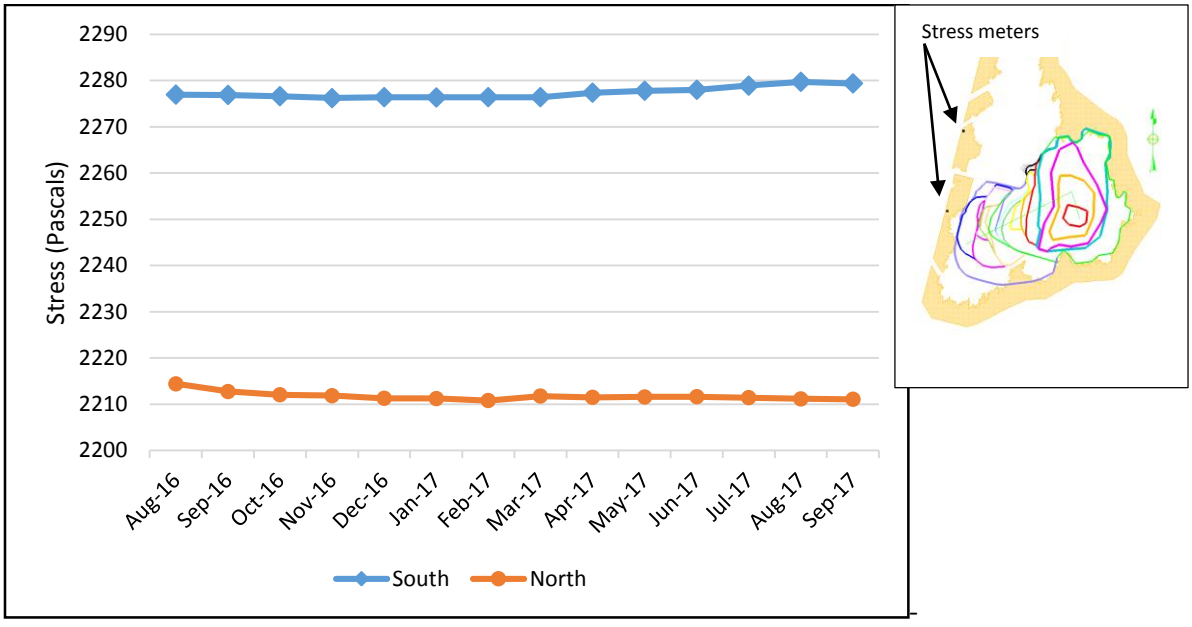

Figure 4.20 Stress meter readings and position of stress meters (insert)

From the single collapse event post the installation of the stress meters, this system could potentially provide important information as the graph for the south shows an increase in stress towards the August 2017 collapse.

4.6 Formulation of the Migration Model.

From the preceding analysis, key independent variables that contribute to the direction of the collapse migration can be listed. These are;

1. Direction of major faults formed from tectonic movements around the craton hosting the area of analysis e.g. along mobile belts / orogenic events
2. Direction and density of major vertical-subvertical joint sets
3. Existence of very poor ground conditions
4. Thickness and position of major shears around the mining horizon
5. Pillar factor of safety
6. Creep
7. Rainfall

From the result of the monitoring program detailed, four distinct collapse events can be seen based on increased migration rate, seismic events, increased closure and the actual collapse seen on the ground. These were July 2014, October 2014, January 2016 and August 2017 events. The four events form three legs of migration which can be used for analysis. In order to formulate a migration model, the first five key variables are analysed on the three event legs in order to obtain the most probable direction and compared with the actual behaviour observed on the ground. For the three legs, detailed analysis is done to compare the failed and the areas where failure is still to occur particularly in the north. Figure 4.21 shows the different areas analysed;

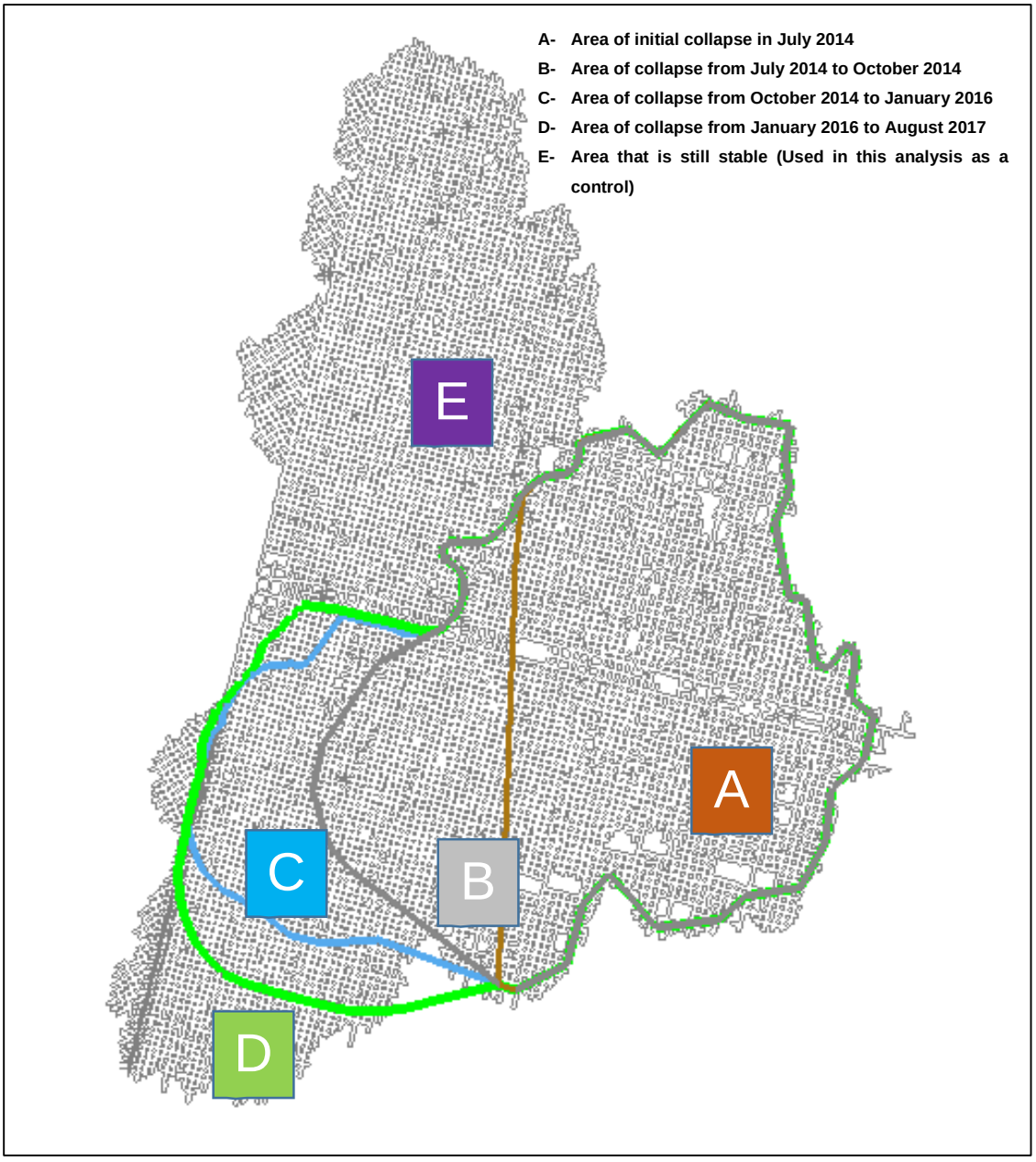

Figure 4.21 Failure areas by period

The result of analysis is summarised in Table 4.7 which gives the average values obtained.

Table 4.7 Key variables in the different areas.

Variable	A	B	C	D	E
1	1.63	2.30	0.68	1.31	0.66
2	2.18	2.69	2.73	2.85	2.76
3	0.36	0.07	0.05	0	0.06
4	-1	1	1	1	1
5	2.54	1.83	2.05	1.95	2.15

Legend:
1 – Density of Aplitic dyke (Structures that formed at the time of dyke emplacement) (per square hectare)
2 – Very poor ground conditions (Q)
3 – Thickness of shear (mm)
4 – Position of shear with respect to mining horizon (m)
5 – Factor of safety

In order to pick any trends and correlations, the data was plotted following the legs of collapse as shown in Figure 4.22. The Figure 4.22 also shows the correlations (indicated by R in the graph) obtained from this analysis. The correlation coefficient was calculated between the observed direction of propagation in the five areas (from A, through B, C and D to E) in relation to each of the five key variables (Density of Aplite dykes, Q-Ratings, Shear thickness, Shear position and factor of safety). An example of the detailed calculation of the correlation coefficient (R) is shown in Appendix 3.

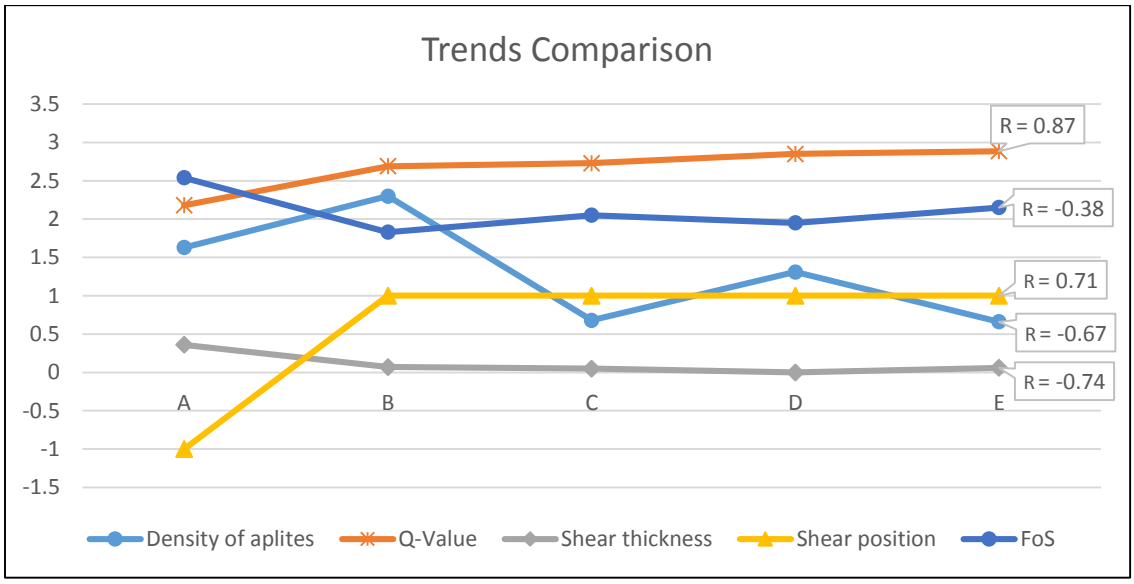

Figure 4.22 Plot of the key variables analysed with respect to the different areas

The correlations are strong except for the Factor of Safety (FoS) which has a low negative correlation of 0.38. These correlations do confirm the key variables that govern the propagation of failure as described in this analysis. Ideally if all the variables are accurately enumerated and incorporated, the FoS should have a high correlation. A low correlation for FoS could be an indication that the design did not accurately consider all the variables.

4.6.1 Formulation of a probability function

From the correlation analysis, using the correlation coefficient, the order of influence on the direction of migration can be stated as follows (from the highest to the lowest)

1. Rock mass condition as established from the Q-Value
2. The shear thickness
3. Position of the major shear with respect to the mining horizon
4. Density of aplite dykes
5. Pillar factor of safety

Additionally as discussed in section 3.3.2 and shown in Table 3.1, the angle (θ) between the strike of the aplite dykes and direction of migration under consideration (bearing difference) also influence the direction of migration.

These variables can thus be reduced into a formulation based on the correlations established. The formulation is thus governed by the following constraints

1. Area where the rock mass quality is lowest (Inversely proportional to Q)
2. Area where the thickness of the shear is highest (Directly proportional to T)
3. Inversely proportion to footwall position (P) of the shear with respect to mining horizon
4. Directly proportional to density of aplitic jointing (D)
5. Directly proportional to the bearing difference

In order to enumerate the most probable area of failure, a failure number (F) is introduced which takes into account all the above key variables. It is important to note that the calculation of the Q-value already takes into consideration the density of joints and thicknesses of shears or any geological structures in the rockmass. However, it does not incorporate position of the shear and orientation of the adverse joint sets. In order to incorporate these to variables in the enumeration, the failure number (F) is established by reducing the Q –value by factors that take these two variables into account.

4.6.1.1 Angle θ

From this research, it has been established that the factor that takes the angle into account should have maximum influence when the angle is 45° and reducing in either directions towards 0° and 90°. A review of the trigonometric curves of angles in Figure 4.23 shows that both the sine and cosine curves are not maximum at 45° and can only be maximum at 45° if a product of the two is taken.

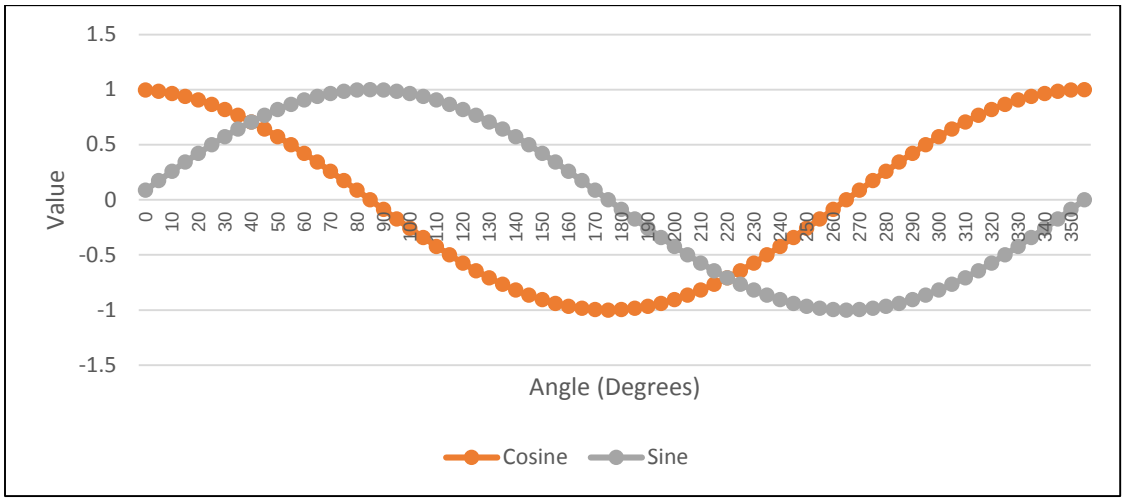

Figure 4.23 Sine – Cosine curves

In order to ensure that the factor that takes the angle into account is always positive, a square function of the product is considered and gives the curve shown in Figure 4.24.

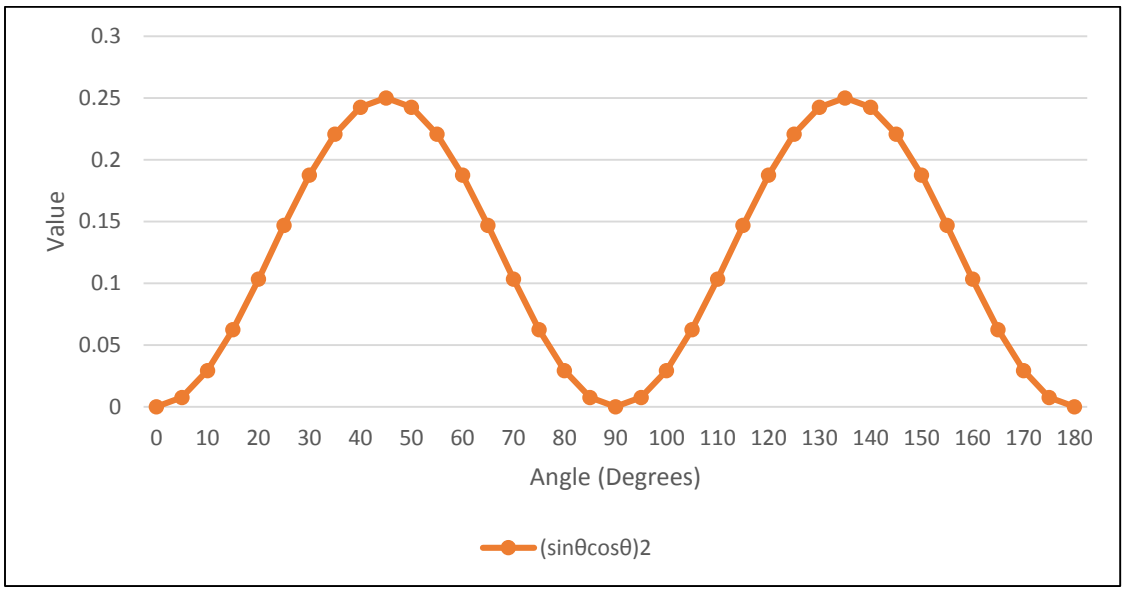

Figure 4.24 Angle difference $(sin\theta cos\theta)^2$ curve

A factor that takes the angle between the direction of migration and the orientation of the major joint set is therefore best represented by $(sin\theta cos\theta)^2$, and were be used in this analysis.

4.6.1.2 Shear position

The second factor that takes into account the position (P) of the shear is considered directly from the location with respect to the reef horizon. The distance is taken as the factor and in this analysis hangingwall is considered positive and footwall considered negative.

Considering these two key factors, equation 4 is proposed to establish the failure factor where a lower value indicates a high risk of failure while a high value represents a low risk of failure. Table 4.8 compares the failure factors for the actual areas observed on the ground.

$$F = (Q * P)/(sin\theta cos\theta)^2 \quad \text{- - - -

4.7 Conclusion

Some strong correlations between the direction of propagation (observed from A, B, C, D and E) and each of the key variables confirm the impact of the key variables that govern failure propagation. The influence of tectonic events within the sub-region is a factor that is not normally given much focus but this research has shown the need to always consider their influence. Analysis of the pillar geometry parameters where the distribution of pillar heights tends to be skewed towards the higher pillar heights while the same trend is not reflected in the width to height ratio point towards control of the quality of blocking out of pillars. The practices of analyzing the geotechnical conditions around a pillar before taking a split is therefore important in reducing cases of low width to height ratio due to height over-break. While the influence of other factors like pillar position to direction of failure migration has shown to be limited, the need to block out regularly positioned pillars as planned is important as it ensures even distribution of the overburden load. On a micro-scale, in the analysis of the direction of failure migration, the influence of joint roughness and joint alteration may be low, but the fact that the thickness of shear has influence on propagation proves that as the alteration gets higher and joints have fill, the influence on propagation is bound to increase. The parameters therefore need to be continually assessed because of their potential influence on failure migration direction. The results of the monitoring system implemented confirm the observation from the macro and micro-scale analysis that there are a number of factors that influence the direction of failure migration. These same results also provide important information on failure trends in relation to the collapse which is important in decision making on evacuation. The failure function formulated correlates well with the actual trends observed on the ground and can therefore be used in predicting failure propagation behaviour.

5 Conclusions and Recommendations

5.1 Conclusions

The research shows that the direction of migration / propagation of failure depends on multiple variables with one new key variable being established from the analysis. Simply put, it is the angle between the direction of propagation and the strike of the major vertical joint set. The density of the major joint set also influences the direction of propagation. Rock mass quality (which incorporates in its calculation the joint condition), major shear position and thickness are other key variables that influence the direction. The fair to strong correlations of these variables with the observed direction of failure propagation confirm the suitability of the use of a formulation with these variables' ability to predict behaviour.

This research also shows that there are other factors like pillar factor of safety, moisture or water in the rock mass and creep that are also at play in the establishment of the direction of propagation/migration. Factor of safety is normally used to identify potential hotspots, however, complex and salient variables like creep do also have influence on failure behaviour and need to be considered in failure propagation prediction.

The fact that the failure front was stopped by a barrier pillar on the western extremity on the southern part of the case study mine as well as the slowing down in migration towards the north past the bigger decline pillars proves the importance and the role played by the larger pillars in stopping or slowing down the failure migration. With further numerical modelling the actual pillar sizes that can stop propagation can then be determined and optimized. Once the correct size pillars for the geotechnical environment have been established, the pillars can then be incorporated into mine design.

However, once failure has initiated, the difficulty in stopping it if the initial design is not appropriately designed, the damage/loss and time of evacuation can only be predicted with a formulation such as established in this research with great

success. This analysis also shows that there is a relationship between closure rate and major collapse events which can be used to inform evacuations plans and prevent human exposure to collapses and failures.

5.2 Recommendations

Barriers pillars have capacity to stop failure propagation and are therefore important for inclusion in designs. The design of the orientation of barrier pillars should take into account the orientation of the major sub-vertical joint sets.

Systems must be put in place to minimize the water that gets into the rock mass through use of efficient pumping arrangements for water used for operations like drilling. Proper drainage facilities must be constructed on surface to minimize percolation of water into the rock mass by use of water diversion trenches.

Areas where the position and thickness of the shear are adverse to the stability of the mine must be left unmined or mined out at extractions that ensure the strength of the pillar is not compromised to induce instability and failure.

5.3 Recommendations for further study

Whilst this research has established some important relationships between geological structures and direction of propagation, there are areas that can be studied further in order to understand the propagation of failure. These include study of impact on failure propagation and stability of the position of major shears further down in the footwall. The depth where the influence is worst and where the influence becomes insignificant or zero is important for consideration in pillar design.

Establishment of a relationships, if any, between the influencing depths of position of shear to the pillar size and direction of propagation failure.

A study or test of the in situ stress field with a view to establishing the orientation of the major and minor horizontal stresses. This stress field can then be

compared to the direction of migration of the failure to establish any potential relationships.

Once the in situ stress field has been established, it is recommended to conduct numerical modelling to test the observed behaviour as well as the formulation with further work into the establishment of design pillar orientation with respect to geological structures. The modelling can also be used to model the actual pillar sizes required to stop failure migration.

REFERENCES

Barton, N. (1988). Rock Mass Classification and Tunnel Reinforcement selection using the Q-System. NGI.

Bieniawski, Z.T. (1989). Engineering Rock Mass Classification. New York. John Wiley & Sons Inc.

Blenkinsop, T. (2014). Structural interpretation Ngezi Mines - Internal report.

Brady, B. H., & Brown, E. T. (2005). Rock Mechanics for underground mining. New York: Kluwer Academic Publishers.

Carla, T.E., Intrieri, P., Farina, N., & Casagli. (2017). A new method to identify impending failure in rock slopes. *International Journal of Rock Mechanics & Mining Sciences*, 93 (2017), 76-81.

Drescher, K., & Handley, M. F. (2003). Aspects of time-dependent deformation in hard rock at great depth. *The Journal of the Southern African Institute of Mining and Metallurgy*, 103 (Issue 6), 325-336.

Esterhuizen, G. (2000). Jointing Effects on Pillar strength. *19th Conference on ground control in Mining* (pp. 286-290). The British Library.

Implats Rock Engineering. (2003). Strata Control Course for Production Officials. Rustenburg: Implats.

Hanekom, J.W.L. (2017). Fundamental understanding underground pillar design process and methods. *AfriRock 2017 Rock Mechanics for Africa* (pp. 1081-1094). Cape Town: SAIMM.

Hedley, D.G.F, & Grants, F. (1972). Stope-and-Pillar Design for the Elliot Lake Uranium Mines. Canadian Institute of Mining

Khoshboresh, A. R. (2013). A study on deformation of tunnels excavated in fractured rocks. M. Sc Research. Quebec: Laval University.

Milne, D.M (1997). Underground design and deformation based on surface geometry. D. Phil Research. University of British Columbia.

Malan, F. (1999). Time dependent behaviour of deep level tabular excavations in hard rock. Rock Mechanics and Rock Engineering, 32 (2), 123-155.

Malan, F. (2012). Pillar design in Hard Rock Mines of South Africa. International Journal of Mining Geological Engineering, Volume 46, No. 2, Dec. 2012, 163-191

Martin, C., & Maybe, W. (2000). The strength of hard-rock pillars. *International Journal of Rock Mechanics and Mining Sciences*, 37, (2000), 1239-1246.

Moore, D. S. (2004). The basic practice of statistics. New York: W.H. Freeman and Company.

More O'Ferrall, G. C., & du Plessis, M. (2017). The influence of geological structures-an often over-looked but important aspect affecting the stability of operating mines. *AfriRock 2017 Rock Mechanics for Africa* (pp. 947-958). Cape Town: The Southern Africa Institute of Mining and Metallurgy.

More O'Ferral, G. C., & Malan, F. D. (2012). The Effect of Weak Layers on Pillar Performance in South African Chrome and Platinum Mines. Canadian Institute of Mining.

Muaka, J. J., Duma, S., Mushangwe, P., Gardner, L., Chindedza, T., Walls, J., & Joughin, W. (2017). Modelling hard rock jointed pillars using a distinct element and discrete network approach considering the effect of clay-filled shear structure. Deep Mining 2017: *Eighth International Conference on Deep and High Stress Mining* (pp. 311-328). Perth: Australian Centre for Geomechanics.

Potvin, Y. (1985). Investigation of underground mine pillar design procedure - *MSc Thesis*. Vancouver: University of British Columbia.

Pritchard, C., & Hedley, D. (1993). Progressive failure and rock bursting at Denison Mine. *3rd International symposium on Rockbursts and Seismicity in Mines* (pp. 111-116). Kingstone Rotterdam: AA Balkema.

Ryder, J., & Jager, A. (2002). Rock Mechanics for tabular hard rock mines. Johannesburg: SIMRAC.

Spencer, D. (1999). A case study of a pillar system failure at shallow depth in a Chrome Mine. Spencer Rock Mechanics Consultancy.

Van Der Merwe, J. (2006, December). Beyond Coalbrook: What did we really learn? *The Journal of The Southern African Institute of Mining and Metallurgy*, 106 (12), 857-868.

Walls, J., & Mpunzi, P. (2017). Geotechnical characterisation and revision of the pillar design for a hard-rock bord and pillar mine. *AfriRock 2017 Rock Mechanics for Africa* (pp. 847-860). Cape Town: SAIMM.

Wilson, A. H., & Prendergast. (2001). Platinum-group element mineralisation of the Great Dyke, Zimbabwe and its relationship to Magma evolution and magma chamber structure. *South African Journal of geology*, Volume 104, 319-342.

Youssof, M., Thybo, H., Artemieva, I., & Levander, A. (2013). Moho depth and crustal composition in Southern Africa. *Tectonophysics*, Volume 608 (November 2013), 267-287.

Zimplats. (2014). Internal Report on initial collapse details.

Zimplats. (2017). Zimplats - 2017 Integrated Annual Report. Harare: Zimplats.

Zimplats Internal report (2016a). Elastic Modelling report. Done by SRK Consulting, Johannesburg.

Zimplats Internal Report (2006). Feasibility Study Ngezi Expansion Vol 3. Done by SRK Consulting, Johannesburg.

Zimplats Internal Report (2016b). Portal 6 Feasibility report. Done by SRK Consulting, Johannesburg.

Zimplats Internal report. (2014). Mutambara Shear Report. Harare: Zimplats.

Zimplats Internal report. (2015). Ground Truthing of the Zimplats Geological model. Done by Kock, S of Implats.

Zimplats Internal report, (2015). Report on the influence of weak clay parting on mine stability. Done by Jacobsz, S.W of Business Enterprises at University of Pretoria.

Zipf, K. (1996). Simulation of Cascading Pillar Failure In Room and Pillar Mines Using Boundary Element Method. Montreal, Quebec, Canada.

Zipf, K. R. (2000). Toward Pillar Design to Prevent collapse of Room and Pillar Mines. Spokane: NIOSH.

.

APPENDICES

APPENDIX 1

JOINT ANALYSIS

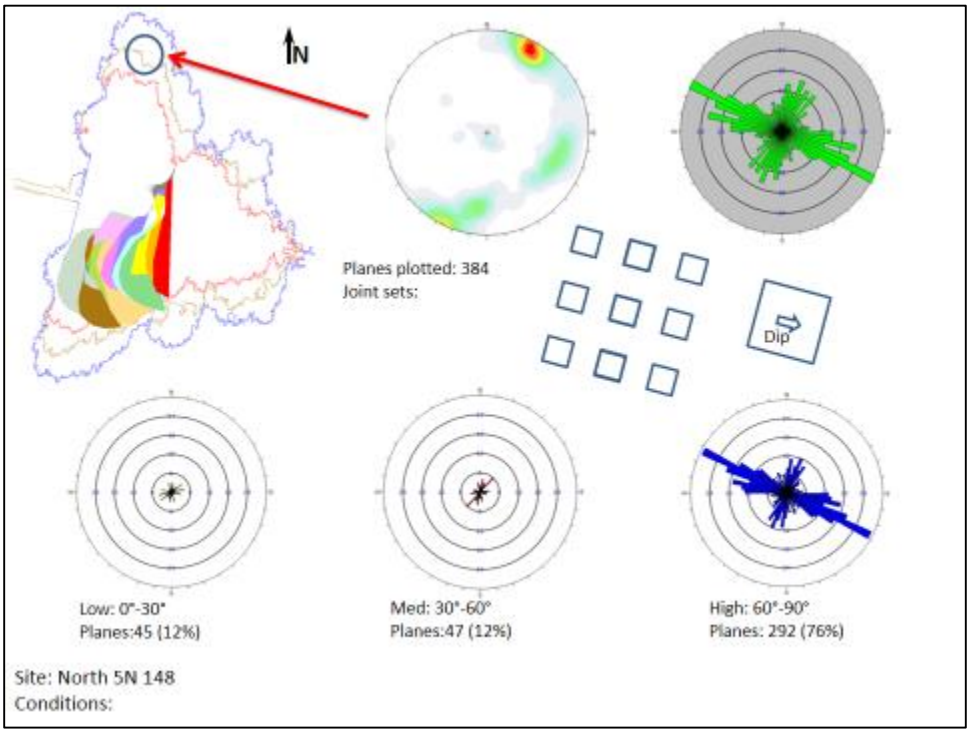

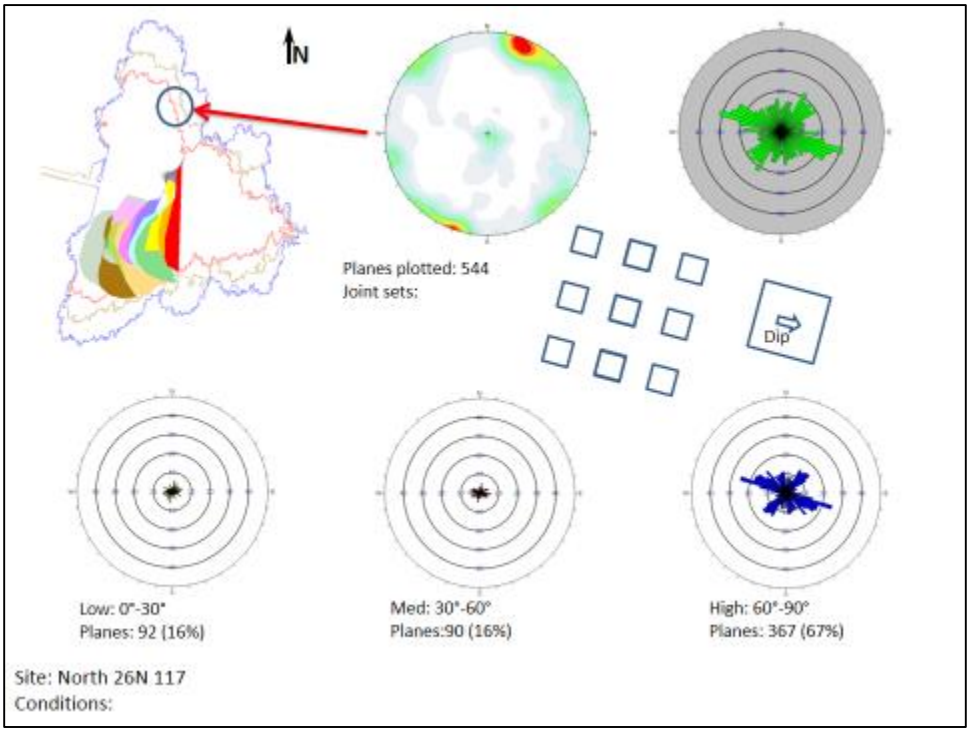

Site: North 26N 117
Conditions:

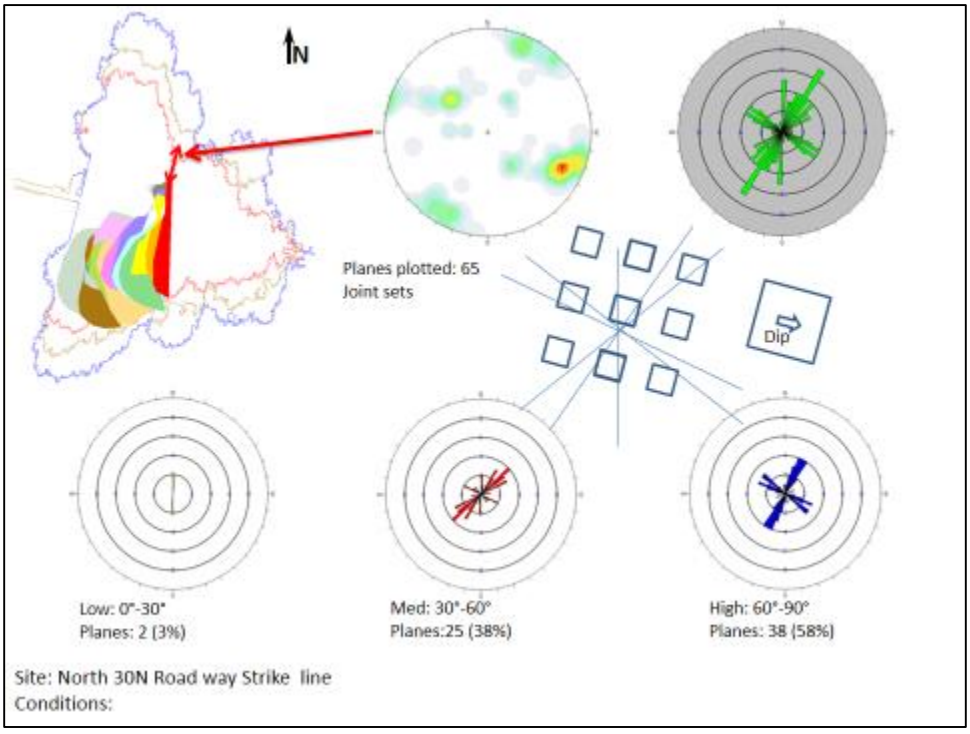

Site: North 30N Road way Strike line
Conditions:

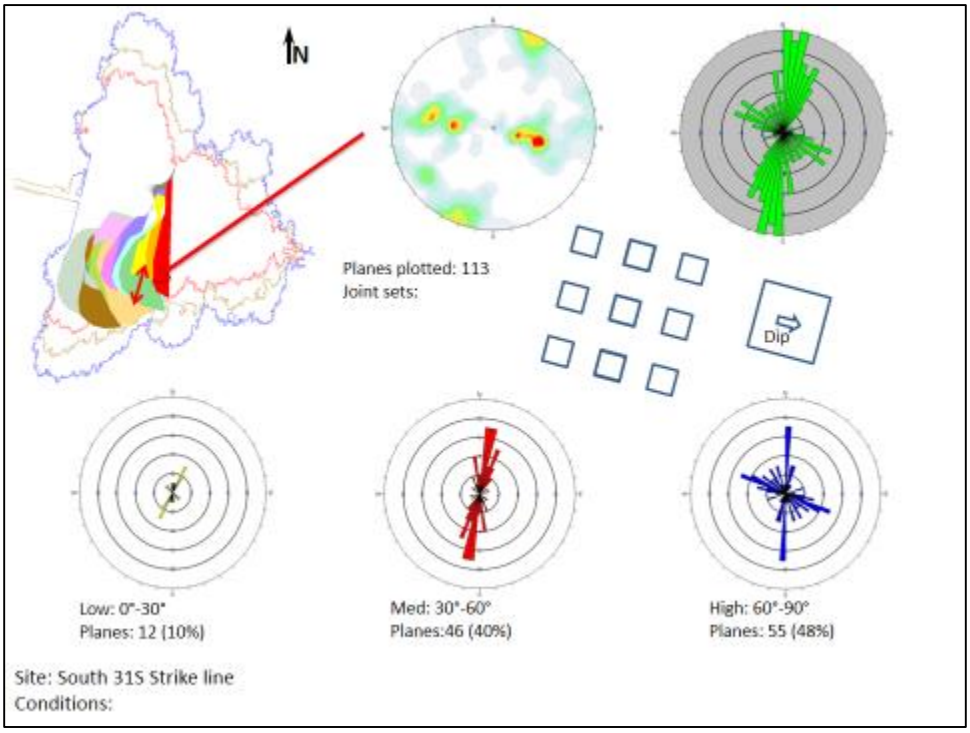
N
Planes plotted: 113
Joint sets:
Dip
Low: 0°-30°
Planes: 12 (10%)
Med: 30°-60°
Planes:46 (40%)
High: 60°-90°
Planes: 55 (48%)
Site: South 31S Strike line
Conditions:

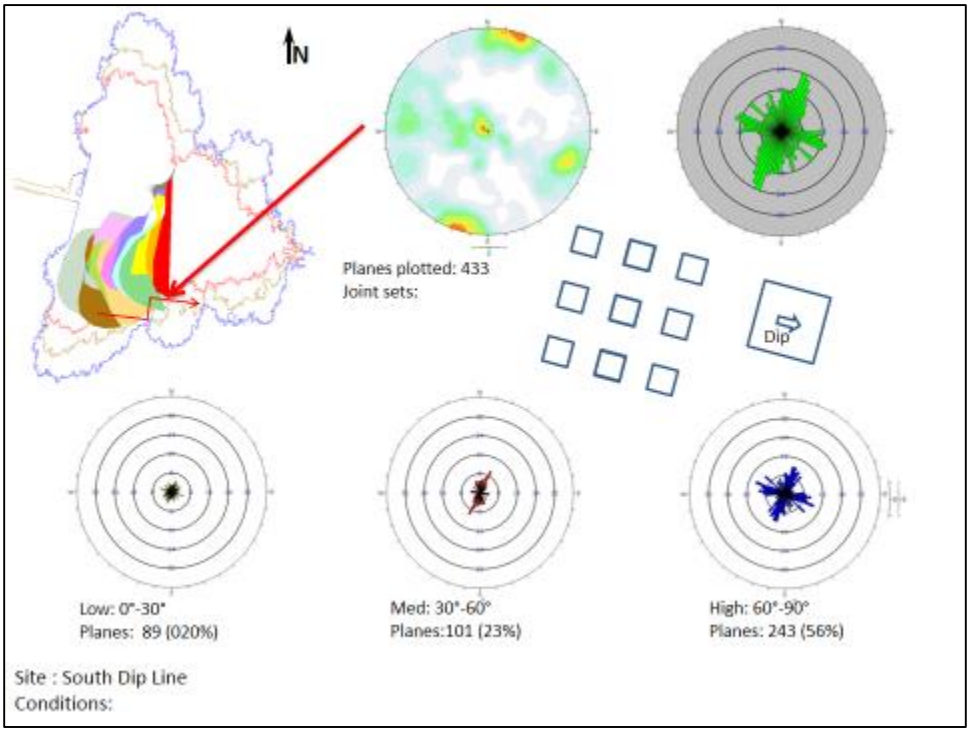
N
Planes plotted: 433
Joint sets:
Dip
Low: 0°-30°
Planes: 89 (020%)
Med: 30°-60°
Planes:101 (23%)
High: 60°-90°
Planes: 243 (56%)
Site : South Dip Line
Conditions:

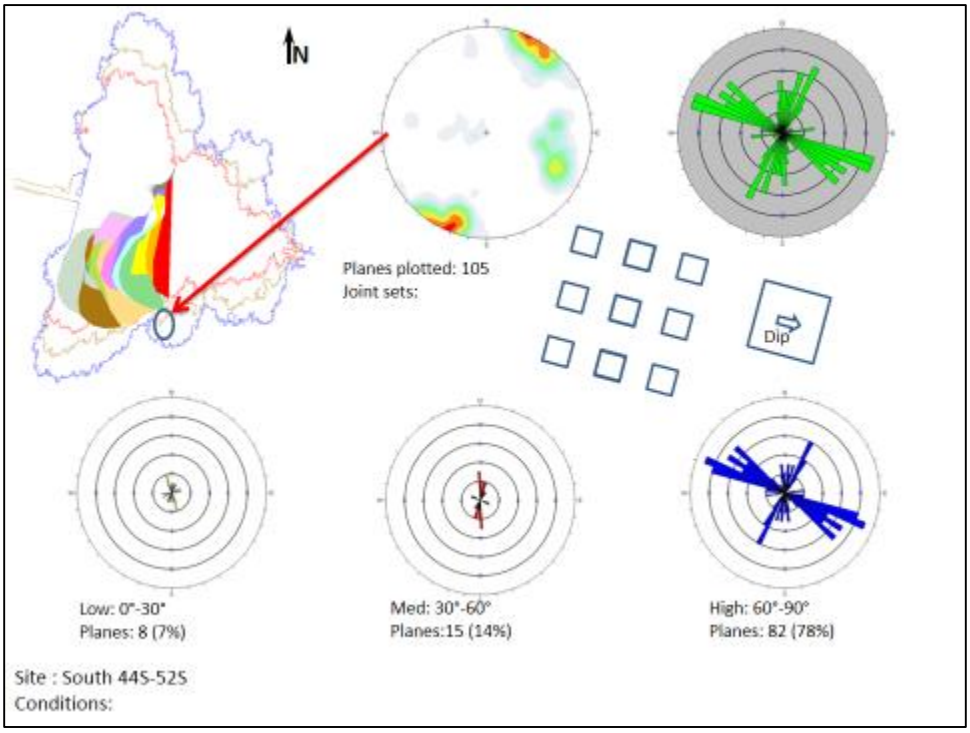
N
Planes plotted: 105
Joint sets:
Dip
Low: 0°-30°
Planes: 8 (7%)
Med: 30°-60°
Planes:15 (14%)
High: 60°-90°
Planes: 82 (78%)
Site : South 44S-52S
Conditions:

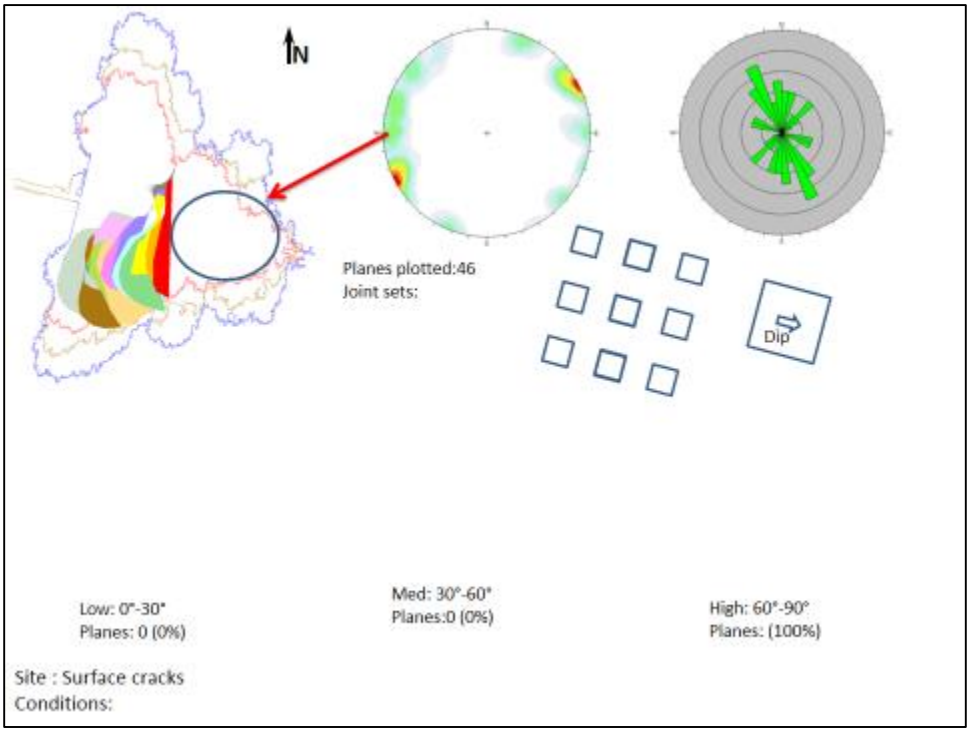
N
Planes plotted:46
Joint sets:
Dip
Low: 0°-30°
Planes: 0 (0%)
Med: 30°-60°
Planes:0 (0%)
High: 60°-90°
Planes: (100%)
Site : Surface cracks
Conditions:

LABORATORY TEST RESULTS

TABLE 1 RESULTS OF UNIAXIAL COMPRESSIVE STRENGTH TESTS WITH MODULUS & POISSON'S RATIO MEASUREMENTS BY MEANS OF STRAIN GAUGES

Client: Zimplats Sampling Site: 13-Jan-11

SPECIMEN PARTICULARS					SPECIMEN DIMENSIONS					SPECIMEN TEST RESULTS								
Rocklab Specimen No 4195-	Hole ID	Sample ID	Sample Zone	Rock Type	Diameter mm	Height mm	Ratio of Height to Diameter	Mass g	Density g/cm³	Failure Load kN	Strength (UCS) MPa	Tangent Elastic Modulus @ 50% UCS GPa	Secant Elastic Modulus @ 50% UCS GPa	Poisson's Ratio Tangent @ 50% UCS	Poisson's Ratio Secant @ 50% UCS	Linear Axial Strain at Failure mm/mm	Failure Code	Note
UCM-01		AB57295	MLE03-1		47.59	103.4	2.2	603.6	3.28	453.1	254.7	166.0	162.0	0.22	0.21	0.001586	3B	
UCM-02	MLE03	AB57296	MLE03-2		47.60	104.8	2.2	607.9	3.26	165.1	92.8	148.0	146.0	0.20	0.18	0.000626	3B	
UCM-03		AB57297	MLE03-3		47.57	101.6	2.1	591.8	3.28	143.9	81.0	153.0	154.0	0.18	0.15	0.000521	2B	
UCM-16		AB57325	MLE40-1		47.42	102.7	2.2	594.2	3.28	437.3	247.6	154.0	158.0	0.21	0.20	0.001759	XB	
UCM-17	MLE40	AB57326	MLE40-2		47.40	105.7	2.2	610.0	3.27	449.7	254.8	142.0	146.0	0.18	0.16	0.001973	XA	
UCM-18		AB57327	MLE40-3		47.39	101.7	2.1	587.3	3.27	448.8	254.4	148.0	149.0	0.22	0.21	0.002044	XA	
UCM-31		AB57365	MLF13-1		47.35	105.6	2.2	589.3	3.17	205.4	116.6	80.9	85.3	0.21	0.16	0.001422	1B	
UCM-32	MLF13	AB57366	MLF13-2		47.40	111.3	2.3	637.2	3.24	392.9	222.7	147.0	151.0	0.24	0.22	0.001779	XA	
UCM-33		AB57367	MLF13-3		47.32	98.4	2.1	564.4	3.26	361.7	205.7	143.0	142.0	0.24	0.21	0.001873	XB	
UCM-49		AB57405	MLF43-1		47.57	103.6	2.2	606.7	3.30	522.4	293.9	152.0	153.0	0.20	0.18	0.002033	XB	
UCM-50	MLF43	AB57406	MLF43-2		47.56	100.6	2.1	590.0	3.30	514.2	289.4	198.0	189.0	0.28	0.25	0.001609	XB	
UCM-51		AB57407	MLF43-3		47.58	97.0	2.0	569.7	3.30	421.5	237.1	155.0	155.0	0.20	0.19	0.001727	5B	
UCM-64		AB57445	MLG02-1		47.18	104.5	2.2	592.8	3.25	268.9	153.8	135.0	135.0	0.23	0.21	0.001160	2B	
UCM-65	MLG02	AB57446	MLG02-2		47.27	96.5	2.0	551.5	3.26	332.1	189.2	171.0	171.0	0.21	0.20	0.001110	6B	
UCM-66		AB57447	MLG02-3		47.23	98.8	2.1	565.6	3.27	293.9	167.8	161.0	162.0	0.23	0.22	0.001051	3B	
UCM-79		AB57465	MLG07-1		47.47	102.7	2.2	591.4	3.25	325.5	183.9	129.0	140.0	0.25	0.19	0.001768	XA	
UCM-80	MLG07	AB57466	MLG07-2		47.44	102.5	2.2	588.5	3.25	269.3	152.4	143.0	146.0	0.25	0.20	0.001215	1B	
UCM-81		AB57467	MLG07-3		47.42	103.7	2.2	595.8	3.25	283.0	160.2	131.0	140.0	0.25	0.22	0.001273	1B	

Note: All tests were conducted according to the ISRM's sp 1 - No specimen could be prepared for the test.

TABLE 2 RESULTS OF BRAZILIAN TENSILE STRENGTH TESTS

Client: Zimplats Sampling Site: 6-Jan-10

SPECIMEN PARTICULARS					SPECIMEN DIMENSIONS				SPECIMEN TEST RESULT		
ROCKLAB Specimen No 4195-	Borehole ID	Sample ID	Sample Zone	Rock Type	Diameter mm	Height mm	Mass gram	Density g/cm³	Failure Load kN	Brazilian Tensile Strength MPa	Note
UTB-13		AB57319	MLE03-25		47.59	25.21	146.6	3.27	45.3	24.0	
UTB-14	MLE03	AB57320	MLE03-26		47.59	23.64	136.9	3.26	43.0	24.3	
UTB-15		AB57321	MLE03-27		47.59	22.27	129.0	3.26	40.1	24.1	
UTB-43		AB57381	MLF13-17		47.30	24.57	139.4	3.23	30.1	16.5	
UTB-44	MLF13	AB57382	MLF13-18		47.30	23.99	136.6	3.24	28.4	15.9	
UTB-45		AB57383	MLF13-19		47.29	26.87	152.6	3.23	35.3	17.7	
UTB-61		AB57419	MLF43-15		47.71	25.96	150.3	3.24	42.3	21.7	
UTB-62	MLF43	AB57420	MLF43-16		47.59	28.10	162.9	3.26	54.8	26.1	
UTB-63		AB57421	MLF43-17		47.58	24.82	141.6	3.21	35.1	18.9	
UTB-76		AB57461	MLG02-17		47.28	25.06	141.1	3.21	28.1	15.1	
UTB-77	MLG02	AB57462	MLG02-18		47.25	26.05	148.9	3.26	30.4	15.7	
UTB-78		AB57463	MLG02-19		47.27	26.22	150.4	3.27	35.6	18.3	

Note: All tests were conducted according to the ISRM's suggested method.

TABLE 3 RESULTS OF TRIAXIAL COMPRESSIVE STRENGTH TESTS

Client: Zimplats Sampling Site:

12-Jan-11

SPECIMEN PARTICULARS					SPECIMEN DIMENSIONS					SPECIMEN TEST RESULTS				
Rocklab Specimen No 4195-	Borehole ID	Sample ID	Sample Zone	Rock Type	Diameter mm	Height mm	Ratio of Height to Diameter	Mass g	Density g/cm³	Confining Pressure σ_3 MPa	Failure Load P kN	Strength (TCS) σ_1 MPa	Failure Mode	Note
TCS-04		AB57301	MLE03-7		47.59	93.6	2.0	548.0	3.29	5	580.2	326.2	2B	
TCS-05		AB57302	MLE03-8		47.61	96.4	2.0	565.5	3.29	5	394.6	221.7	1B	
TCS-06		AB57303	MLE03-9		47.59	96.0	2.0	561.4	3.29	5	628.4	353.3	XA	
TCS-07		AB57307	MLE03-13		47.62	96.8	2.0	567.0	3.29	10	419.4	235.5	3B	
TCS-08	MLE03	AB57308	MLE03-14		47.54	100.2	2.1	587.1	3.30	10	677.9	381.9	2B	
TCS-09		AB57309	MLE03-15		47.58	94.5	2.0	553.8	3.30	10	690.2	388.2	2B	
TCS-10		AB57313	MLE03-19		47.59	97.4	2.0	570.1	3.29	15	617.3	347.0	2B	
TCS-11		AB57314	MLE03-20		47.58	95.8	2.0	561.6	3.30	15	425.5	239.3	3B	
TCS-12		AB57315	MLE03-21		47.68	98.0	2.1	575.2	3.29	15	739.7	414.3	XA	
TCS-19		AB57333	MLE40-9		47.50	94.7	2.0	547.6	3.26	5	607.4	342.7	XA	
TCS-20		AB57334	MLE40-10		47.38	97.0	2.0	562.5	3.29	5	499.8	283.4	XA	
TCS-21		AB57335	MLE40-11		47.38	94.1	2.0	545.9	3.29	5	577.7	327.6	XA	
TCS-22		AB57341	MLE40-17		47.40	95.3	2.0	551.7	3.28	10	534.4	302.8	2B	
TCS-23	MLE40	AB57342	MLE40-18		47.46	96.5	2.0	559.8	3.28	10	513.4	290.2	3B	
TCS-24		AB57343	MLE40-19		47.42	97.8	2.1	568.4	3.29	10	570.3	322.9	3B	
TCS-25		AB57349	MLE40-25		47.28	96.4	2.0	555.1	3.28	15	659.3	375.5	XA	
TCS-26		AB57350	MLE40-26		47.44	94.8	2.0	548.2	3.27	15	613.6	347.1	3B	
TCS-27		AB57351	MLE40-27		47.58	91.4	1.9	531.2	3.27	15	706.3	397.3	XA	
TCS-34		AB57369	MLF13-5		47.26	98.1	2.1	561.3	3.26	5	452.8	258.1	XA	
TCS-35		AB57370	MLF13-6		47.24	101.7	2.2	579.8	3.25	5	483.7	276.0	XA	
TCS-36		AB57371	MLF13-7		47.24	98.9	2.1	562.2	3.24	5	243.7	139.0	7B	
TCS-37		AB57373	MLF13-9		47.26	98.6	2.1	563.5	3.26	10	320.4	182.6	3B	
TCS-38	MLF13	AB57374	MLF13-10		47.26	96.0	2.0	548.9	3.26	10	410.7	234.1	5B	
TCS-39		AB57375	MLF13-11		47.44	97.5	2.1	560.4	3.25	10	524.5	296.7	2B	
TCS-40		AB57377	MLF13-13		47.28	87.3	1.8	502.3	3.28	15	550.5	313.5	2B	
TCS-41		AB57378	MLF13-14		47.29	98.9	2.1	568.0	3.27	15	559.1	318.3	2B	
TCS-42		AB57379	MLF13-15		47.27	97.1	2.1	557.3	3.27	15	488.6	278.4	2B	
TCS-52		AB57408	MLF43-4		47.56	95.9	2.0	561.4	3.30	5	668.0	376.0	XA	
TCS-53		AB57409	MLF43-5		47.57	97.1	2.0	569.1	3.30	5	634.6	357.1	XA	
TCS-54		AB57410	MLF43-6		47.57	95.0	2.0	557.2	3.30	5	653.1	367.5	XA	
TCS-55		AB57411	MLF43-7		47.63	100.9	2.1	591.8	3.29	10	695.2	390.2	XA	
TCS-56	MLF43	AB57412	MLF43-8		47.57	97.4	2.0	571.3	3.30	10	698.9	393.2	XA	
TCS-57		AB57413	MLF43-9		47.67	97.4	2.0	570.4	3.28	10	621.0	347.9	7B	
TCS-58		AB57415	MLF43-11		47.56	101.6	2.1	594.6	3.30	15	780.6	439.4	XA	
TCS-59		AB57416	MLF43-12		47.57	94.6	2.0	555.0	3.30	15	754.6	424.6	XA	
TCS-60		AB57417	MLF43-13		47.58	97.4	2.0	572.4	3.30	15	754.6	424.4	XA	
TCS-67		AB57449	MLG02-5		47.25	96.8	2.0	554.7	3.27	5	382.2	218.0	4B	
TCS-68		AB57450	MLG02-6		47.22	92.5	2.0	529.6	3.27	5	450.3	257.1	XA	
TCS-69		AB57451	MLG02-7		47.20	97.2	2.1	557.3	3.28	5	534.4	305.4	XA	
TCS-70		AB57453	MLG02-9		47.24	98.5	2.1	566.9	3.28	10	480.0	273.8	5B	
TCS-71	MLG02	AB57454	MLG02-10		47.23	96.5	2.0	554.8	3.28	10	282.0	161.0	4B	
TCS-72		AB57455	MLG02-11		47.25	97.2	2.1	561.1	3.29	10	520.8	297.0	3B	
TCS-73		AB57457	MLG02-13		47.43	99.7	2.1	573.6	3.26	15	674.2	381.6	XA	
TCS-74		AB57458	MLG02-14		47.27	95.2	2.0	546.8	3.27	15	519.5	296.0	4B	
TCS-75		AB57459	MLG02-15		47.24	89.4	1.9	514.1	3.28	15	665.5	379.7	XA	
TCS-82		AB57469	MLG07-5		47.41	97.7	2.1	561.1	3.25	5	392.1	222.1	XA	
TCS-83		AB57470	MLG07-6		47.42	95.8	2.0	549.1	3.25	5	376.1	212.9	XA	
TCS-84		AB57471	MLG07-7		47.43	97.1	2.0	556.1	3.24	5	421.8	238.7	XA	
TCS-85		AB57473	MLG07-9		47.42	95.1	2.0	542.8	3.23	10	480.0	271.8	XA	
TCS-86	MLG07	AB57474	MLG07-10		47.43	90.6	1.9	518.8	3.24	10	491.1	277.9	XA	
TCS-87		AB57475	MLG07-11		47.45	95.3	2.0	546.9	3.24	10	445.3	251.8	XA	
TCS-88		AB57477	MLG07-13		47.46	96.8	2.0	555.2	3.24	15	238.8	135.0	5B	
TCS-89		AB57478	MLG07-14		47.46	100.1	2.1	582.5	3.29	15	551.7	311.9	XA	
TCS-90		AB57479	MLG07-15		47.46	101.7	2.1	585.3	3.25	15	487.4	275.5	5B	

Note: All tests were conducted according to the ISRM's Specification.

TABLE 1 RESULTS OF UNIAXIAL COMPRESSIVE STRENGTH TESTS WITH MODULUS & POISSON'S RATIO MEASUREMENTS BY MEANS OF STRAIN GAUGES

Client: Zimplats

Sampling Site: Bimha Mine

7-Aug-14

SPECIMEN PARTICULARS					SPECIMEN DIMENSIONS					SPECIMEN TEST RESULTS								
Rocklab Specimen No 5853-	Hole ID	Sample ID	Depth From.. To..	Rock Type	Diameter mm	Height mm	Ratio of Height to Diameter	Mass g	Density g/cm³	Failure Load kN	Strength (UCS) MPa	Tangent Elastic Modulus @ 50% UCS GPa	Secant Elastic Modulus @ 50% UCS GPa	Poisson's Ratio Tangent @ 50% UCS	Poisson's Ratio Secant @ 50% UCS	Linear Axial Strain at Failure mm/mm	Failure Code	Note
UCM-04	45S34 Up Hole	UCM 1	2.10 - 2.25		54.60	137.6	2.5	1059.36	3.29	575.5	245.8	148.0	150.0	0.22	0.23	0.001916	XB	
UCM-05	45S34 Up Hole	UCM 2	1.85 - 2.00		54.60	139.5	2.6	1076.22	3.29	559.9	239.1	153.0	155.0	0.23	0.22	0.001781	XA	
UCM-06	45S34 Up Hole	UCM 3	5.25 - 5.40		54.57	139.1	2.5	1061.52	3.26	430.8	184.2	127.0	109.0	0.23	0.17	0.001695	XA	
UCM-07	45S34 Up Hole	UCM 4	2.65 - 2.80		54.63	139.0	2.5	1068.04	3.28	541.3	230.9	148.0	153.0	0.25	0.25	0.001766	XB	
UCM-08	45S34 Up Hole	UCM 5	2.45 - 2.60		54.64	139.4	2.6	1069.73	3.27	486.7	207.6	150.0	153.0	0.24	0.24	0.001716	XA	
UCM-09	45S34 Up Hole	UCM 6	2.28 - 2.43		54.63	139.6	2.6	1068.88	3.27	504.1	215.1	144.0	146.0	0.24	0.23	0.001706	XB	

Note: All tests were conducted according to the ISRM's specfications.

APPENDIX 3

Example calculation of the coefficient of correlation (R)

Equation 1 gives the Pearson's correlation coefficient (Moore, 2004)

$$r = \frac{n(\Sigma xy) - (\Sigma x)(\Sigma y)}{\sqrt{[\, n\Sigma x^2 - (\Sigma x)^2 \,][\, n\Sigma y^2 - (\Sigma y)^2 \,]}} \qquad \ldots\ldots\ldots\ldots\ldots (1)$$

Density of Aplite dykes is used as an example in the calculation of the correlation coefficient (R). The areas A,B,C,D and E have been numerated 1,2,3,4,5 for the purpose of calculating R.

	Area (X)	**Density (Y)**	**XY**	**X^2**	**Y^2**
	1	1.63	1.63	1	2.6569
	2	2.3	4.6	4	5.29
	3	0.68	2.04	9	0.4624
	4	1.31	5.24	16	1.7161
	5	0.66	3.3	25	0.4356
SUM	15	6.58	16.81	55	10.561

$$R = \frac{5(16.81) - (15) \times (6.58)}{\sqrt{[5 \times 55 - 15^2] \times [5 \times 10.56 - 6.58^2]}}$$

= -0.671884

= -0.67